A CLUSTER ANALYSIS OF TROPICAL CYCLONE TRAJECTORIES IN THE SOUTH INDIAN OCEAN: THE INFLUENCES OF THE EL NINO-SOUTHERN OSCILLATION AND THE SUBTROPICAL INDIAN OCEAN DIPOLE

By

KEVIN D. ASH

A THESIS PRESENTED TO THE GRADUATE SCHOOL
OF THE UNIVERSITY OF FLORIDA IN PARTIAL FULFILLMENT
OF THE REQUIREMENTS FOR THE DEGREE OF
MASTER OF SCIENCE

UNIVERSITY OF FLORIDA

2010

To the Captain of the cargo vessel in the Indian Ocean who did not listen to my advice and motivated me to learn more.

ACKNOWLEDGMENTS

I would like to first extend thanks to my parents and my brother for their love and support. I am also grateful to Ann Foster and the United States Geological Survey for employing me during my first year in Gainesville and affording me the opportunity to earn a decent paycheck while in graduate school. I am appreciative as well to the Department of Geography for funding and the opportunity to work as a Teaching Assistant during my second year. I am grateful to the Poehling family and all who graciously supported the establishment of a new fellowship this year in memory of their son, Ryan. Many thanks as well to my thesis committee members Peter Waylen and Tim Fik for their valuable advice. Finally, thank you to my committee chair and advisor Corene Matyas for her dedication and wisdom in challenging and guiding me during the last two years.

TABLE OF CONTENTS

page

LIST OF TABLES

LIST OF FIGURES

LIST OF ABBREVIATIONS

ANOVA	analysis of variance
CA	cluster analysis
ENSO	El Niño-Southern Oscillation
hPa	hectopascals
ITCZ	inter-tropical convergence zone
JTWC	Joint Typhoon Warning Center
$m\ s^{-1}$	meters per second
MSLP	mean sea level pressure
NCEP	National Centers for Environmental Prediction
NH	Northern Hemisphere
NOAA	National Oceanic and Atmospheric Administration
RSMC	Regional Specialized Meteorological Center
SH	Southern Hemisphere
SICZ	South Indian Convergence Zone
SIO	South Indian Ocean
SLP	sea level pressure
SO	Southern Oscillation
SST	sea surface temperature
SSTA	sea surface temperature anomaly
TC	tropical cyclone
TTT	tropical-temperate trough
$W\ m^{-2}$	Watts per square meter
WMO	World Meteorological Organization
WNP	Western North Pacific

Abstract of Thesis Presented to the Graduate School
of the University of Florida in Partial Fulfillment of the
Requirements for the Degree of Master of Science

A CLUSTER ANALYSIS OF TROPICAL CYCLONE TRAJECTORIES IN THE SOUTH INDIAN OCEAN: THE INFLUENCES OF THE EL NINO-SOUTHERN OSCILLATION AND THE SUBTROPICAL INDIAN OCEAN DIPOLE

By

Kevin D. Ash

May 2010

Chair: Corene Matyas
Major: Geography

Tropical cyclones (TCs) are a regular feature over the South Indian Ocean (SIO) during the austral warm season from November to April. The storms often pass in close proximity to the islands of Madagascar, Mauritius, and Reunion, or pass through the Mozambique Channel. In addition to threatening human lives, cyclones are also capable of negative societal impacts in this economically developing region, ruining crops and disrupting the region's busy shipping lanes. It is therefore important to investigate the causes and controls that shape the tracks of the SIO TCs. The goal of this research is to relate variability of TC motion to the oceanic-atmospheric circulation.

Cluster analysis is employed to group SIO TC trajectories by their initial and final positions. The clusters are then used to compare group median index values that represent El Niño-Southern Oscillation (ENSO) and the Subtropical Indian Ocean Dipole (SIOD) using Kruskal-Wallis analysis of variance (ANOVA) on ranks and post-hoc multiple comparisons. ENSO is known to influence TC trajectories in the SIO through modulation of the semi-permanent SIO subtropical high. However, though ENSO plays a role in altering the oceanic-atmospheric environment within the basin, it

is not always simultaneously associated with either a strong or weak subtropical high. The SIOD is known to exert strong influence on precipitation patterns in the SIO region, also through modulation of the SIO subtropical semi-permanent high. Both ENSO and SIOD have likewise been linked to shifts in the austral summer tropical-temperate troughs (TTTs) from the African continent to northeast of Madagascar over the western SIO.

The results of the multiple comparison tests in this study suggest that both ENSO and SIOD are significantly associated with TC trajectories. This significant link between SIOD and SIO TCs has not been documented in the known SIO TC literature, and this study proposes TTTs as the physical mechanism responsible for the strong eastward component of TC motion when ENSO is in warm phase and SIOD is in negative phase. When ENSO is in cool phase and SIOD is simultaneously in positive phase, TC trajectories tend to show strong westward movement, remain farther north and do not recurve into the mid-latitude westerlies. This study is important because the findings suggest that anti-phase interactions of ENSO and SIOD frequently associate with anomalous westward or eastward TC trajectories.

CHAPTER 1
INTRODUCTION

Tropical cyclones (TCs) are among the most devastating natural forces on earth. On a global scale, they are responsible for a large portion of casualties and damages attributed to natural hazards (Emanuel, 2005b). TCs are broadly defined as warm core low pressure systems originating over tropical water bodies, which derive their energy largely from heat fluxes between the warm ocean surface and the overlying atmosphere (Emanuel, 2003). The term 'tropical cyclone' is used throughout this document as a general term encompassing tropical systems of varying levels of intensity including hurricane intensity (> 33 m s^{-1}), tropical storm intensity (>17 m s^{-1}), and tropical depression intensity (<17 m s^{-1}), all using the United States (US) standard 1-minute average sustained wind speed. Since the TC data source utilized in this study is the US Joint Typhoon Warning Center (JTWC) best-tracks, no further explanation is necessary regarding the differing criteria used by various other meteorological agencies in their respective TC nomenclatures. Chapter 3 provides further details of a more precise definition of a TC as relevant to the analyses presented herein.

Whether intense or weak, landfalling or in the open ocean, TCs have great capacity to threaten human life and disrupt society with their combinations of fast winds, heavy rain, and coastal water rise (Pielke and Pielke, 1997). Thus, scientists, social policy makers, military commanders, and even investors maintain great interest in improvements of TC prediction both in real time and on longer time horizons. TCs follow variable paths, or trajectories, from their development regions over tropical waters, but frequently they exhibit trajectories with some component of westerly and poleward movement. Quite often, TCs that stray into the subtropics begin to take

recurving poleward trajectories and move with an easterly component, influenced by mid-latitude westerly jet streams (Knaff, 2009). To fully understand TCs is to be able to consistently predict their frequency, movement, and intensity within useful and acceptable margins of error. The ability to predict may then afford greater warning lead time, which can save lives or mitigate profit loss (Murnane, 2004).

The South Indian Ocean (SIO) is an important region for TC research and accounts for about 14% of the average annual global TC activity, a similar percentage to the North Atlantic (Jury, 1993). The peoples of southern Africa, Madagascar, and the Mascarene Islands (Figure 1-1) are vulnerable to repeated TC strikes and their concomitant hazards (Table 1-1). Madagascar has endured many devastating events, particularly on the northern half of the island. Landfalls of intense TCs Andry and Kamisy (both Saffir-Simpson category 4) impacted northern Madagascar in 1983-84 (Jury *et al*., 1993). Successive storm surges up to six meters accompanied three TCs (Daisy, Geralda, and Litanne) that made landfall within the same 100km stretch of coastline early in 1994 (Naeraa and Jury, 1998). These systems destroyed critical shipping and energy infrastructures, brought flooding rainfall, and caused hundreds of deaths (Chang-Seng and Jury, 2010b). Northern Madagascar is also a leading vanilla-producing region and is subject to widespread agricultural losses, as transpired in 2000 and again in 2007 (Brown, 2009).

Southern Africa has seen the adverse impacts of TCs as well, though landfalls are much less frequent than in Madagascar. Reason and Keibel (2004) observed that less than 5% of cyclones in the SIO made landfall on the east coast of Africa over the period 1954-2004. Still, Mozambique has endured unusually severe impacts from TCs in a few

instances, with widespread flooding from rainfall causing the most casualties and damage. Cyclone Eline in 2000 struck as serious seasonal flooding was already underway and exacerbated the catastrophic flooding across the region, killing hundreds and affecting millions of people (Vitart *et al*., 2003; Reason and Keibel, 2004). Disastrous flooding in Mozambique from heavy rainfall also accompanied the passages of Cyclone Dera in 2001 and Favio in 2007 (Reason, 2007; Klinman and Reason, 2008).

The larger inhabited islands of the Mascarene Archipelago (Mauritius and Réunion) are precariously positioned with respect to SIO TCs. TC Dina devastated Réunion in 2002 and TC Hollanda likewise wrought widespread damage on Mauritius, though casualties in both cases were few, a testament to the well-organized and executed cyclone preparedness and warning systems of these islands (Parker, 1999; Roux *et al*., 2004). While these are relatively small islands with small populations, their locations are strategic along busy shipping lanes. SIO TCs are a significant threat to the lives of ship crews and their expensive cargoes, as hundreds of large commercial vessels sail daily around the Cape of Good Hope and across the region between economic hubs in Europe and the Americas and in South Asia and the Far East (Roberts and Marlow, 2002; Chang-Seng and Jury, 2010b).

TCs of the SIO have not been scrutinized as closely as those of the Northern Hemisphere or the Australian region over the past thirty years (Jury, 1993). Most recently, improvements in technology and gathering volumes of reliable observations in this economically poor and once data-sparse region are allowing for an increase of climatological studies of SIO TCs. Great leaps forward in weather/climate monitoring

and forecasting have followed from a succession of novel inventions in communications, transportation, space-borne remote sensing, and computer science over the past 200 years. The advent of satellite remote sensing particularly revolutionized tropical cyclone science beginning from the launch of the experimental weather satellite TIROS I in 1960, which provided the first pictures of a TC from space (Fritz and Wexler, 1960). Weather satellite images now allow atmospheric scientists to locate and track TCs with greater precision and even estimate their intensities based on cloud patterns (Dvorak, 1975).

These technologies have not been evenly deployed across the globe, thus the accuracy and lengths of record of TC climatologies are also unequal across the earth's oceans. In the SIO, the infrared satellite imagery needed to apply the Dvorak intensity estimation technique has been available since about 1980; therefore, reliable measures of TC positions and intensities begin from that time (Knaff and Sampson, 2009; Chang-Seng and Jury, 2010a). Another significant improvement for SIO TC observation was realized in 1998 with the placement of the Meteosat geostationary satellite over the region (Caroff, 2009; Chang-Seng and Jury, 2010a). With a useable record back to 1980, and as TC observation capabilities continue to evolve, there is sufficient data quantity and quality to study TCs of the SIO in greater depth.

Using these satellite observations, this research focuses on the trajectories or tracks of SIO TCs since 1979. Much scholarly research has previously focused on TC movement in order to improve short-term prediction of individual storm tracks, arguably the most important aspect of TC prediction (Chan, 2005). One method is to predict a TC's movement by comparing it to several similar TCs in the historical record in terms of

storm location, direction and speed of forward movement, and intensity (Hope and Neumann, 1970; Neumann and Randrianarison, 1976; Bessafi *et al*., 2002). This may be referred to as a statistical analog model or a climatology and persistence model (CLIPER), a method long used and, though increasingly falling into disfavor for short-term prediction, still used as of 2005 at the Joint Typhoon Warning Center (JTWC) as a baseline for assessing TC track predictions (Sampson *et al*., 2005).

The preferred method for short-term prediction is now based upon physical equations to model oceanic and atmospheric variables that influence the net directional heading and forward speed of each TC. There are two principal factors that account for TC movement. One is the latitudinal variation of the Coriolis effect across a cyclone's wind field, inducing poleward advection of positive vorticity which appears in aggregation over time as gentle poleward bending of the TC's track (Chan and Gray, 1982; Elsner and Kara, 1999). This is referred to as beta drift or the beta effect (Chan, 2005).

The second and more substantial influence on TC movement is the environmental steering flow. Essentially, a TC vortex is embedded within the larger scale atmospheric wind pattern and carried along with the mean flow (Chan and Gray, 1982; Chan, 2005). Dominant steering features include subtropical ridges of high pressure and troughs of low pressure. A TC's movement may be approximated using the environmental mid-tropospheric flow surrounding a TC vortex at 700, 650, or 500 hPa (Chan and Gray, 1982; Wang and Holland, 1996). A weaker and less vertically developed TC is steered more by lower tropospheric flow, whereas a strong and vertically stout TC is steered by deep layer tropospheric flow (Wang and Holland, 1996).

It is at this point that this study can be viewed in the proper context. Physical numerical modeling of TC movement has proven to be more skillful overall than climatology and persistence (Chan, 2005). Without a doubt, this is invaluable for short-term TC prediction, warning, and risk mitigation. However, statistical and climatological methods are still quite useful for longer term prediction. Given the vast improvements in TC observation techniques and computing abilities over the past fifty years, statistical analysis of a spatially and temporally homogenous global TC dataset can provide a first approximation for prediction of TC frequency and movement on intraseasonal or perhaps even interannual time scales (Klotzbach *et al*., 2010). Such statistical predictions of TC frequency have shown promise over the past thirty years, though substantial improvements are still possible (Hastenrath, 1995; Klotzbach 2007).

Much of the improvement already made in seasonal TC frequency prediction owes to greater understanding of the scope and influence of larger scale, low frequency modes of ocean-atmosphere variability such as the El Niño-Southern Oscillation (ENSO) (Klotzbach *et al*., 2010). Research has recently turned to ENSO and other global and regional ocean-atmosphere modes as likely drivers of variability in steering flow on intraseasonal and interannual time scales. Statistical associations linking these modes of variability to identifiable patterns of TC trajectories can spur future research and inform longer term trajectory predictions, even if the physical mechanisms between the two cannot be explicitly described initially. Furthermore, statistical linkages may be used for longer term disaster planning purposes, if the linkages are strong and stable enough for reliable predictions.

The goal of this study is to enhance understanding of South Indian Ocean (SIO) TC activity by testing the hypotheses that sea surface temperature anomalies (SSTA) in the equatorial Pacific Ocean and/or the tropical and subtropical Indian Ocean (IO) are contemporaneously associated with particular types of SIO TC trajectories. This is important because SSTA can be used as a proxy measure of the strength of the atmospheric circulation around the semi-permanent SIO subtropical high, thus potentially providing insight into forcing mechanisms for the above mentioned TC trajectories. Chapter 2 will review relevant literature regarding known oceanic-atmospheric global and regional pattern changes linked to the SST anomalies (SSTA) in the above stated regions, discuss how these changes relate to TCs in other ocean basins, and set a framework for how these may influence SIO TC trajectories. Chapter 3 explains the cluster analysis used here to assign a sample of 191 SIO TCs to groups according to their trajectories and then discusses the defining characteristics of each group. Chapter 4 then uses the clustering structure of Chapter 3 to test the above stated hypotheses using SST composites and statistical tests of indices representing the El Niño-Southern Oscillation (ENSO) and Subtropical Indian Ocean Dipole (SIOD). The conclusions and potential applications of this research are then summarized in Chapter 5, and results will show significant links between ENSO, SIOD, and SIO TC trajectories. It is hoped that the results presented here will contribute to a better understanding of the relationship between SIO TC tracks, ENSO, and regional modes of variability internal to the IO. The implications of skillful monthly, multi-monthly, or even up to seasonal TC trajectory forecasts would be beneficial for long term disaster planning and risk mitigation for those vulnerable to TC impacts in the region.

Table 1-1. Tropical Cyclone Close Passes in the South Indian Ocean. Number of times during the period 1979-2008 that a tropical cyclone passed within 200 kilometers (km) of the coast of the four main countries. Note that Reunion is an overseas department of France.

Country	TC Passes <= 200 km
Madagascar	58
Mauritius	49
Reunion	37
Mozambique	25

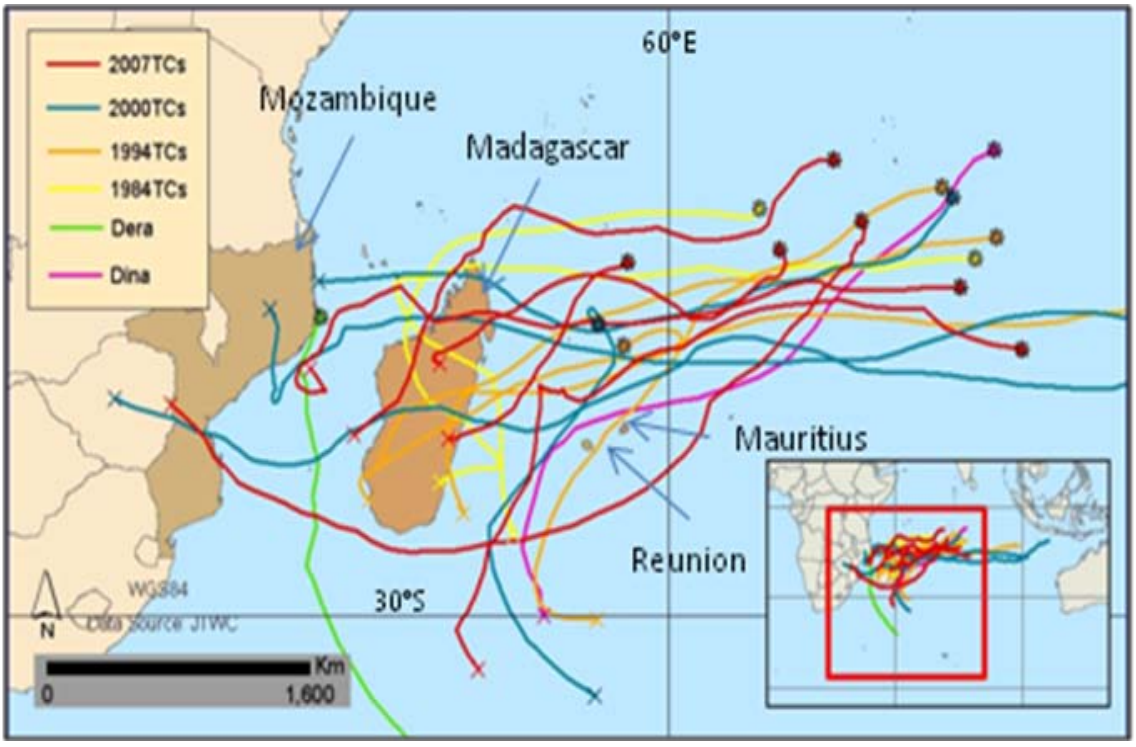

Figure 1-1. South Indian Ocean Region Map. Notable tropical cyclones Dera (2001) in green and Dina (2002) in purple. Notable cyclone seasons for TC impacts include: 1984 in yellow, 1994 in orange, 2000 in blue, and 2007 in red.

CHAPTER 2
LITERATURE REVIEW

Tropical Cyclones of the South Indian Ocean

Introduction

In order to set the context for the analyses in Chapters 3 and 4, this chapter reviews the existing relevant literature on previous tropical cyclone (TC) research in the South Indian Ocean (SIO). A brief note on the beginning of TC research in the basin will be followed by an updated basic TC climatology leading into a literature-based climatological description of typical favorable conditions for TCs in the basin. There will also be a substantial section reviewing the literature on the known oceanic-atmospheric effects of El Niño-Southern Oscillation (ENSO) within the SIO and how these effects are thought to influence TC activity in the SIO. The chapter will also outline the basic understanding of the other oceanic-atmospheric phenomenon that will be tested here, namely the Subtropical Indian Ocean Dipole (SIOD). Finally, the concluding portion of this chapter will summarize and link together the most important concepts in preparation for the data exploration and analyses in Chapters 3 and 4.

Brief History and Early Research

The term cyclone was first applied in reference to the tropical systems of the Indian Ocean. Sir Henry Piddington coined the word while stationed in India during the first half of the 19th century to describe the rotating nature of the wind fields of the violent storms observed in the Bay of Bengal (Emanuel, 2005a). In the SIO, TC research was likewise pursued in earnest by the latter half of the 19th century through British colonial resources. These early research efforts were conducted in great part by Charles Meldrum, inaugural director of the Royal Alfred Observatory and founding

member of the Meteorological Society of Mauritius (Buchan, 1901; Visher, 1922). Through collections of observations of wind direction and velocity, pressure, humidity, and cloud types both from Mauritius and from ocean vessel reports, he approximated TC paths across the SIO and advised ships at sea in TC avoidance tactics (Buchan, 1901).

Unfortunately, for all of Meldrum's curiosity, ingenuity, and ability to synthesize information, his burgeoning TC research program did not withstand the changing winds of global commerce. The opening of the Suez Canal in 1869, coupled with the rise of steam ships beginning in the 1850s, shifted important shipping lanes between Britain, India, and Asia away from Mauritius to the Red and Arabian Seas and the Bay of Bengal (Anderson, 1918; Pearson, 2003). The shift was deleterious to Meldrum's work, and the number of reporting ocean vessels in the SIO dropped from 787 in 1878 to 283 by 1900 (Ward, 1902). His work bears mention here because it was not completely lost to the annals of science. Merging Meldrum's TC data and German records (now apparently lost), early 20th century American geographer and climatologist Stephen Visher surmised that about twelve TCs occur annually in the SIO between 40°E and 100°E, an accurate estimation that remains valid over the long term up to the present (Visher, 1922).

Very little research was published in English in the peer-reviewed literature on SIO TCs after Visher until the early 1990s. This is likely attributable to the relatively low economic status of the SIO region and a coincident lack of access to the newer communications and remote sensing technologies that were being pioneered in Northern Hemisphere weather/climate research. One important exception was

Neumann and Randrianarison's (1976) work on short-term statistical prediction of TC motions in the SIO. This paper, while focused more on methodology and forecast verification than climate scale research, also included an updated climatological SIO TC narrative. The authors estimated that roughly ten TCs traverse the region each year, with the majority occurring between December and April. More recent papers gave varying accounts of the baseline SIO TC climatology specific to their respective time periods and study area boundaries (Jury, 1993; Bessafi and Wheeler, 2006; Ho *et al*., 2006; Kuleshov *et al*., 2008). Therefore, to provide appropriate context for this study a short descriptive SIO TC climatology is offered in the following subsection.

Basic Tropical Cyclone Climatology

For the present study, an updated thirty-year climatology of SIO TC counts was derived using the best-track archives from the TC forecasting and monitoring arm of the United States military, the Joint Typhoon Warning Center (JTWC) (Chu *et al*., 2002). The archive is updated annually and is freely available at http://www.usno.navy.mil/NOOC/nmfc-ph/RSS/jtwc/best_tracks/shindex.html. The period 1979-2008 is used here, following the recommendation of Knaff and Sampson (2009) that JTWC Southern Hemisphere (SH) TC data are most accurate, consistent, and suitable for scientific research from about the year 1980 and forward.

A total of 339 SIO TCs of any intensity occurred during this period of record, not counting those in the Australian region generally east of 90°-100°E (Figure 2-1). It should be noted here that because austral summer spans successive calendar years, annual TC counts begin anew each July. The twenty-nine-year annual mean number of SIO TCs was 11.7 with a standard deviation of 2.4. The minimum was 6 in 1982-83 and the maximum was 17 in 1996-97, with a median of 12 TCs. Estimates of total annual

frequency discussed above were 12 in the 1920s and 10 in the 1970s, both within one standard deviation of the mean given here for the more recent period.

TCs formed in the SIO in every calendar month during the thirty year period, though the region's TC season typically spans austral summer from November through April (Figure 2-2). The peak months were January through March, during which 56% of all SIO TCs occurred, and on average, there were two cyclones in each of those months. Storms forming between June and September were usually weak and short-lived. October and May TCs, while not numerous, occasionally were of hurricane intensity. As the present work focuses on SIO TC tracks, a track map of the SIO TCs analyzed in Chapter 4 is provided for geographical context (Figure 2-3).

A Climatologically Favorable Environment

In the North Atlantic basin, tropical easterly waves are important foci for nascent TCs (Landsea *et al*., 1998). While tropical easterly waves also exist in the SIO, they typically propagate slower, are less pronounced in structure, and are not the primary source of tropical disturbances that undergo TC genesis (Parker and Jury, 1999). The primary sources of tropical disturbances that become TCs in the SIO are northerly and westerly wind surges that penetrate from near the equator southward and locally enhance convergence and vorticity along the inter-tropical convergence zone (ITCZ) (Jury *et al*., 1994; Jury *et al*., 1999). In austral summer, the ITCZ is a region in the SIO where persistent easterly and southeasterly trade winds associated with the semi-permanent South Indian subtropical high pressure ridge converge with northerly and westerly monsoon outflow winds that cross the equator and are associated with the massive continental boreal high pressure systems of central and east Asia (Jury *et al*., 1994). This area of sustained convergence is characterized by relatively persistent

convective clusters, a portion of which may intensify and become more symmetrically organized when a favorable thermodynamic environment exists (Gray, 1998).

The position and orientation of the ITCZ varies within and between the seasons, and peaks in convective activity within the ITCZ generally coincide with peaks in TC activity. In October during the monsoon transition, the ITCZ sets up close to the equator (Jury *et al*., 1994). It migrates gradually southwestward to its most poleward configuration at the height of austral summer, and returns quickly to the north during the monsoon transition months of March and April (Jury *et al*., 1994). The orientation of the SIO ITCZ during austral summer is generally southwest to northeast, extending from the Mozambique Channel to Sumatra. The boundary is approximately coincident with the average 28°C SST (sea surface temperature) isotherm and rarely shifts south of 15°S (Figures 2-4 and 2-5) (Liebmann and Smith, 1996; Parker and Jury, 1999; Reynolds *et al*., 2002). This configuration allows for the uplift of the moisture laden boundary layer and subsequent latent heat release through condensation, a principal energy source for TCs.

Jury (1993) offered a synopsis of climatological features that are associated with variability of TC frequency in the SIO. Greater TC activity is likely when easterly wind anomalies at 200 hPa are centered near 15°S, inducing enhanced anticyclonic shear. This suppresses unfavorably strong jet stream westerlies south of 20°S and allows for a moderate background easterly flow from the equator southward to near 10°S. The results are favorable levels of vertical wind shear and divergent flow across the region, which provide a favorable environment of outflow mechanisms for developing TCs

(Merrill, 1988). When upper level troughs intrude to near 15°S, these favorable wind shear and divergent patterns are greatly reduced over the tropical SIO

In the lower troposphere, more TCs occur when both the northern and southern Hadley cells are simultaneously stronger than normal (Jury, 1993). This allows for strong convergence of Indian monsoon outflow and brisk subtropical trade winds in the 10°S-15°S zone, resulting in increased convection, low-level cyclonic vorticity, and upper-level poleward outflow (Love, 1985). Shanko and Camberlin (1998) also observed that when SIO TCs are active the northeasterly Indian monsoon outflow bypasses east Africa and flows across the equator into the SH, leading to reduced onshore flow and resultant drought in Ethiopia. When the Hadley cells are weak, Indian monsoon outflow is deflected west over east Africa bringing seasonal rains while SIO TC activity is reduced. Not surprisingly, positive SST anomalies in the SIO are likewise associated with an increase in TC frequency (Jury *et al*., 1999; Leroy and Wheeler, 2008; Chang-Seng and Jury, 2010a).

The focus of much previous SIO TC research was largely on their frequency and/or regional environmental features that influence their frequency. The basic conditions for formation are not substantially different from other ocean basins, and the basic climatology of the region is now relatively well established. Intraseasonal to interannual scale studies were restricted in the past because the historical TC data of the region are not of high quality. Since the 1970s, this situation has been improving and more recent literature focused on potential relationships between SIO TCs and the most important tropical low-frequency source of ocean-atmosphere variability, ENSO, which itself requires a thorough discussion.

El Niño-Southern Oscillation

Introduction

ENSO is well known as the leading mode of interannual ocean-atmosphere variability in the tropics, with important teleconnections influencing a significant proportion of interannual variability in extratropical regions as well (Trenberth *et al*., 2005). The Southern Oscillation (SO) was so termed by Walker and Bliss during the 1920s to describe the inverse relationship between the relatively high surface pressure readings over the eastern South Pacific Ocean and typically low surface pressure readings near the maritime continent and eastern Indian Ocean (Julian and Chervin, 1978). The El Niño phenomenon was known originally as an annual occurrence of warming sea surface temperatures off the coast of Peru and Ecuador, with onset near or just after the austral summer solstice coincident with a seasonal slacking of southeast trades (Wyrtki, 1975). Subsequently, the term El Niño has become associated with excessive warm anomalies of SST off the west coast of South America and extending westward along the equator to the international dateline, a result of reduced equatorial easterly winds and concomitant Ekman pumping-induced cold upwelling (Trenberth, 1991).

The linkages of these atmospheric and oceanic phenomena were first explained in detail by Bjerknes (1969), who suggested that the equatorial zonal wind circulation (the so-called Walker Circulation) was thermally driven by equatorial SSTs and that variability in these could then affect the strength of the meridional Hadley circulations. Additional important pieces of the ENSO puzzle were discovered in the 1970s. Kidson (1975) quantitatively identified the SO signal in the global pressure and precipitation fields, and Wyrtki (1975) described the reduced sloping of sea level across the

equatorial pacific as a response to weakened southeasterly trades during El Niño. In 1976, Trenberth (1976) suggested the importance of moisture convergence and enhanced convection over the expanding warm pool near the dateline in strengthening the Hadley cell while weakening the Walker cell.

As the basic understanding of the coupled oceanic-atmospheric nature of ENSO evolved, it became apparent that it constitutes an integral part of the global climate system. Namias (1976) noticed low pressure anomalies and a southward dip of the jet stream off the coast of California during El Niño, and both van Loon and Madden (1981) and Horel and Wallace (1981) provided further evidence that ENSO modulates pressure, wind patterns, rainfall, and temperature on a global scale. Philander (1985) first applied the term La Niña to those conditions which are approximately opposite to El Niño, chiefly characterized by strong equatorial easterlies and a tongue of cold SST anomalies extending from the coast of South America westward in the equatorial Pacific Ocean to near the dateline with a warm pool near the maritime continent (Trenberth, 1991). The known oceanic-atmospheric teleconnection links between ENSO and the SIO are discussed in the next section.

ENSO Influences in the South Indian Ocean

A plethora of research exists on the impacts of ENSO on SST and atmospheric circulation variability in the SIO in all seasons. However, because this study is focused on TCs of the SIO, special attention is given here to the influences of ENSO within the SIO during austral warm season from October to April. Particular mention is made of changes in ocean-atmospheric variables known to be important in TC formation and movement.

It is very well established that El Niño (La Niña) is associated with an increase (decrease) of SSTs in the western tropical SIO. During warm ENSO events from October until February, anomalous easterly lower tropospheric winds are present in the tropical eastern SIO west to near 90°E, coincident with raised mean sea level pressures (MSLP) over subtropical eastern SIO and Australia due to the shift of the downward branch of the Walker circulation (Pan and Oort, 1983; Gutzler and Harrison, 1987; Harrison and Larkin, 1998; Reason *et al*., 2000; Larkin and Harrison, 2001; Lau and Nath, 2003; Yoo *et al*., 2006). These easterlies force a downwelling, westward-propagating oceanic Rossby wave, which coupled with equatorial Ekman transport induces warming of SST and deepening of the thermocline in the tropical western SIO (Chambers *et al*., 1999; Klein *et al*., 1999; Xie *et al*., 2002). This warm pool in the western SIO is most often coincident with positive SST anomalies (SSTA) in the equatorial Pacific Ocean near 130°W, which is within the commonly used Niño-3.4 index region (Pan and Oort, 1983; Nicholson, 1997). The positive SSTA in the western SIO would support a greater probability of TC genesis, while the easterlies in the eastern SIO would not favor TCs due to anticyclonic wind curl and cool SSTA.

With a warm pool over the western SIO during ENSO warm events, convection is enhanced and MSLP is lowered (Oort and Yienger, 1996; Reason *et al*., 2000; Trenberth and Caron, 2000; Larkin and Harrison; 2001; Lau and Nath, 2003). Positive zonal wind anomalies are noted in the western tropical and subtropical SIO (van Loon and Rogers, 1981; Meehl, 1987; Karoly, 1989; Reason *et al*., 2000; Yoo *et al*., 2006). These westerlies are a vital feature of El Niño as related to SIO TC trajectories, as they

would likely influence a more easterly movement away from southern Africa and Madagascar.

The proclivity for westerly anomalies over the western SIO during El Niño has been very well researched in relation to southern African rainfall. The tropical-temperate troughs (TTTs) of southern Africa are known to shift northeastward over Madagascar when the SIO subtropical high weakens. This allows mid-latitude upper troughs to intrude equatorward and provide outflow for tropical convection, with cloud bands extending southeastward into the central SIO (Lindesay *et al*., 1986; Mason and Jury, 1997; Cook, 2000; Tyson and Preston-Whyte, 2000; Nicholson, 2003; Pohl *et al*., 2009; Manhique *et al*., 2009). The importance of ENSO and the TTTs for TC trajectories are key components of this paper, and the TTT phenomenon will be discussed again in another section.

Many authors have confirmed that the La Niña spatial pattern is largely characterized by opposite signed anomalies of SST, MSLP, and winds that are present during El Niño (Wolter, 1987; Reason *et al*., 2000; Larkin and Harrison, 2001). Notably, Wolter (1987) found that during La Niña the southeasterly trades are stronger than average in the SIO and the monsoon northeasterlies across the Bay of Bengal and South China Sea are also simultaneously stronger. The stronger northeast monsoons penetrate southward across the equator in the central and eastern SIO and deflect back eastward under Coriolis forcing, increasing lower tropospheric westerlies in the eastern SIO during La Niña from October-February (Hastenrath, 2000; Larkin and Harrison, 2001). The enhanced moisture flux convergence over this region is associated with increased cloudiness and convection (Wolter, 1987). These associations suggest a

broad favorable area for TC activity across the tropical SIO during La Niña, with persistent southeasterly trade winds and a strong subtropical high likely to influence TC movement toward the west. Farther south in the SIO, there are weakened subtropical and mid-latitude westerlies associated with La Niña (Reason *et al*., 2000). Again, this suggests a poleward retreat of the troughs that would potentially influence recurvature in a TC. Using NOAA SST and NCEP reanalysis data, difference maps of SST, SLP, and 500 hPa zonal winds were constructed to illustrate the changes in spatial patterns that accompany El Niño and La Niña in the SIO (See Figures 2-6, 2-7, and 2-8) (Kalnay *et al*., 1996; Reynolds *et al*., 2002). Using the Niño-3.4 region index and based on the definitions of El Niño and La Niña periods as defined by the National Oceanic and Atmospheric Administration (NOAA), El Niño years are 1982-83, 1986-87, 1987-88, 1991-92, 1994-95, 1997-98, 2002-03, 2004-05, and 2006-07. La Niña years are 1984-85, 1988-89, 1995-96, 1998-99, 1999-2000, 2000-01, and 2007-08. This information is available at http://www.cpc.noaa.gov/products/analysis_monitoring/ensostuff/ensoyears.shtml. These ENSO-TC associations have been explored in the peer-reviewed literature and the next section will discuss the findings.

Tropical Cyclones and El Niño-Southern Oscillation

Many volumes and articles are available on the connection between ENSO and TCs, and the relationship therein is particularly well established in the Northern Hemisphere (NH). However, it is of note that where the global ENSO-TC literature has been reviewed, the SIO is often an afterthought, if not completely omitted from consideration (Gray and Sheaffer, 1991; Landsea, 2000; Chu, 2004; Camargo *et al*., 2009). Furthermore, studies that include the SIO in aggregation of hemispheric or

global ENSO and TC signals are difficult to interpret for any one basin. For example, Frank and Young (2007) found global numbers of TCs increase during ENSO, with positive contributions to this increase from all TC regions except the North Atlantic. However, this study haphazardly considered the entire SH as one ocean basin and therefore the results are very difficult to relate to more specific regional findings. Since the focus of this work is the SIO, this section surveys and integrates literature relevant to the ENSO-TC association only in that region.

Having reviewed the larger scale SIO-ENSO relationship in the previous section, this section will present the known links between these ENSO-influenced changes and TCs. There is no basin-wide correlation between ENSO and TC genesis frequency in the SIO, just as in the North and South Pacific regions (Jury, 1993; Revell and Goulter, 1986; Lander, 1994). It is instead the spatial patterns of TC genesis and movement that exhibit links to ENSO. TC genesis is more active over the western SIO during El Niño (Evans and Allan, 1992; Xie *et al*., 2002). Favorable conditions are generated when strong easterlies appear near Sumatra early in the austral warm season, exciting a westward propagating oceanic Rossby wave that couples with off-equatorial Ekman transport to induce an unusually deep warm pool centered near 15°S, 60°E (Jury *et al*., 1999; Reason *et al*., 2000; Xie *et al*., 2002). At the height of austral summer, the TTTs often shift from the African continent to near the vicinity of the warm pool, resulting in an intersection of the South Indian Convergence Zone (SICZ) and the SIO Intertropical Convergence Zone (ITCZ). This combination of favorable thermodynamics and a lifting mechanism leads to more convective activity in the western tropical SIO (Lindesay *et al*., 1986; Mason and Jury, 1997; Cook, 2000; Xie *et al*., 2002; Ho *et al*., 2006;

Manhique *et al*., 2009). During an ENSO warm event, cooler SSTs in the eastern SIO and anticyclonic shear from equatorial lower tropospheric easterlies account for a reduction of TC genesis, particularly in early summer (Ho *et al*., 2006; Camargo *et al*., 2007c; Kuleshov *et al*., 2009). Conversely, during an ENSO cool event the western SIO suffers reduced TC genesis while the eastern SIO experiences more, with positive SST anomalies, mid-tropospheric relative humidity, and increased cyclonic vorticity contributing to the eastern shift in genesis (Wolter, 1987; Camargo *et al*., 2007c; Kuleshov *et al*., 2009).

The tracks of SIO TCs have also been studied, and in terms of track density there is some disagreement in the literature. One group of authors have consistently conveyed their finding of a partition at 85°E with greater (reduced) TC activity in the western (eastern) SIO during El Niño years and the reverse relationship during La Niña (Kuleshov and de Hoedt, 2003; Kuleshov *et al*., 2008). Ho *et al*. (2006) found a similar split with their cut point at 75°E, however Chang-Seng and Jury (2010a) observed in SST compositing that those years of greater TC activity between 50°E-70°E exhibited a La Niña signal in the eastern Pacific. The contrasting results could be attributed to the use of different data sets, different definitions of El Niño/La Niña years, and different intensity thresholds for the definition of a TC. In any case, the fact that varying results have been obtained lends support to the notion that east to west differences in yearly TC activity within the SIO cannot be clearly established based solely on ENSO.

As noted in the previous section, wind anomalies were found to be more westerly to the south of 10°S across the SIO during strong warm ENSO events, especially over the western SIO (van Loon and Rogers, 1981; Meehl, 1987; Karoly, 1989; Cook, 2000;

Reason *et al*., 2000; Xie *et al*., 2002; Yoo *et al*., 2006). Also, the zonal steering flow averaged over 850-200 hPa across the tropical and subtropical SIO was found to be more westerly (easterly) during El Niño (La Niña) (Vitart *et al*., 2003; Ho *et al*., 2006). This was hypothesized to lead to a greater risk of landfall for Mozambique during La Niña, when steering flow is highly zonal (Vitart *et al*., 2003; Reason and Keibel, 2004). Ho *et al*. (2006) suggested from track density maps that westerly steering flows could increase the incidences of recurving TCs just east of Madagascar during El Niño. Similar recurvature trends can be inferred from track density maps in Camargo *et al*. (2007c).

Given the associations already noted above between ENSO phase and the presence of westerly winds near Madagascar, the notable shift of TTTs over the western SIO during warm ENSO events, and the observed tendency for recurving TCs during warm ENSO phases, it is perplexing why no link has been explored between the three. Several very recent studies have used outgoing longwave radiation (OLR) and rainfall anomalies to bolster the long suggested strong links between the location of TTTs and ENSO phase (Fauchereau *et al*., 2009; Pohl *et al*., 2009; Manhique *et al*., 2009). There seems to be a gap in the literature here where the westerly wind anomalies and negative OLR convective anomalies at the source of these maritime based El Niño TTTs could be tested for associations with SIO TCs. It stands to reason that during El Niño TCs may often develop and move southeastward as integral parts of the TTTs, or perhaps TCs tracking through the SIO could interact with the troughs and be shunted south and eastward.

In addition, many authors have noted the insufficiency of ENSO phase aggregated to the seasonal time scale as the sole predictor of convective variability over Africa and extending into the SIO (Waylen and Henworth, 1996; Mason and Jury, 1997; Fauchereau *et al*., 2009; Pohl *et al*., 2009; Manhique *et al*., 2009; Chang-Seng and Jury, 2010a). The work presented in this paper builds on this notion to demonstrate a link between ENSO, TTTs, and TCs in tandem with a regional mode of SIO SST variability. A more integrated understanding of the Pacific teleconnection and the local SST will also allow consideration of these relationships at the sub-seasonal temporal scale, rather than the more typical season-aggregated paradigm. The other important mode of variability for SIO TC trajectories that must be accounted for in tandem with ENSO is the SIOD, which will be discussed in the following section.

Subtropical Indian Ocean Dipole

As demonstrated in the previous section, ENSO is undoubtedly linked to SIO ocean-atmospheric variability, including TC frequency and trajectories. However, a significant portion of this variability cannot be solely attributed to ENSO. There are modes of variability internal to the SIO that must also be taken into account, and these would be expected to interact with the ENSO phenomenon to potentially affect SIO TC tracks. As will be demonstrated in Chapter 4, the most relevant phenomenon in relation to TC trajectories in the SIO is the Subtropical Indian Ocean Dipole (SIOD). This phenomenon has been independently quantified as the second EOF of SIO SSTA at least three times in the literature, though not always identified explicitly as the “SIOD” (Behera *et al*., 2000; Behera and Yamagata, 2001; Huang and Shukla, 2007; Leroy and Wheeler, 2008). It has been implicated as equal in importance with ENSO in understanding warm season rainfall variability in both Africa and Australia (Reason,

2001; England *et al*., 2006). The pattern peaks during austral summer and is characterized in the positive (negative) mode by warm (cool) SST anomalies centered about 25°S-40°S and 55°E-75°E, with cool (warm) anomalies to the west of Australia centered about 18°S-30°S and 85°E-105°E (Behera and Yamagata, 2001; Suzuki *et al*., 2004; Huang and Shukla, 2008). Most importantly, the SIOD pattern has been shown to occur largely independent of ENSO phase (Behera *et al*., 2000; Reason, 2001).

The SIOD is known in positive mode to enhance precipitation over southeastern Africa and southwestern Australia (Behera and Yamagata, 2001; Reason, 2001; England *et al*., 2006). In particular, when the warm pole is shifted west closer to southern Africa the potential for heavy precipitation is further increased, owing to anomalous onshore southeasterlies advecting humid maritime air over the sub-continent (Reason, 2001; Reason, 2002). The mechanism for cooling in the eastern pole is strengthened southeast trades and resultant increased ocean surface evaporation and mixing, while the western warm pole develops concurrently with increased southward Ekman transport of warm SSTs from the tropical SIO combined with decreased northward Ekman transport of cool SSTs from the mid-latitudes (Behera and Yamagata, 2001).

In negative mode, the SIOD is associated with drier conditions over far southeastern Africa, as well as in southwestern Australia. The SSTA poles are generally reversed, with warm anomalies stretching from the eastern subtropical SIO back to the west-northwest toward Madagascar in association with slackened southeasterly trades. The western pole cools south and southeast of Madagascar in conjunction with enhanced latent and sensible heat loss from enhanced westerlies and

the advection of drier, cooler air masses from higher latitudes (Behera and Yamagata, 2001). Reason (2002) noted the strong similarity between the positive SIOD SST and wind anomaly patterns and the atmospheric anomalies associated with tropical-temperature troughs (TTTs). This is important because it raises the possibility of local SSTA influence in the variability of TTTs, which are often attributed to remote forcing mechanisms from ENSO as discussed previously in this chapter.

The potential association between SIO TCs and SIOD has not been explored explicitly. In Leroy and Wheeler (2008), the second EOF of Indo-Pacific region SSTA is used as one of several predictors of TC activity in the western SIO. This pattern is identified by the authors as the tropical Indian Ocean Dipole of Saji *et al*. (1999) and Webster *et al*. (1999), though the visual loadings strongly suggest the SIOD pattern of Behera and Yamagata (2001) and later Suzuki *et al*. (2004). Thus, there is precedence, albeit inadvertent, for a significant association between SIO TCs and SIOD. As discussed earlier in the chapter, it stands to reason that an eastward shift of TTTs over the western SIO could in theory influence TCs to take a poleward or even eastward turn. Therefore, if SIOD is also associated with the occurrence of TTTs, and if the SIOD occurs largely independent of ENSO (Fauchereau *et al*., 2003; Washington and Preston, 2006), then an interactive consideration of ENSO and SIOD is necessary to associate one or both with the variability in TTTs and/or in SIO TC trajectories. A more detailed discussion of the literature on TTTs follows in the next section.

Tropical-Temperate Troughs

While it is well known that recurving TCs often are steered by and interact with atmospheric troughs, the synoptic patterns of the trough-TC relationship as potentially altered by ENSO and/or SIOD have not been fully explored in the SIO. The present

study is aimed at this gap in the literature, and TTTs are implicated as an important steering mechanism for SIO TCs. In this section, a summary is provided of the extant literature on TTTs.

Lower tropospheric convergence zones, characterized by positively tilted poleward moisture plumes or cloud bands, were an early discovery after the advent of weather satellite remote sensing in the 1960s. Streten (1973) noted the existence of these diagonal cloud bands in each of the SH oceans, located equatorward and to the west of the semi-permanent subtropical highs. This region of enhanced convection is sometimes referred to as the South Indian Convergence Zone (SICZ), and is only prominent during austral summer (Cook, 2000; Todd *et al*., 2004). Over southern Africa and into the western SIO, these are referred to as tropical-extratropical cloud bands or tropical-temperate troughs (TTTs). They have been very well known for many years as the principal source of summer precipitation over southern Africa (Harangozo and Harrison, 1983; Lindesay *et al*., 1986; Mason and Jury, 1997).

Their structure over the African continent is in the coupling of a thermally induced tropical low often located over southeast Angola or southwest Zambia near 20°S with an upper level westerly transient wave passing south of Africa (Harangozo and Harrison, 1983; Lyons, 1991; Mason and Jury, 1997; Todd and Washington, 1998). TTTs do not always reside over Africa, but sometimes shift north and eastward over Madagascar and into the SIO (Mason and Jury, 1997; Washington and Todd, 1999). TTTs represent important extrusions of heat and moisture into the upper troposphere which are then redistributed into the higher latitudes (Todd *et al*., 2004).

The relevance of TTTs to SIO TC trajectories has been mentioned here in earlier sections. The longitudinal placement of TTTs has been linked to phases of ENSO, with the warm phase representing a shift of sustained convection over the western SIO (Lindesay *et al*., 1986; Mason and Jury, 1997; Cook, 2000; Tyson and Preston-Whyte, 2000; Nicholson, 2003; Fauchereau *et al*., 2009; Pohl *et al*., 2009; Manhique *et al*., 2009). Similar eastward shifts have been observed during negative SIOD events (Reason, 2002; Pohl *et al*., 2009). These studies demonstrated anomalous westerlies over Madagascar and into the tropical/subtropical SIO in accompaniment of the eastward-displaced TTTs. Previous studies of TCs suggested a possible link between recurving SIO TCs and El Niño, and between westward moving TCs and La Niña (Jury *et al*., 1999; Xie *et al*., 2002; Vitart *et al*., 2003). The longitudinal shifting of the TTTs, in conjunction with the vacillation of the SIO trade winds, are likely related to monthly or perhaps even seasonal trends in the directional motion of TCs through the control mechanisms of ENSO and/or SIOD.

Conclusion

This literature review has surveyed the SIO TC literature and discussed two of the most important known sources of intraseasonal to interannual variability in the tropical and subtropical SIO: ENSO and SIOD. ENSO is known to exert a strong influence on oceanic-atmospheric variables that are linked to SIO TC frequency and trajectories. However important ENSO's role may be in the variability of either TTT or TCs, it is not sufficient alone to explain changes in convection and the associated wind patterns that steer TCs. The SIOD has been shown to exert influence on convective patterns in the absence or in opposition to the influence of ENSO. There has not been a comprehensive study of potential associations between SIOD and SIO TC activity. The

only known possible link in the literature between the two was in Leroy and Wheeler (2008), wherein the second EOF of Indo-Pacific SSTs displayed an SIOD pattern but was not clearly identified as such by the authors. Additionally, the southern African TTTs and the so-called SICZ (which are both linked to ENSO and SIOD) have not been linked with variability of TC trajectories, though their coincident seasonal natures, geographic locations, and atmospheric structures strongly suggest a meaningful association.

The rest of this study explores the identified gaps in the literature of the relationships between SIO TC trajectories, ENSO, and SIOD. The presence/absence of TTTs and associated weakness/strength of the SIO trade winds and subtropical high are proposed as key mechanisms in these relationships. In the next chapter, cluster analysis will be utilized to classify SIO TC tracks according to their genesis and final locations in order to test whether patterns of local (SIOD) and/or remote (ENSO) SSTA associate with the different types of TC tracks.

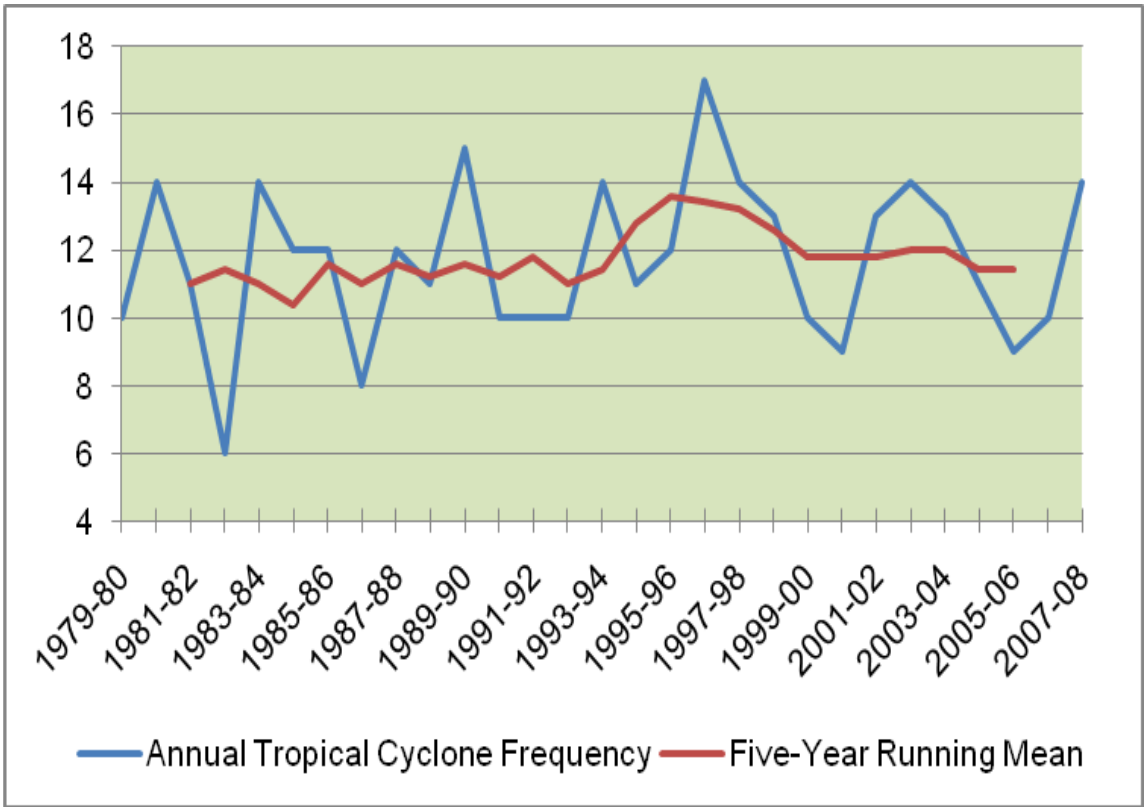

Figure 2-1. Annual frequencies of South Indian Ocean tropical cyclones in blue. Five year running mean in red. Period of record is 1979-80 to 2007-08 during which a total of 339 storms occurred.

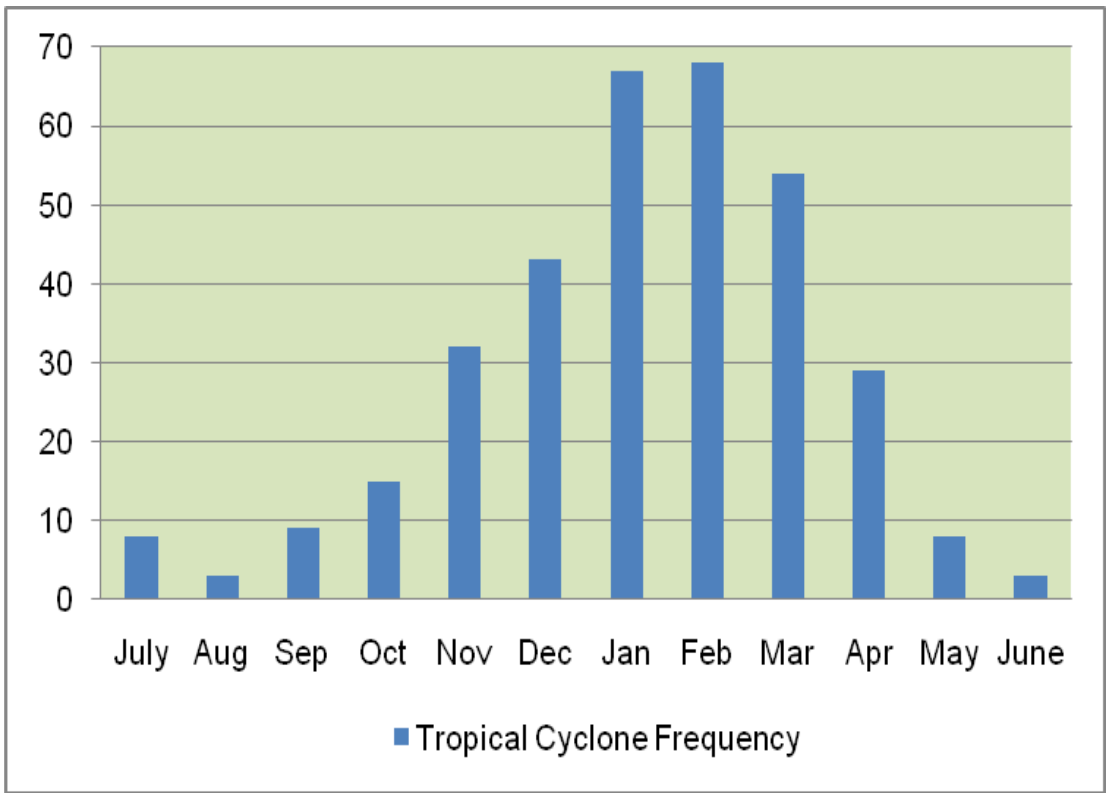

Figure 2-2. Monthly frequencies of South Indian Ocean tropical cyclones. Period of record is 1979-80 to 2007-08 during which a total of 339 storms occurred.

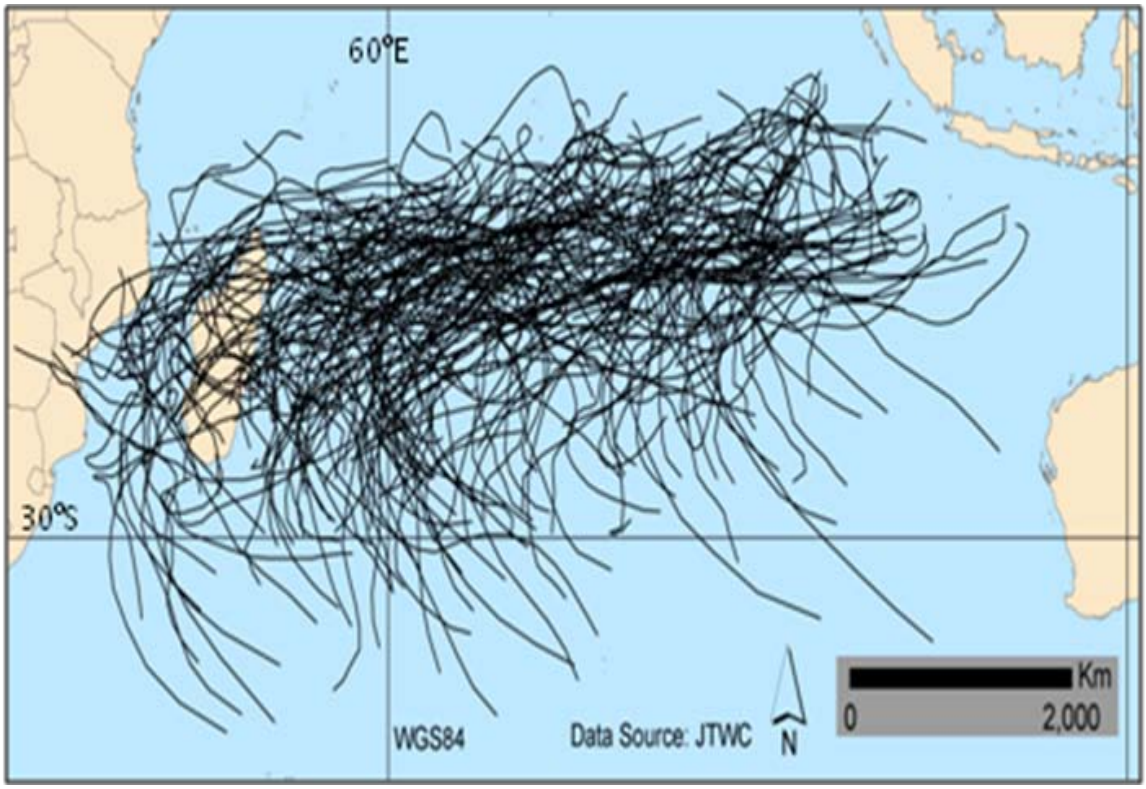

Figure 2-3. South Indian Ocean Tropical Cyclone Trajectories. Trajectory map of the tropical cyclones included in this study.

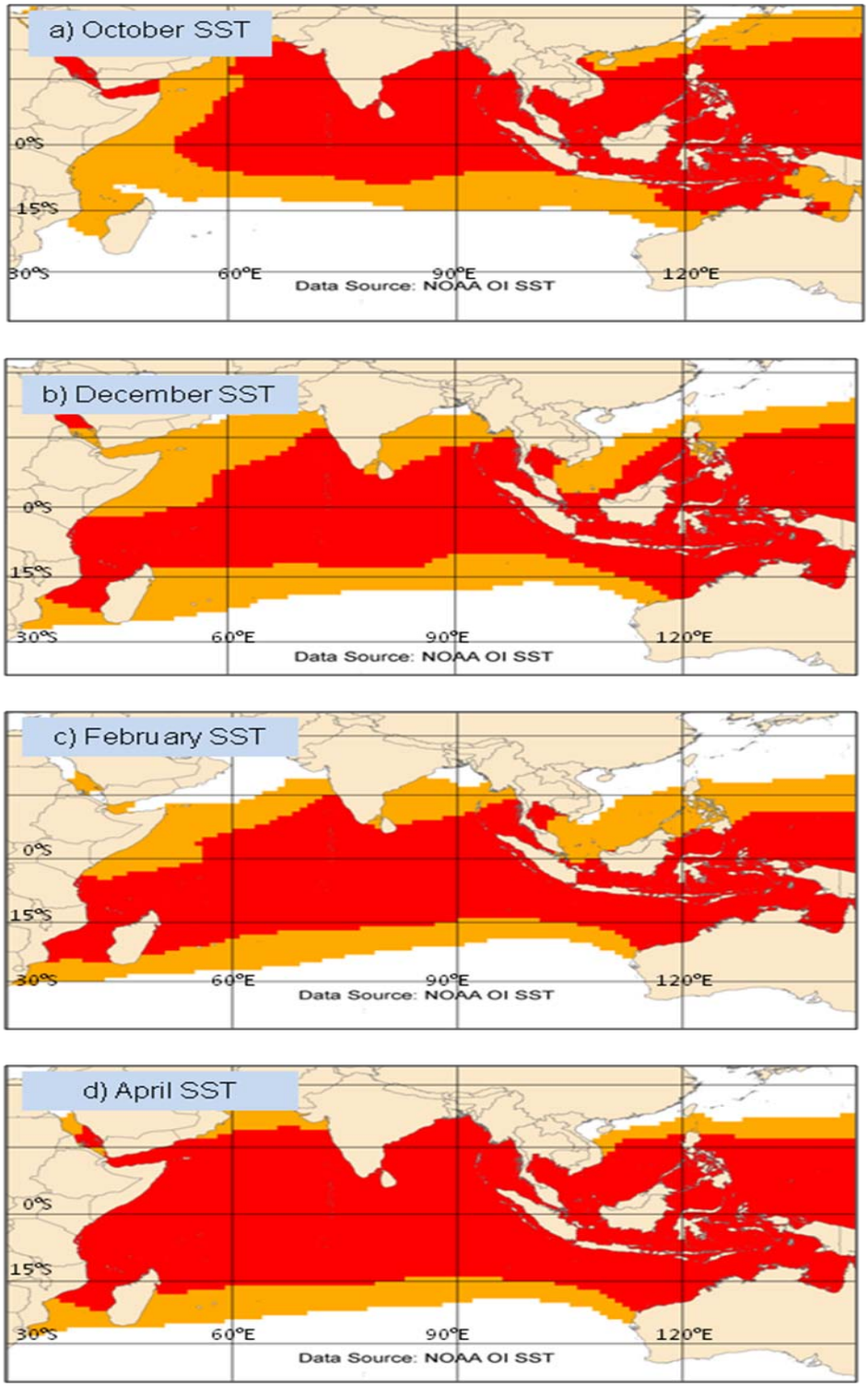

Figure 2-4. Indian Ocean Sea Surface Temperatures, averaged from 1979-2008. From top, October, December, February, April. Orange shading represents SSTs greater than 26°C and red shading represents SSTs greater than 28°C.

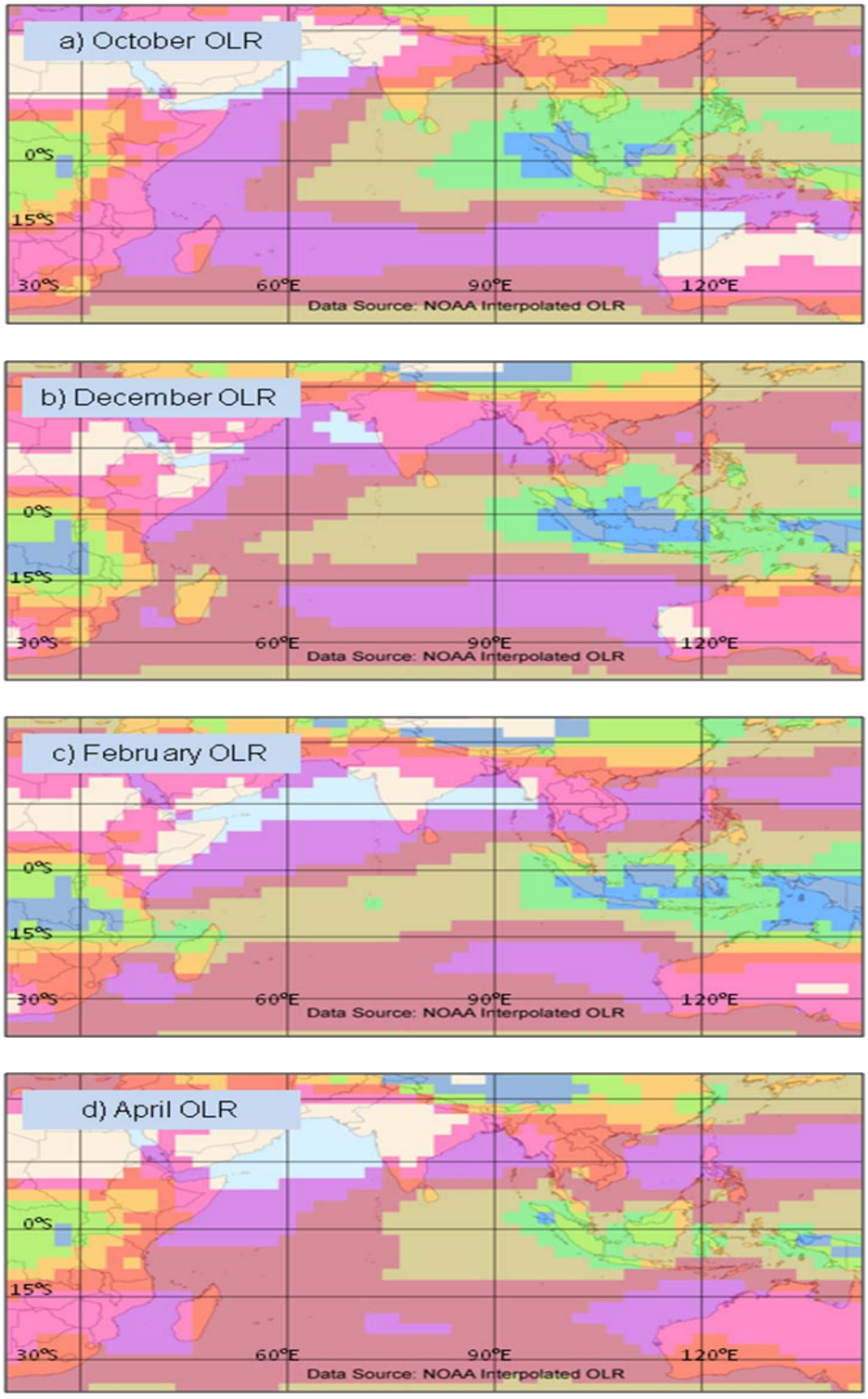

Figure 2-5. Indian Ocean Outgoing Longwave Radiation, averaged from 1979-2008. From top, October, December, February, April. Color Key: Blue 180-200 W m^{-2}, Green 200-220 W m^{-2}, Orange 220-240 W m^{-2}, Red 240-260 W m^{-2}, Pink 260-280 W m^{-2}, Clear >280 W m^{-2}.

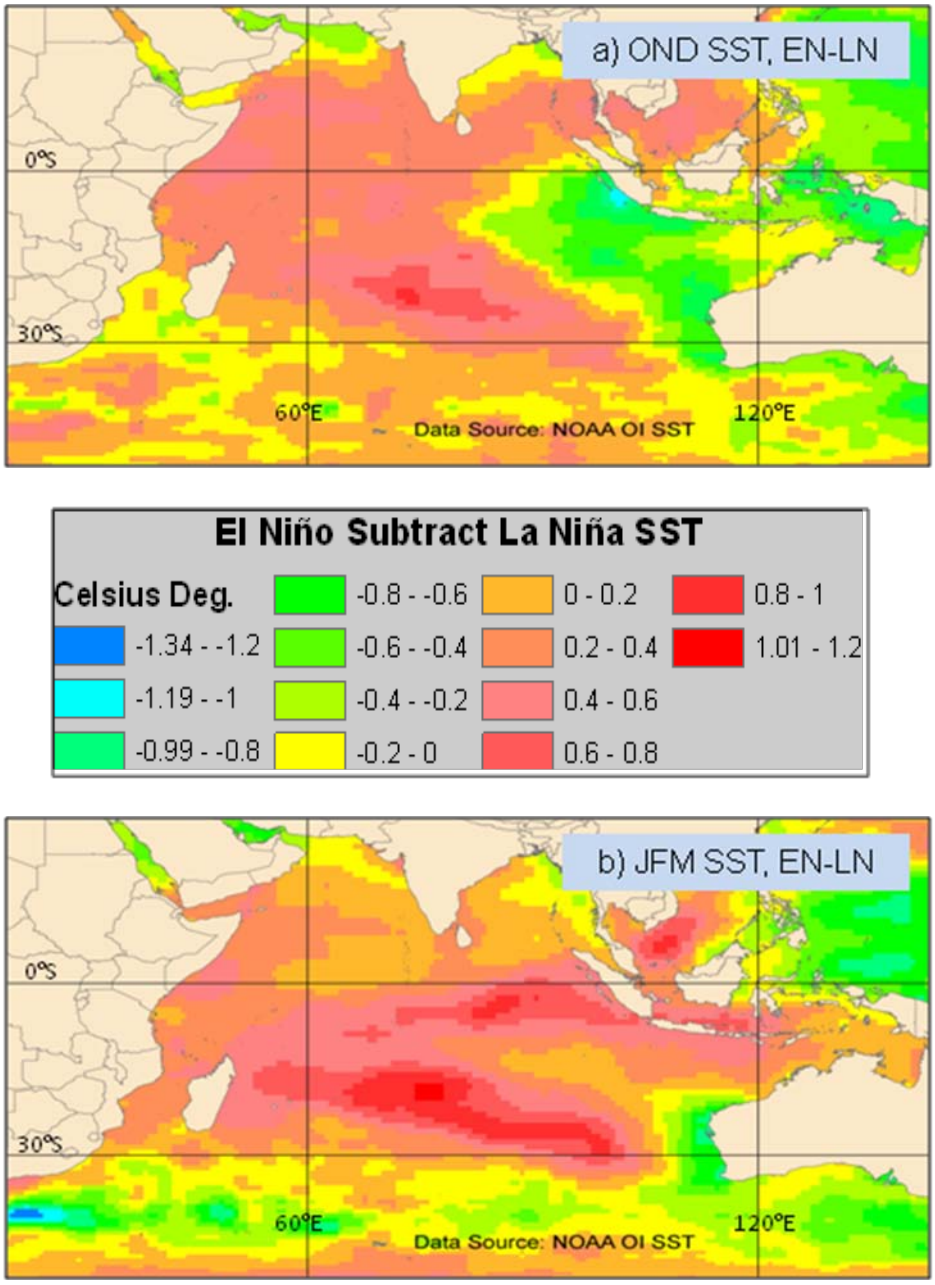

Figure 2-6. Difference of El Niño and La Niña SST patterns in the SIO.

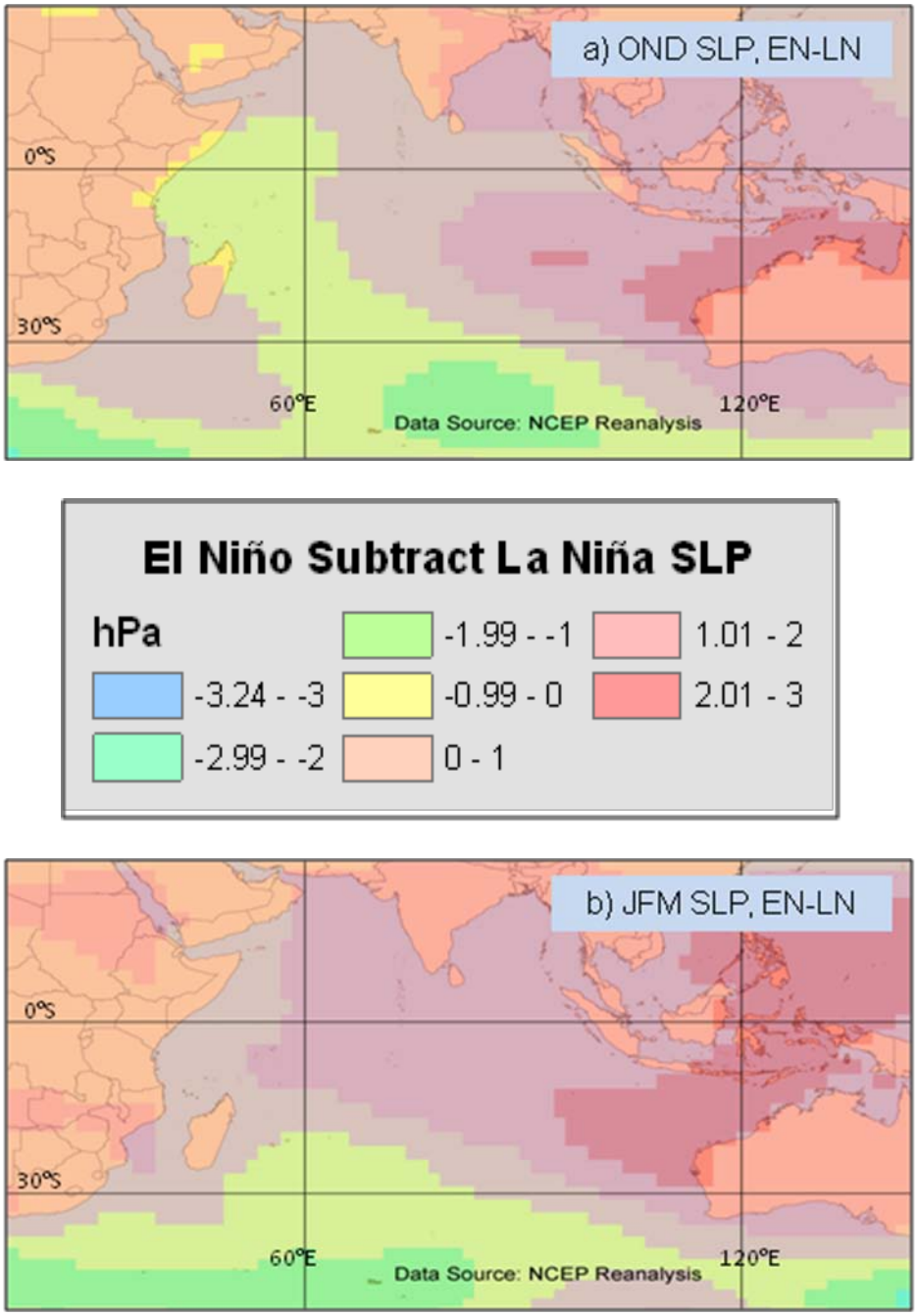

Figure 2-7. Difference of El Niño and La Niña SLP patterns in the SIO.

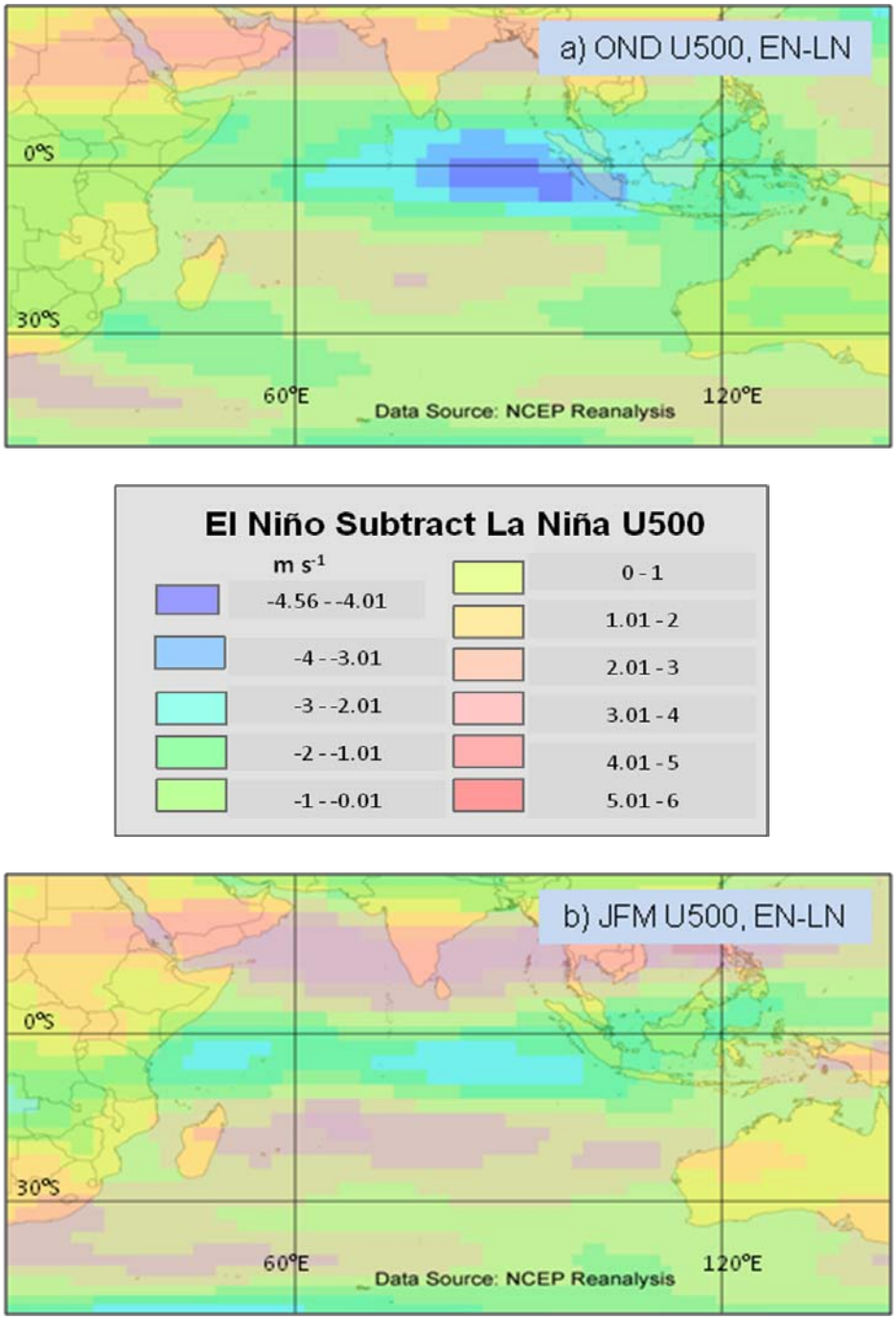

Figure 2-8. Difference of El Niño and La Niña 500 hPa zonal wind patterns in the SIO.

CHAPTER 3
A CLUSTER ANALYSIS OF SOUTH INDIAN OCEAN TROPICAL CYCLONE TRAJECTORIES

Introduction

The literature review in the previous chapter demonstrated that very little research has considered the potential relationship between the Subtropical Indian Ocean Dipole (SIOD) and South Indian Ocean (SIO) tropical cyclones (TCs). Other potential interactions between El Niño-Southern Oscillation (ENSO), SIOD, tropical-temperate troughs (TTTs), and TC trajectories have likewise not been explored. Copious volumes have been written on many of these topics with reference to African or Australian rainfall, and it seems much of that research could be extended and applied with respect to TCs.

As noted previously, tropical cyclones are not scarce in the SIO, but occur in similar abundance to hurricanes of the North Atlantic. Unfortunately, the difficulty in conducting ocean-atmosphere research in the Southern Hemisphere (SH) is that reliable observations are few and far between. However, remote sensing technology began filling in the vast SH observational voids during the 1960s and particularly since the late 1970s. It is now accepted in the scientific community that sufficient satellite-derived measurements and estimates of ocean-atmosphere phenomena in the SH exist beginning from about 1979-1980 (Uppala *et al*., 2006; Knaff and Sampson, 2009).

Given thirty years of consistent SH data, opportunity exists to attempt more comprehensive explanation of the links between SIO TCs, the synoptic scale ocean-atmospheric patterns in which their life cycles are embedded and larger scale sources of regional and global importance such as SIOD and ENSO. The balance of the work presented here is devoted to filling in the gaps in the literature on the links between

SIO-TC trajectories, ENSO, and SIOD. The approach described herein is to first reduce dimensionality of the TC data by classification of the storms into a manageable yet meaningful structure by way of cluster analysis. This is intended to facilitate statistical analyses of the TCs and interpretation of the findings in relation to known physical mechanisms governing their directions of motion guided by ENSO and/or SIOD-influenced synoptic patterns. In Chapter 4, analysis of variance (ANOVA) will be applied to the clusters to compare the median values of ENSO and SIOD indices. Global composite maps of sea surface temperature anomalies (SSTA) will also be constructed to complement the statistical results.

Tropical Cyclone Data and Study Area Definition

The Joint Typhoon Warning Center (JTWC) best-track dataset for the SH provided the latitude/longitude fixes of SIO TCs at six hour intervals, which are deemed reliable and suitable for scientific and statistical research from about 1980 onward (Knaff and Sampson, 2009). A subsequent desirable effect of using the recent thirty year period from 1979-2008 is to research principally the teleconnections operating after the known Pacific Ocean climate shift of 1976-77, as it has been shown that spatial patterns of ENSO-SIOD interaction differ on multi-decadal time scales (Trenberth, 1990; Zinke *et al*., 2004). Yet, permanent geostationary weather satellite coverage over the entire SIO was not realized until May 1998 (Caroff, 2009; Chang-Seng and Jury, 2010a). This means that estimates of TC intensity may not be reliable prior to 1998, and that weak and/or short-lived TCs may not be accurately accounted-for during this period. Thus, only SIO TCs which attained a maximum lifetime intensity of at least 30 m s^{-1} (or 60 knots maximum 1-minute sustained wind) are included in the analysis.

The decision to include only relatively well-organized TCs is intended to alleviate concerns about TC fix data quality, which are most error-prone in analyses of weaker, less organized tropical systems (Yip *et al*., 2006). For each of the 191 TCs in this study, all fixes provided in the JTWC best-track data are utilized, regardless of the estimated intensity. This means that a portion of the fixes near each storm's beginning and end points likely include position estimates made when the systems were not yet well developed, or near the end of their life cycle when they were undergoing extratropical transition. The inclusion of all fixes is justified in order to construct a meaningful classification of TC trajectory types over their full life cycles from cyclogenesis to cyclolysis. Weak TCs do not typically exhibit a well-defined, axisymmetric vertical vortex structure, thus their movements in relation to the larger background steering flow can be quite aberrant. As this study is primarily concerned with TCs whose movement behaves more or less in concert with the mean steering flow, the decision not to consider weak storms is upheld.

The spatial extent of the study region is restricted according to the eastern most boundary of the regional SIO TC forecasting agency. Official TC forecast responsibilities and data archives for the World Meteorological Organization (WMO) are assigned to the La Réunion Regional Specialized Meteorological Center (RSMC) for the Indian Ocean south of the equator and eastward from the African continent to 90°E (Caroff, 2009). East of 90°E in the SIO, the responsibility is assigned to WMO RSMC Perth in Western Australia. The intended region of study here is the western SIO including southern Africa, Madagascar, and the Mascarene archipelago, but not the Australia region. Thus, the artificial 90°E boundary is applied here to further truncate

the number of storms in the analysis, leaving out all TCs which formed in the SIO east of 90°E and never crossed that meridian into RMSC La Réunion's area of responsibility.

Finally, a brief comment is necessary regarding the use of JTWC TC data here instead of WMO La Réunion TC data. The latter dataset does not contain complete records of TCs that began well east of 90°E and later crossed the boundary on a westerly tack. A WMO SH TC best-track archive was recently assembled which incorporated La Réunion and Perth data and eliminated the anthropogenic boundary effect; however, these data are not available to this author (Kuleshov *et al*., 2008). Ho *et al*. (2006) addressed dataset concerns by performing the same analysis on both the JTWC and La Réunion datasets, with spatially and temporally consistent results. Thus, the JTWC data are utilized here without further deliberation. A total of 191 SIO TCs are included in the cluster analysis (See Appendix).

Cluster Analysis in Tropical Cyclone Research

Cluster analysis (CA) is a widely known quantitative classification and data exploration method that has been frequently employed in geophysical research over the last fifty years (Gong and Richman, 1995). The most common use of CA is as an exploratory tool to reduce highly heterogeneous data sets to a few manageable and internally similar groups such that variability is maximized between groups while simultaneously minimized within groups (Lattin *et al*., 2003). In CA, there is no foreknowledge of an optimum number of clusters in the data, such that the final cluster solution may result in a number of groups that does not necessarily reflect the natural modality of the data. A well structured clustering solution, whether it reveals the optimum natural modality of the data or not, can aid a researcher to understand

mechanisms which shape differences and similarities of places, events, or phenomena (Wilks, 2006).

Classification schemes, both subjective and objective, have been applied to both extratropical and tropical cyclone trajectories. Many have successfully employed CA to sift through the complex and chaotic nature of these transient entities and group observations into recognizable and interpretable archetypes (for examples see Wolter, 1987; Blender *et al*., 1997; Trigo *et al*., 1999; Gaffney *et al*., 2007; Manhique *et al*., 2009). Of special interest here are those which have classified TCs based on their trajectories. These types of analyses have been performed for TC trajectories in the western North Pacific (WNP), North Atlantic, and eastern North Pacific. Harr and Elsberry (1991) qualitatively identified straight moving, recurving-north, and recurving-south TCs in the western North Pacific (WNP). In the same basin, Elsner and Liu (2003) used four geographic variables in a *k*-means clustering algorithm and identified three types of TC paths: recurving, north oriented, and straight moving. Camargo *et al*. (2007a) employed a regression mixture model to further categorize WNP TCs into seven clusters, taking into account geographic location as well as forward speed and the actual shape of each TC's entire trajectory. Most recently, Choi *et al*. (2009) used a fuzzy clustering approach to identify four different types of TC trajectories that make landfall on the Korean peninsula.

In the North Atlantic, Elsner (2003) also employed *k*-means clustering to identify three types of hurricane tracks, two of which often make landfall in the United States. Camargo *et al*. (2008) built upon the regression mixture model clustering from their WNP study and found three clusters of TC trajectories in the eastern North Pacific. In

each of the TC clustering studies listed above, the respective clusters were used to draw conclusions about each trajectory type's potential for landfall, their seasonality, and relationships to prominent low-frequency sources of atmospheric variability such as ENSO. Following from these analyses in other oceans, the goal here is to use CA to complete the first known classification of TC trajectories in the SIO. The categorization scheme is subsequently used to identify which trajectory types associate closely with ENSO and SIOD.

The Clustering Procedure

The clustering algorithm implemented in this study is a two-stage agglomerative hierarchical approach using a Euclidean distance measure and the group average linkage method. Stage one delineates TC genesis regions within the SIO while stage two examines the direction of storm motion for TCs within each genesis region. Agglomerative hierarchical clustering begins with each observation as its own group and then iteratively joins the two closest groups until there is one group that includes every observation (Lattin *et al*., 2003). The criteria for determining the closest proximity group is the average Euclidean distance between all available pairs in any two groups being compared (Wilks, 2006). The statistical software package NCSS is utilized to complete the clustering procedures.

The variable utilized to perform the initial clustering procedure is based upon previous research demonstrating that El Niño (La Niña) is associated with more TCs forming west (east) of about 75°E to 85°E (Ho *et al*., 2006; Camargo *et al*., 2007c; Kuleshov *et al*., 2009). This is theoretically justified in that a favorable pool of anomalously warm SSTs and deeper than normal thermocline are present in the western SIO during strong ENSO warm events (Xie *et al*., 2002; Camargo *et al*., 2007c),

along with unfavorable negative SST anomalies, stronger lower tropospheric easterlies, and elevated mean sea level pressure (MSLP) in the eastern SIO (Pan and Oort, 1983; Reason *et al*., 2000; Larkin and Harrison, 2001). It follows then that a zonal stratification in the initial longitude points echoes the established regional physical characteristics of ENSO in relation to TC genesis. Thus, the longitudes of the initial center fixes for each TC are clustered in the first stage of the analysis.

In hierarchical CA, one diagnostic of the strength of a clustering structure is the cophenetic correlation, which is related to the dendrogram. A dendrogram is a tree diagram that illustrates the hierarchy of linkages carried out by the clustering algorithm (Wilks, 2006). Cophenetic correlation indicates how well the visual structure and dissimilarity index of a dendrogram reflects the clustering structures and dissimilarity measures in the actual data matrix (Romesburg, 1984). If the cophenetic correlation is near 0.8 or greater, the clustering structures as depicted in the dendrogram are more likely to reflect real clusters in the data. If the cophenetic correlation is significantly less than 0.8, the clustering structures as visualized in the dendrogram are more likely exaggerations of reality and the results of the CA are not suitable for further analysis (Romesburg, 1984). The cophenetic correlation corresponding to the dendrogram for the first stage of the CA is 0.77, which indicates that visual inspection of the dendrogram should allow for discernment of an appropriate number of clusters (Figure 3-1).

It is important here to discuss the reasoning behind the chosen number of clusters. One subjective method for choosing the number of clusters is by visually identifying a cut line in the tree diagram where the average dissimilarity between the groups jumps

considerably between grouping iterations (Wilks, 2006). In Figure 3-1 this jump occurs at approximately 8-10 on the dissimilarity index, with groups 2-5 all agglomerating near this point. Therefore, the cut line is placed such that there are five clusters. Group 1 is small and clearly different from all other groups. Group 2 is likewise separated from groups 3-5.

With five clusters tentatively identified, these are then mapped using ArcGIS to visualize the geographic pattern (Figure 3-2). The map of the five cluster solution helps to justify the choice of that number. In CA there is not always a clear optimum number of groups, especially with larger data sets, and the number of clusters extracted is often partly a function of the researcher's goal for the analysis (Wilks, 2006). Since this study seeks to identify potential links between ENSO, SIOD, and TC trajectories, it makes sense to incorporate previously accepted knowledge on the effects of ENSO in the SIO TC genesis regions. Such incorporation is accomplished with the five cluster solution.

Three of the five groups contain approximately 89% of the TCs and cover the region within which ENSO influences on genesis are thought to be the strongest. Group 3 roughly coincides with the region in the western SIO where TC genesis is more likely during a warm ENSO event, while group 5 coincides with the region in the eastern SIO where genesis is more likely during a cool ENSO event (Ho *et al*., 2006; Camargo *et al*., 2007c; Kuleshov *et al*., 2009). Recall that Ho *et al*. (2006) placed the boundary separating these regions at about 75°E, but Kuleshov *et al*. (2008) found the boundary to be 85°E. Therefore, group 4 is the transition region where the see-saw influences of ENSO phases on TC genesis are not well defined. The other 11% of observations from the remaining two groups are located at the far western and eastern bounds of the

study region. Very little has been published about ENSO and TCs forming in the Mozambique Channel, thus group 2 coincides with a region where the ENSO influence on TCs may be subsidiary to other influences. Finally, group 1 is clearly exceptional, including four TCs with unusually long distance tracks.

One of the principal goals of this study is to investigate the directions of the TC trajectories in relation to ENSO and SIOD. ENSO is generally thought to influence more westerly tracks during a strong cold phase and more easterly tracks during a strong warm phase (Vitart *et al*., 2003). It is also hypothesized that a strong positive SIOD (with anomalously strong trade winds) should influence more westerly tracks, while a strong negative SIOD (weaker trades and eastward shift of TTTs) should influence more easterly tracks (Behera and Yamagata, 2001; Reason, 2002). Thus, a second stage of clustering is undertaken to differentiate the cases where storms that form in a similar geographic location follow very different tracks. Only the three large clusters across the main development regions of the tropical western and central SIO are utilized for this second CA as Group 1 is too small, and TCs within Group 2 were close to land.

This second CA is performed for each group separately so that the TCs within groups 3, 4, and 5 are clustered by the latitude and longitude of their final positions (Figures 3-3, 3-4, and 3-5). The importance of this second round of clustering is to mete out storms that move mostly westward and threaten land from those that track more eastward and remain at sea. The same agglomerative hierarchical method is implemented for the second CA as was described for the first, with a Euclidean distance measure and group average linkage. A total of seven clusters will be discussed in the rest of the study: two motion-based clusters derived from each of the original groups 3,

4, and 5, and one from the original cluster 2. The seven clusters are ranked by their size and then designated simply as C1 through C7 (Table 3-1).

Discussion

The clustering procedure yields three large groups in the three main genesis regions of the SIO (western, central, and eastern) that generally move west or southwest. 60% of the TCs in the study are contained within one of these three groups, confirming that a majority of TCs in the SIO move with a southwesterly component. This is not surprising given that average background conditions absent an ENSO or SIOD influence would allow for such a motion generally around the northwest fringes of the subtropical high. Secondary groups are also found for each of the three main genesis regions, which are likely candidates for association with departures from the average flow regime, such as happen with opposing phases of ENSO or SIOD. Approximately 27% of the TCs examined belong to one of these groups. Seven of the eight clusters are described below to complete this chapter.

Eastern Formation Region: C1 and C6

The largest group overall is C1 with 40 TCs. These form in the eastern SIO east of 90°E and track to the west and southwest before weakening or recurving south and eastward in the area south of 15°S and east of 75°E (Figure 3-6). The peak months of formation for these TCs are February-April with a secondary peak in November, and this type of SIO TC rarely passes within 200 kilometers (km) of populated land masses. Although also forming in the eastern SIO, group C6 has 16 TCs and is distinguished from C1 by longer distance tracks with more westward trajectories, with a few in this group crossing west of 60°E and passing within at least 200 km of land (Figure 3-7).

These unique storms occur most frequently during the SIO peak months of January-March.

Central Formation Region: C2 and C7

Occurring most often during January-March with a secondary peak in November, C2 is also a common type with 39 TCs in the group. These TCs develop in the central genesis area between 75°E and 85°E and track westward or southwestward with a concentration of final points south of 20°S between 50°E and 75°E (Figure 3-8). A second concentration of final points exists near northern Madagascar and within the Mozambique Channel. During the period 1979-2008, 16 of the 39 TCs either made landfall or passed within 200 km Madagascar, Mozambique, or the Mascarene Islands. C7 also forms in the central genesis region and is far less common with only 14 TCs. These storms occur in most every month during the austral summer but show a unique tendency to occur more in October when TCs in other parts of the basin are rare. They track generally southward and southeastward, ending south of 15°S and east of 80°E, and do not threaten any populated regions of the SIO (Figure 3-9).

Western Formation Region: C3 and C4

In the western genesis area, 39 TCs comprise C3; this group has the highest frequency of making landfall or passing close by with 33 out of the 39 impacting Madagascar, Mozambique, or the Mascarene Islands. These TCs occur very frequently from December to March, with very few forming during the transition months of November or April. C3 TCs form in an arc from between 6°S and 12°S and 60°E to 70°E bending south and west to between 10°S and 18°S and 55°E and 60°E (Figure 3-10). C3 final points are heavily concentrated around Madagascar, probably in large part because of deleterious interactions between the TC vortex and the mountainous

Malagasy terrain which exceeds 2500 meters at its heights. A second concentration of TC final positions are found south of the Mascarene Islands between 27°S-33°S and 50°E-60°E. C4, the counterpart to C3 in the western genesis area, shows a tendency to develop near 12°S between 60°E-72°E in Jan.-Feb (Figure 3-11). Movement is southward and southeastward and C4 TCs seldom pass within 200 km of the principal populated islands of the Mascarene archipelago. Trajectory end points are generally south of 20°S and east of 63°E. These two groups represent the greatest opportunity to apply knowledge of the effects of ENSO and SIOD on TC tracks. If the likelihood of C3 versus C4 TC trajectory types could be predicted one month or three months in advance with some confidence, this could be invaluable information for disaster planning purposes in the inhabited regions of the western SIO.

Far West/Mozambique Channel: C5

The last group is located at the far western edge of the SIO (Figure 3-12). 17 TCs in C5 formed near Madagascar or in the Mozambique Channel. Given their close proximity to land at genesis, it is not surprising that they impact populated regions at a high rate with 14 of 17 tracking within 200 km of one of the major inhabited places in the region. TCs in this group that form north of about 12°S exhibit a southwestward and then southward movement, but the remainder of the TCs in the group move mostly to the south and east, which is known to be the common trajectory for TCs with genesis in the Mozambique Channel (Reason, 2007). These occur mainly at the height of austral summer in Jan.-Feb.

Conclusion

In this chapter, a two stage hierarchical CA of TC initial longitudes and final latitudes and longitudes was used to identify eight types of TC trajectories in the SIO.

Similar research methods have been utilized in the literature in other active TC basins, but such a classification for the SIO is not found in the peer-reviewed literature. The results in the first stage corresponded well to the known geographic patterns of TC genesis in relation to ENSO. The second stage of CA parsed out three additional groups by splitting the main genesis region clusters based on the geographic locations of their final positions.

The overarching goal of this study is primarily to investigate the influences of ENSO and SIOD on TC trajectories in the SIO. The cluster solution presented above fits in with changes in the geographic distribution of a favorable environment for TC genesis associated with ENSO. This provides confidence that the clustering solution reflects at least a portion of the underlying physical mechanisms behind the variability of TC genesis and trajectories in the region. Therefore, in the next chapter the groups described above are used as a basis for further inquiry into ENSO and SIOD as sources of TC trajectory variability in the SIO. The method for testing these associations will be to compare the seven groups via ANOVA between median values of ENSO and SIOD indices. Composite maps for each group will also allow for qualitative identification of SSTA anomalies in key regions of the subtropical SIO and the tropical Pacific.

Table 3-1. Eight cluster solution for South Indian Ocean tropical cyclones, ranked by the number of TCs in each group. The group average initial and final longitudes final latitude are displayed in decimal degrees east and south. Movement direction is a generalization to dichotomize the TCs from common genesis regions (western, central, eastern SIO, and Mozambique Channel). The number of TC passing within 200 kilometers of land is given in the far right column.

Cluster Designation	Number of TCs	Initial Longitude	Genesis Region	Final Latitude	Final Longitude	Movement Direction	Close Pass
C1	40	95.60	Eastern	24.73	83.33	Southwest	2
C2	39	78.83	Central	23.76	56.65	Southwest	16
C3	39	62.98	Western	26.95	49.89	Southwest	33
C4	22	65.38	Western	26.55	69.32	Southeast	3
C5	17	44.85	Channel	27.06	48.61	Southeast	14
C6	16	99.01	Eastern	20.20	55.51	West	7
C7	14	81.91	Central	20.89	86.59	Southeast	0
Sum/Average	187	75.51		24.31	64.27		75

Table 3-2. Frequency of TC genesis by month for C1-C7.

Clusters	Sept.	Oct.	Nov.	Dec.	Jan.	Feb.	Mar.	Apr.	May
C1	0	1	6	4	4	6	11	7	1
C2	0	0	7	3	11	8	5	4	1
C3	0	0	0	9	13	7	7	1	2
C4	0	0	1	3	7	6	3	2	0
C5	0	0	0	0	5	8	3	1	0
C6	0	1	2	1	4	3	5	0	0
C7	1	3	1	0	2	2	2	2	1

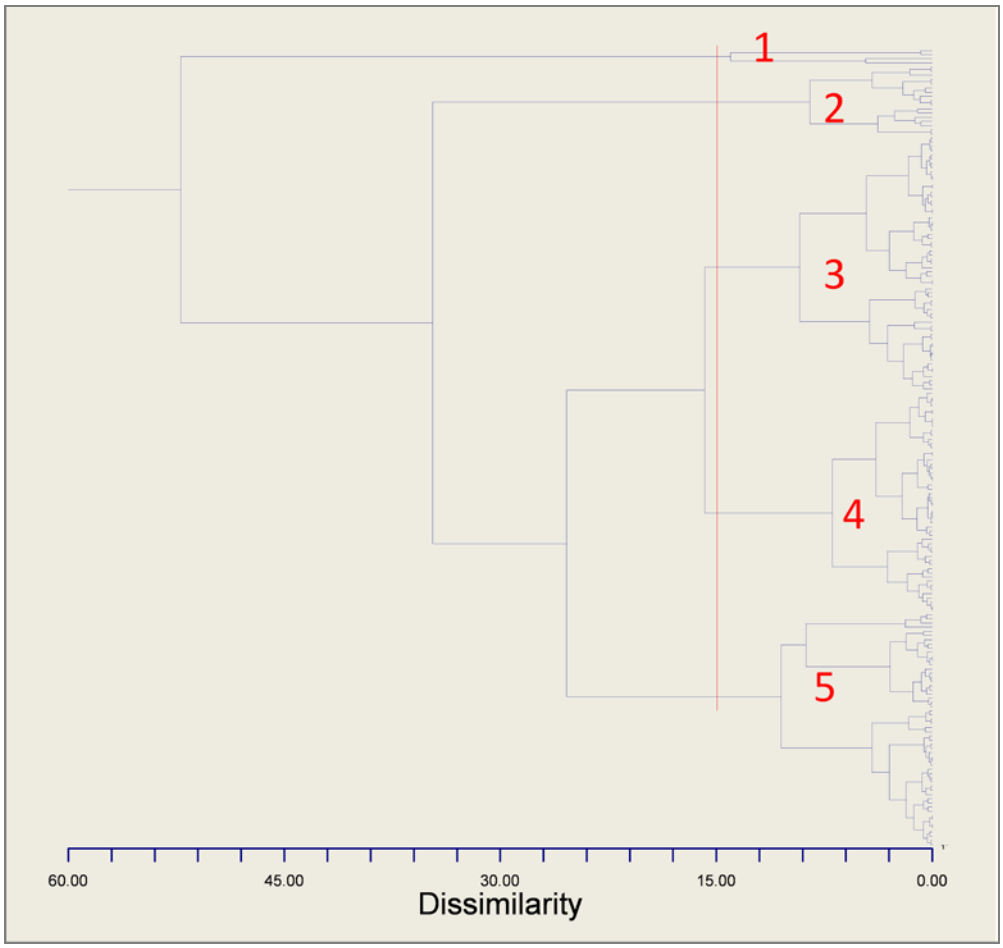

Figure 3-1. Dendrogram of South Indian Ocean tropical cyclones when clustered by their initial longitude. The vertical red line indicates the cut point for a five cluster solution. The cophenetic correlation is 0.77.

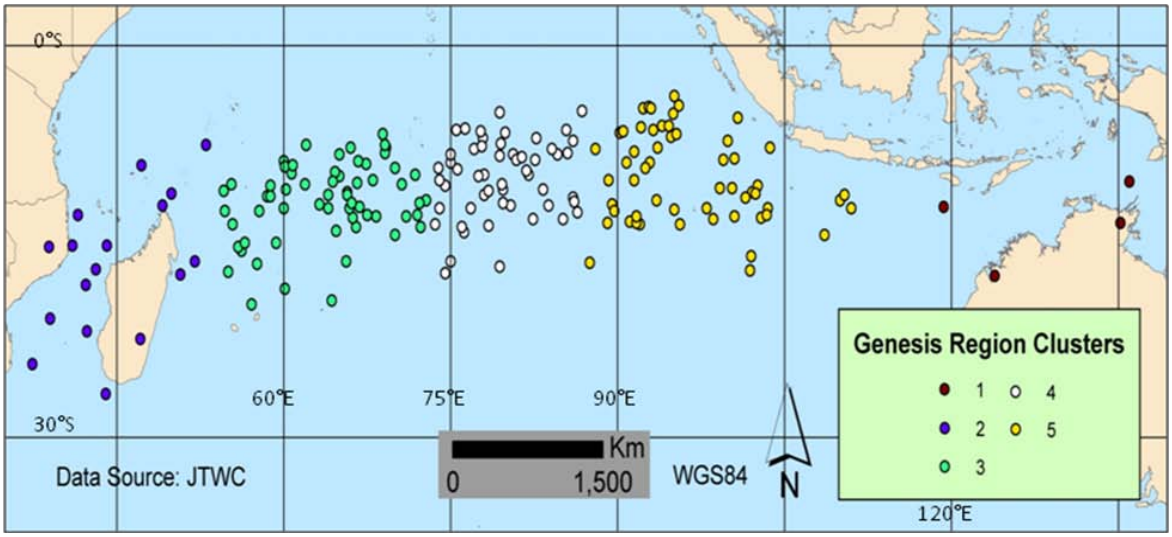

Figure 3-2. Map of five cluster solution of South Indian Ocean tropical cyclones when clustered by their initial longitude. Each point represents the latitude/longitude position at which the system was first identified as a tropical cyclone.

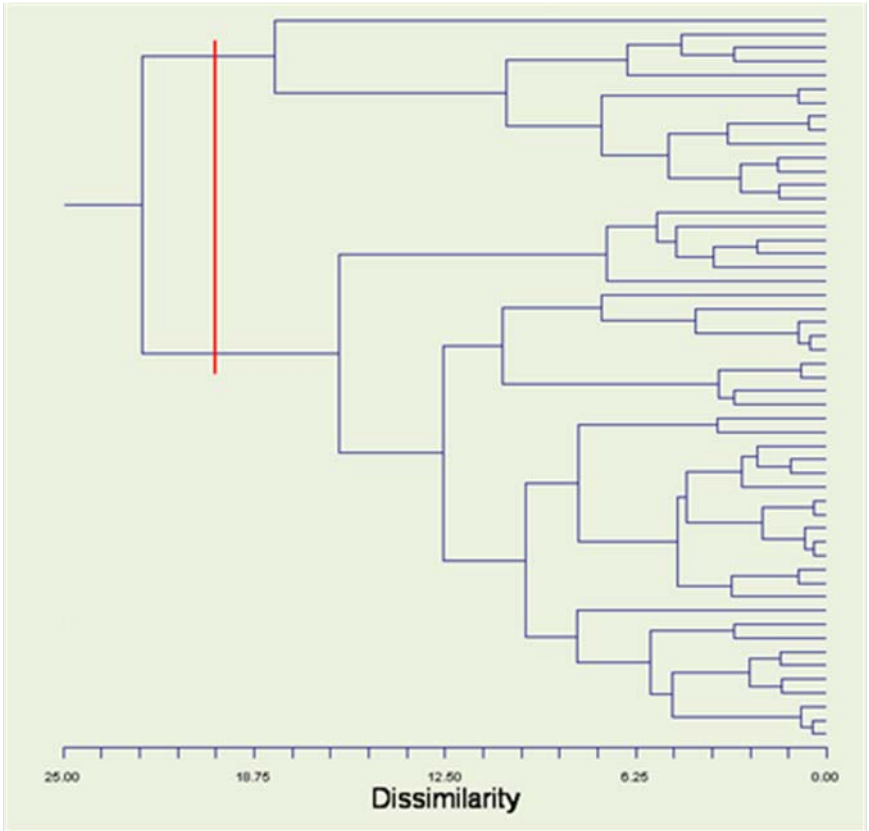

Figure 3-3. Dendrogram of South Indian Ocean tropical cyclones in central region when clustered by their final latitude and longitude. The vertical red line indicates the cut point for a two cluster solution. The cophenetic correlation is 0.72.

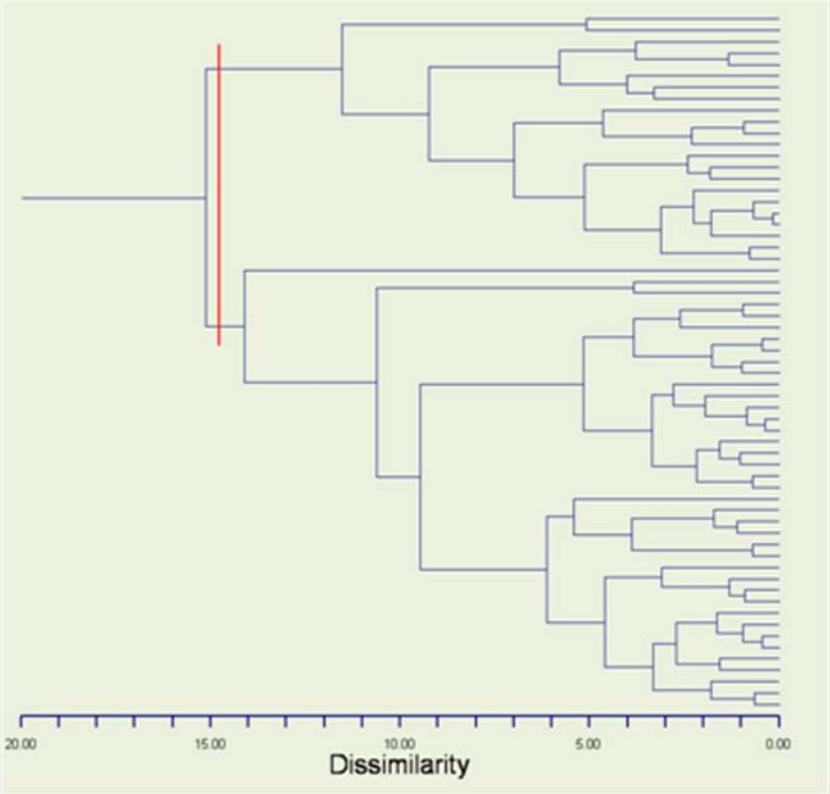

Figure 3-4. Dendrogram of South Indian Ocean tropical cyclones in western region when clustered by their final latitude and longitude. The vertical red line indicates the cut point for a two cluster solution. The cophenetic correlation is 0.71.

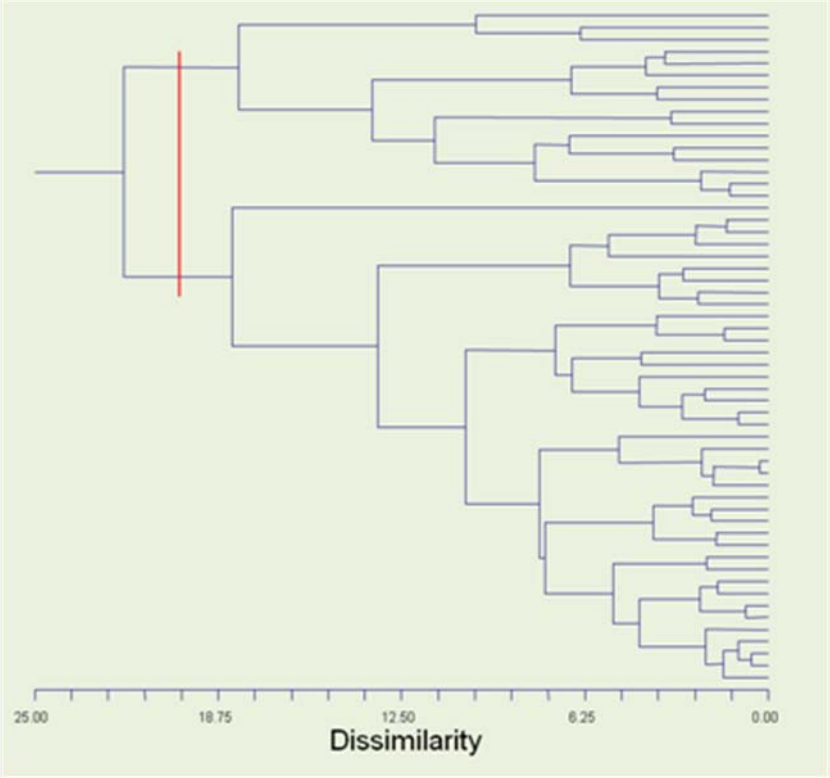

Figure 3-5. Dendrogram of South Indian Ocean tropical cyclones in eastern region when clustered by their final latitude and longitude. The vertical red line indicates the cut point for a two cluster solution. The cophenetic correlation is 0.71.

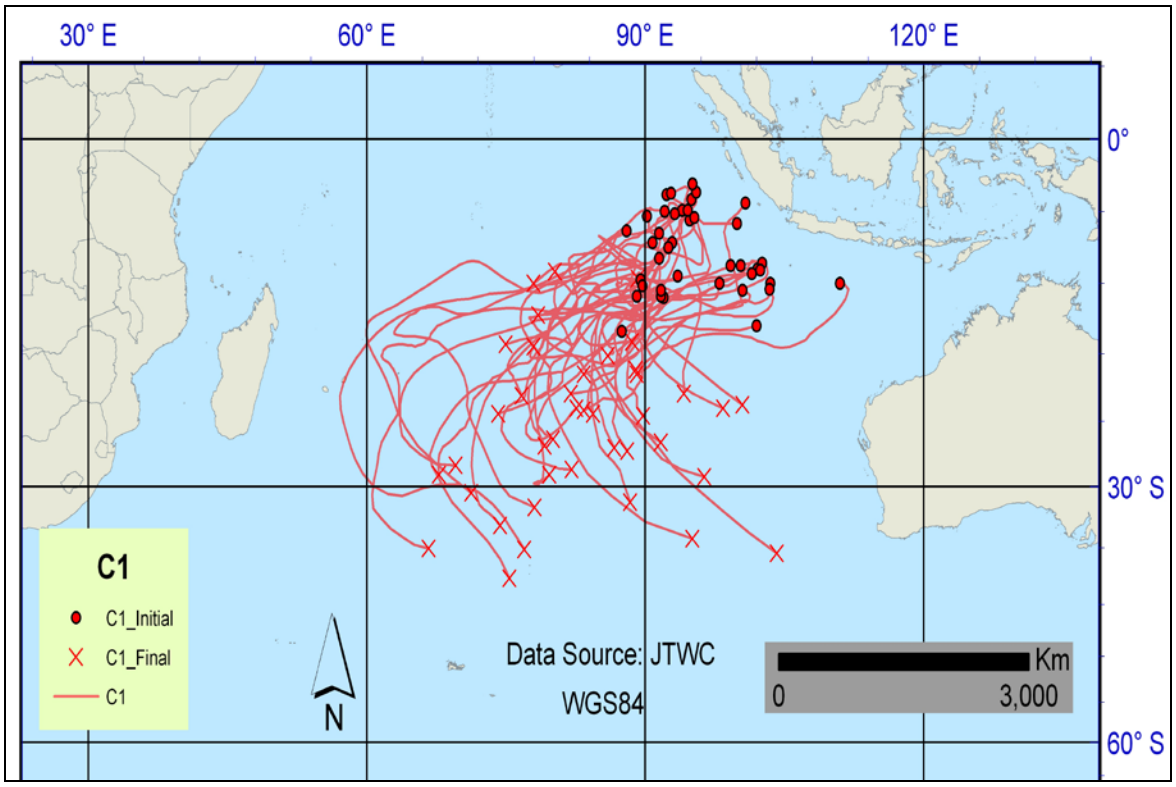

Figure 3-6. Tropical cyclone trajectories in Cluster 1 (C1): eastern region and south motion

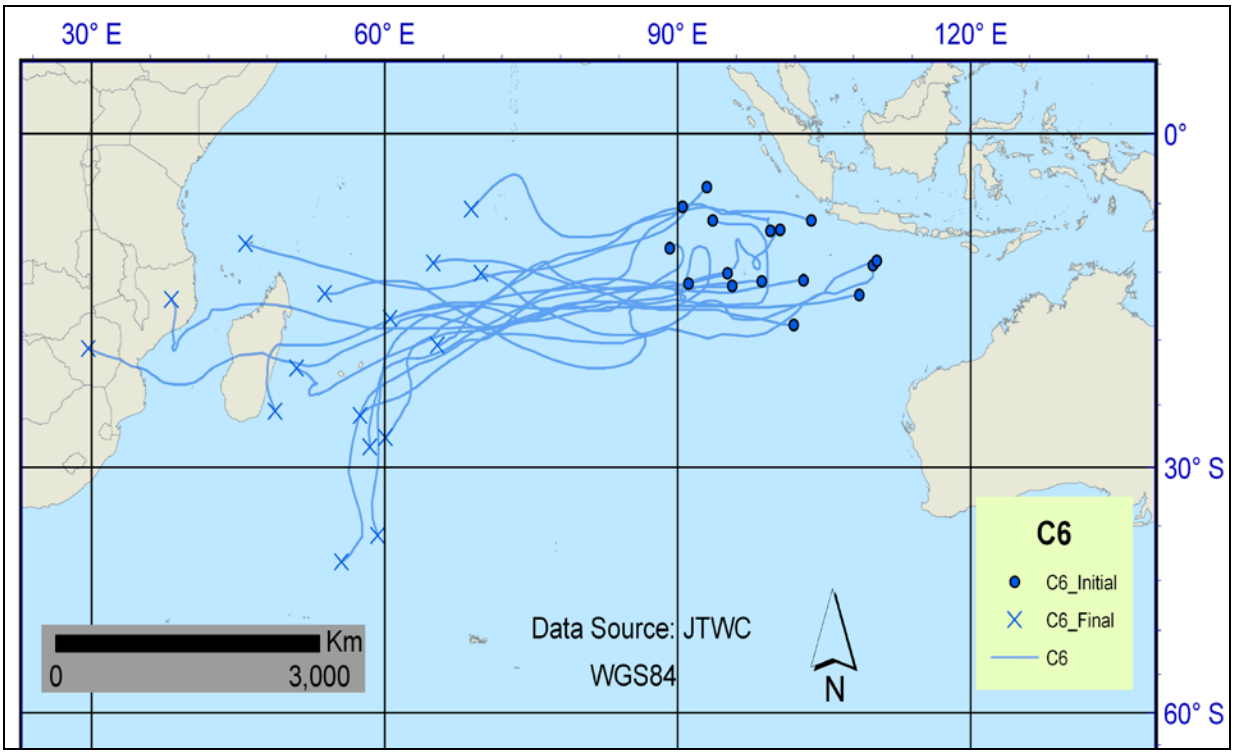

Figure 3-7. Map of tropical cyclone trajectories in Cluster 6 (C6): eastern region and west motion.

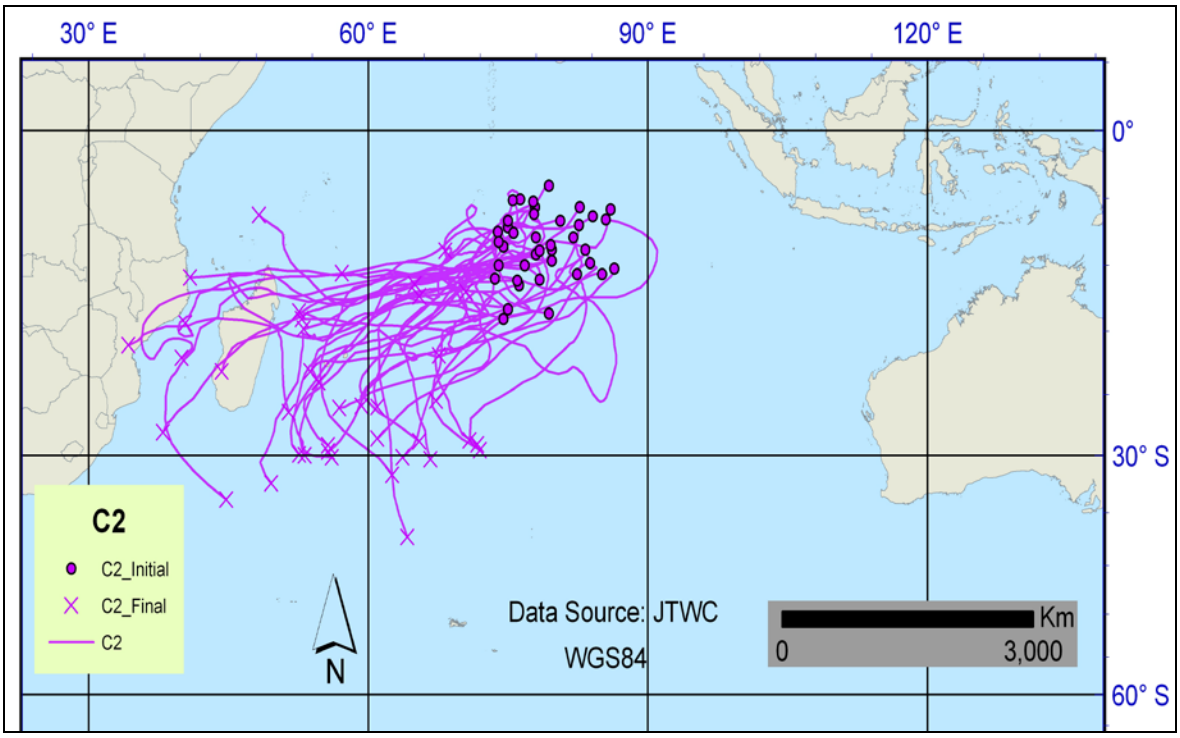

Figure 3-8. Map of tropical cyclone trajectories in Cluster 2 (C2): central region and southwest motion.

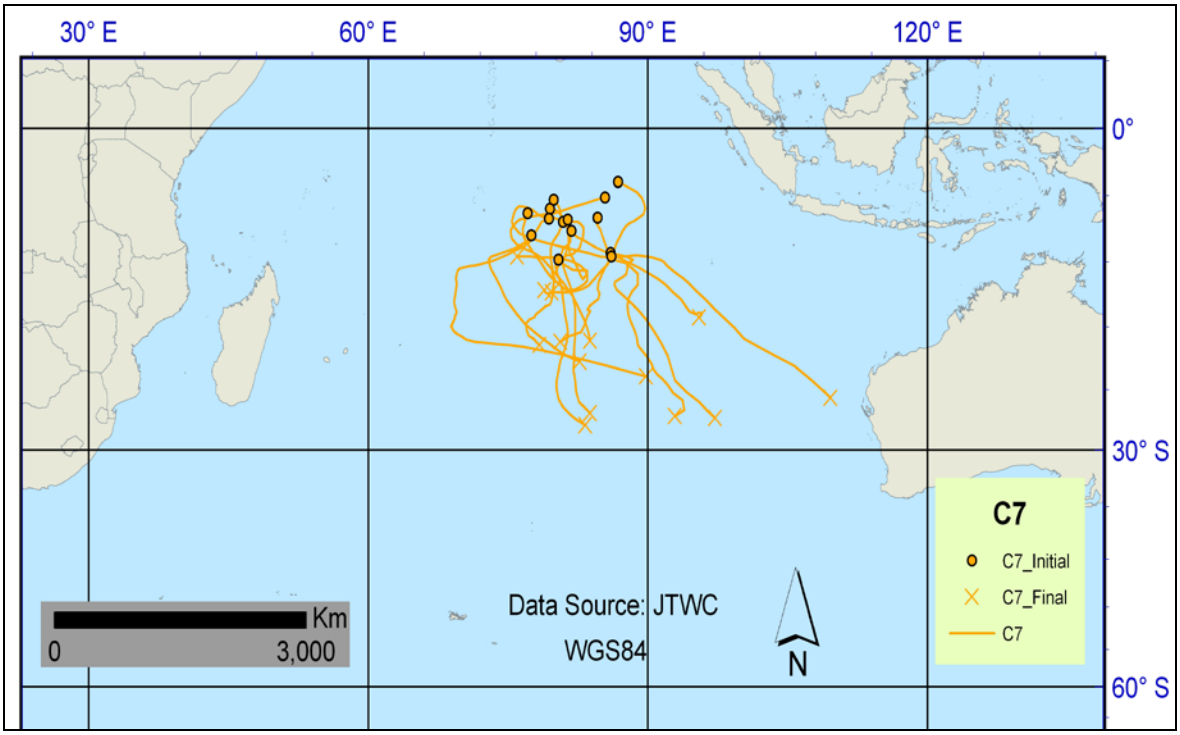

Figure 3-9. Map of tropical cyclone trajectories in Cluster 7 (C7): central region and southeast motion.

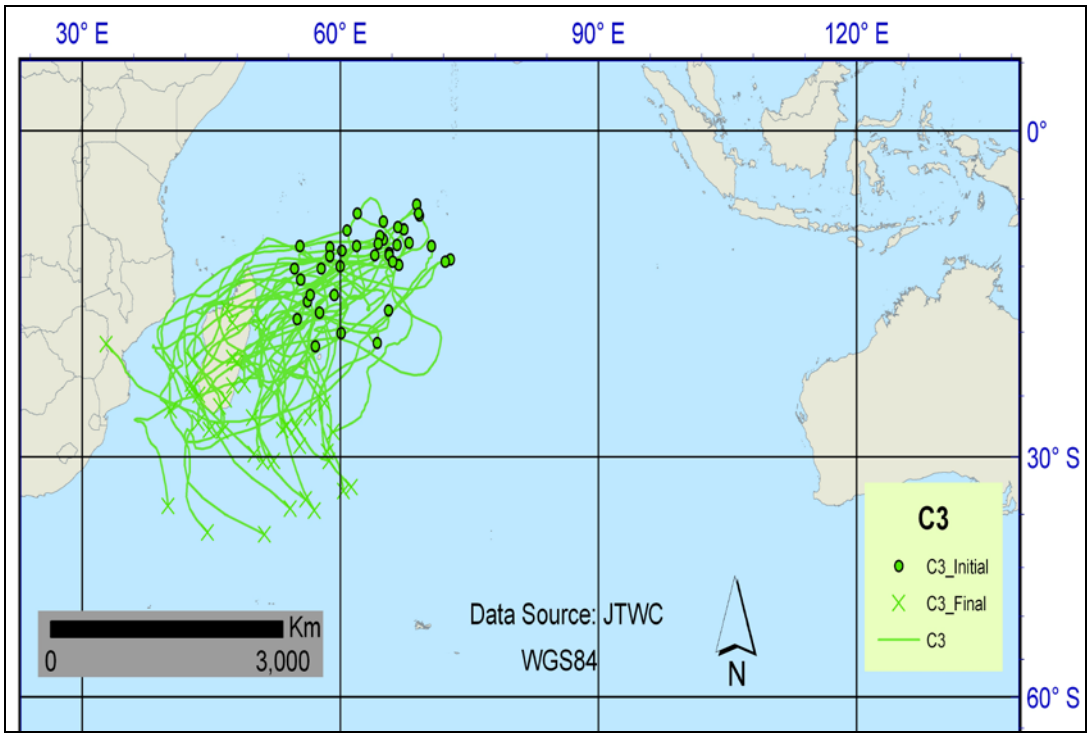

Figure 3-10. Map of tropical cyclone trajectories in Cluster 3 (C3): western region and southwest motion.

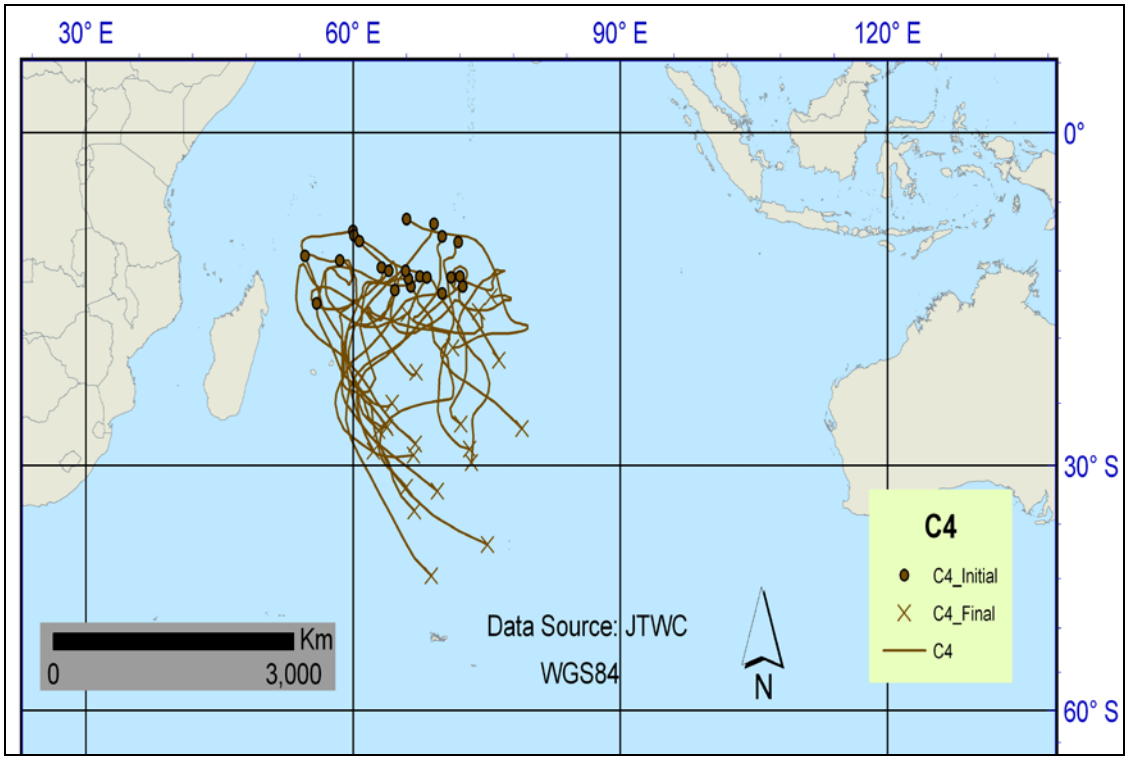

Figure 3-11. Map of tropical cyclone trajectories in Cluster 4 (C4): western region and southeast motion.

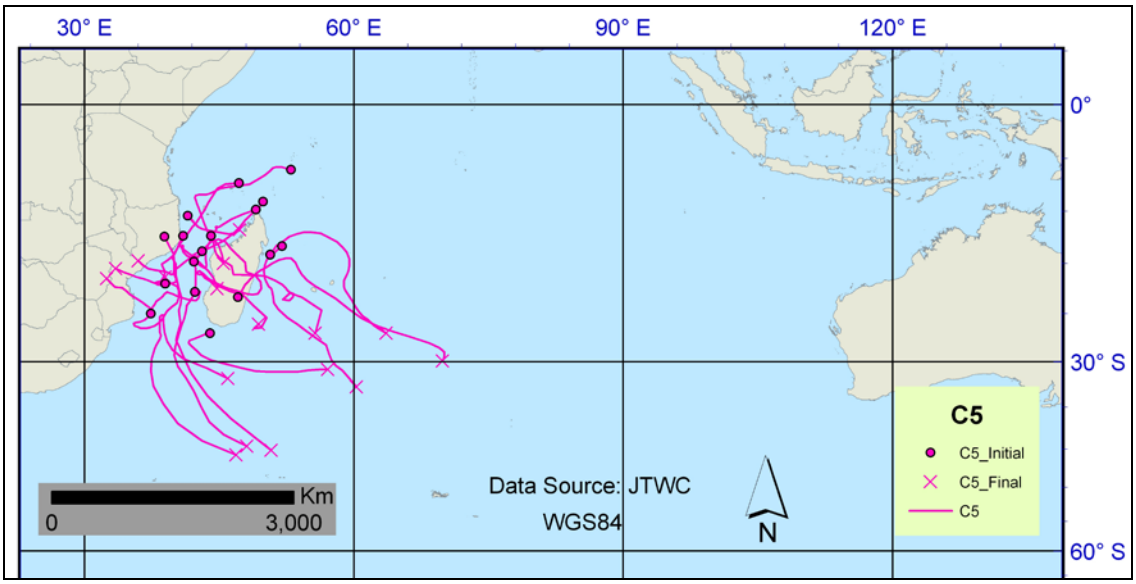

Figure 3-12. Map of tropical cyclone trajectories in Cluster 5 (C5): Mozambique Channel region.

CHAPTER 4
THE INFLUENCES OF EL NINO-SOUTHERN OSCILLATION AND THE SUBTROPICAL INDIAN OCEAN DIPOLE

Introduction

As discussed in Chapter 1, tropical cyclones (TCs) are a recurring phenomenon in the South Indian Ocean (SIO) during austral summer. These damaging and life threatening systems are of particular concern for the inhabitants on the southwest fringe of the basin, especially in Madagascar and Mozambique where social and economic factors may serve to amplify human vulnerability to environmental hazards such as TCs (Brown, 2009; Silva *et al*., 2010). One of the utmost aims of this work is to contribute to scientific understanding of the relationships between SIO TC movements, El Niño-Southern Oscillation (ENSO), and the Subtropical Indian Ocean Dipole (SIOD). It would be useful in the future if the physical risk from TC strikes could be better understood, such that a developing nation like Madagascar might be able to plan one or perhaps three months in advance when a favorable pattern for TC strikes is anticipated.

A survey of previous research in Chapter 2 found that ENSO has a noticeable teleconnection signal in the SIO. During the warm phase, positive sea surface temperature anomalies (SSTA) develop in concert with a deepened thermocline to enhance convection and potential TC genesis northeast of Madagascar and west of about 75°E-85°E (Chambers *et al*., 1999; Jury *et al*., 1999; Klein *et al*., 1999; Reason *et al*., 2000; Xie *et al*., 2002; Ho *et al*., 2006; Camargo *et al*., 2007c; Kuleshov *et al*., 2009). During a cool ENSO event, convection along the Intertropical Convergence Zone (ITCZ) is enhanced east of about 75°E-85°E and TC genesis is more frequent owing to positive SSTA, increased mid-tropospheric relative humidity, and lower tropospheric

shear from near-equatorial westerlies (Wolter, 1987; Larkin and Harrison, 2001; Ho *et al*., 2006; Camargo *et al*., 2007c; Kuleshov *et al*., 2009).

These documented ENSO-TC genesis relationships were accounted for in the first stage of the cluster analysis (CA) of SIO TC trajectories, which was detailed in Chapter 3. The first clustering algorithm separated 187 TC trajectories into four principal groups by their initial longitudes: three in the main development region east of 52°E to near 110°E (western, central, eastern) and one in the far western SIO near Madagascar and within the Mozambique Channel. The western development region is favored with strong El Niño conditions, the eastern region is favored with strong La Niña conditions, and the central region represents an area of variable ENSO influence. A second round of clustering then subdivided each of the three main formation regions into two based on the latitude and longitude of each TC's final position. Using this method, the results of the CA allow for comparative analyses of groups that share a geographic development region but differ in their directions of motion.

ENSO is known to associate with wind anomalies in the SIO that influence TC trajectories. During El Niño, westerly anomalies are present over the tropical and subtropical SIO (van Loon and Rogers, 1981; Meehl, 1987; Karoly, 1989; Reason *et al*., 2000; Ho *et al*., 2006; Yoo *et al*., 2006). It has been suggested that these westerlies steer TCs to recurve to the east away from Madagascar, (Jury *et al*., 1999; Xie *et al*., 2002; Vitart *et al*., 2003; Ho *et al*., 2006). La Niña is associated with easterly steering anomalies stemming from a strong SIO subtropical high, and TCs exhibit straighter westward trajectories during the cool ENSO phase (Wolter, 1987; Vitart *et al*., 2003). Despite these findings however, sole consideration of ENSO to predict seasonal

steering flow, and therefore landfalls, has not sufficiently accounted for spatio-temporal variations of the TC trajectories (Vitart *et al*., 2003; Klinman and Reason, 2008).

This study addresses the ENSO shortcomings through consideration of the SIOD as a second phenomenon associated with significant variability of the SIO subtropical high and therefore TC steering flow. The SIOD represents the second empirical orthogonal function of Indo-Pacific SSTA, and often occurs in the absence of or in opposition to the ENSO teleconnection (Behera and Yamagata, 2001; Fauchereau *et al*., 2003; Washington and Preston, 2006). During the positive phase, SSTA are warm in the western subtropical SIO and cool in the eastern subtropical SIO, similar to La Niña. During the negative phase, anomalies are generally reversed, with a spatial SIO SSTA signature not unlike El Niño (Behera and Yamagata, 2001; Suzuki *et al*., 2004; Huang and Shukla, 2008). SIOD can be used to infer the strength and direction of the TC steering flow anomalies because the SSTA are mainly the result of Ekman transport and latent and sensible heat flux between the ocean surface and the planetary boundary layer (Behera and Yamagata, 2001; Reason, 2002). This study is unique in that SIOD has not previously been tested for association with SIO TC trajectories.

SIOD and ENSO are also implicated in the development and evolution of austral summer tropical-temperate troughs (TTTs). These tropical-extratropical cloud bands are the most important synoptic feature related to precipitation across southern Africa (Harangozo and Harrison, 1983; Lindesay *et al*., 1986; Mason and Jury, 1997). During El Niño and/or a negative SIOD event, the principal tropical convective source of TTTs very often shifts over far eastern Africa, Madagascar, or into the western SIO in conjunction with westerly upper waves that propagate northward to near 10°S (Lyons,

1991; Mason and Jury, 1997; Todd and Washington, 1999; Cook, 2000; Reason, 2002; Fauchereau *et al*., 2009; Manhique *et al*., 2009; Miyasaka and Nakamura, 2010). Thus, given the known relationships between ENSO and SIO TC tracks, it is possible that certain couplings of ENSO and SIOD could show strong relationships to certain SIO TC trajectory types. Previous studies have established that El Niño is associated with positive zonal steering wind anomalies, but they have not tested for nor discussed the relationship in a broader synoptic context that includes the eastward shift of TTTs as the physical mechanism by which TC recurvature may occur with either or both El Niño and negative SIOD.

Additionally, the research presented herein also addresses the inadequacy of the seasonal scale in TC trajectory trend prediction by testing monthly data. Using the trajectory clusters from Chapter 3 to stratify TCs by their initial and final positions, the relationships between the groups and both ENSO and SIOD will be tested using monthly scale SSTA indices via non-parametric analysis of variance (ANOVA). The results will for the first time explicitly link patterns of TC tracks to intraseasonal variability in tropical Pacific SSTs and subtropical SIO SSTs. An ample theoretical framework to understand the mechanisms by which ENSO and SIOD exert steering influence on SIO TCs through longitudinal shifts of TTTs exists in the literature on rainfall variability in southern Africa. From this broader perspective, intraseasonal or perhaps even interannual forecasts of TC trajectories that account for both ENSO and SIOD phases could be utilized for improved predictions of the number of TCs likely to threaten the southwestern rim of the SIO.

Data and Methods

The seven main clusters (C1-C7) from Chapter 3 are used now to analyze and compare the groups' SST anomaly patterns in the important regions relating to ENSO and SIOD. These clusters were identified through an analysis of TC genesis and lysis points for 191 TCs that reached peak intensity of at least 30 ms-1 and passed west of 90°E. The four TCs in C8 that formed very near Australia have been omitted from the analysis as they do not associate strongly with any particular ENSO or SIOD pattern.

SST monthly index values in numerical format were acquired online respectively for SIOD and ENSO at http://www.jamstec.go.jp/res/ress/behera/iosdindex.html and http://www.cpc.noaa.gov/data/indices/. Each TC is assigned the monthly values of the index values corresponding to the month(s) spanning each TC's life cycle. If a storm's life cycle bridged two months, those two months' values were averaged. Then, using the TC clusters as treatment groups, analysis of variance (ANOVA) is performed for three ENSO SSTA indices and for SIOD.

As not every SSTA variable was found to approximate a normal distribution (results not shown here), a nonparametric rank test to compare the medians of the seven clusters, the Kruskal-Wallis Test (KW) with ties adjustment, is carried out using the software package NCSS (Kruskal and Wallis, 1952; Higgins, 2004). The null hypotheses for the tests are that the median values of the index values for the Niño or SIOD regions are not significantly different across all seven TC clusters. The alternative hypotheses are that there exists a significant difference in at least one pair of TC clusters in their median values of the Niño or SIOD indices. To ensure that the results of the KW tests are appropriately interpreted, Modified-Levene Equal-Variance Tests are applied in each case (Brown and Forsythe, 1974). If the groups do not differ

significantly in their variances, the results of the KW tests are accepted and investigated further where appropriate.

Given a rejection of the null hypothesis for the KW tests and given that equality of variance is satisfied, it is then necessary to perform multiple comparisons amongst the groups to determine which TC trajectory groups are significantly different with respect to contemporaneous SST anomalies in the Niño and SIOD regions. Since the data here are not assumed to approximate a normal distribution, Dunn's rank sums procedure is used to test statistical significance in multiple comparisons (Dunn, 1964). Both a standard Z-test and a test using a Bonferroni correction are employed in the multiple comparisons. The decision of how best to account for experiment-wide error rate is often subjective and dependent on the nature of the data being analyzed (Cabin and Mitchell, 2000). Thus, the results will be presented in tables reporting both liberal and conservative significance levels with respect to the probabilities of Type I errors.

As complementation for the ANOVA results, global SSTA composite maps are constructed for each cluster and plotted in ArcGIS with overlaid SSTA centers of action for the Niño and SIOD regions. This allows for qualitative examination of the SSTA patterns to help visualize their geospatial signatures, keeping the formal statistical inferences from the Niño and SIOD indices firmly in mind. The dataset used here is the National Oceanic and Atmospheric Administration (NOAA) Optimum Interpolation (OI) SST Version 2, which is available online (Reynolds *et al*., 2002). The data are weekly SST means with 1.0 degree latitude by 1.0 degree longitude resolution, and the temporal coverage is from October 1981 to the present. An SST average is extracted based on the initial and final dates for each respective TC's life cycle. The spatial scope

of the data is global and the temporal scale is approximately the duration of each storm's life cycle. Composites are then averaged according to cluster membership, such that one global SST composite exists for each of the seven clusters.

To account for seasonality, monthly averages for each month from October to May were also downloaded from the same source (Reynolds *et al*., 2002) and then composited over the period Oct. 1981 to May 2008. To obtain anomaly composites for each TC, the 26 year monthly composite was subtracted from each of the 175 individual TC event composites available during the study period. For example, TC Jaya's life cycle spanned parts of March and April in 2007. Therefore, the final anomaly composite map for Jaya is the SST composite for that TC's life cycle minus the combined March-April 26 year composite.

For the KW ANOVA tests, three SST regions are outlined in the Pacific for ENSO (see Figure 4-1): Niño-1+2 (0°-10°S, 90°W-80°W), Niño-3.4 (5°N-5°S, 170°W-120°W), and Niño-4 (5°N-5°S, 160°E-150°W). The Niño-3.4 (N3.4) index is commonly used alone to represent ENSO events, while the Niño-1+2 (N1.2) region is sensitive to warm events and Niño-4 (N4) is more sensitive to cold events (Trenberth, 1997; Hanley *et al*., 2003). ENSO index data is utilized for all 187 TCs in the seven principal clusters. Two SST regions are also outlined for the SIOD (Figure 4-2): the Subtropical Dipole Index west pole (SDI west, 37°S-27°S, 55°E-65°E), and the Subtropical Dipole Index east pole (SDI east, 28°S-18°S, 90°E-100°E). The Subtropical Dipole Index (SDI) is calculated by subtracting the east pole from the west pole (Behera and Yamagata, 2001). SDI data is not yet available for 2008, therefore six TCs from 2008 were omitted, leaving a total of 181 TCs for the SDI tests.

Results

Kruskal-Wallis ANOVA Results

The results of the KW tests suggest that sea surface temperatures in the tropical Pacific and the subtropical Indian Oceans are significantly and contemporaneously associated with variability of SIO TC trajectories (Tables 4-1, 4-3, 4-4, 4-5, and 4-6; Figures 4-3, 4-4, 4-5, and 4-6). The null hypotheses of no significant differences in the median values of N3.4, N1.2, N4, and SDI across all TC clusters are rejected at $\alpha=0.05$ and N3.4 and SDI are significant even at $\alpha=0.001$. The results of the Modified-Levene Equal-Variance tests for all groups are a failure to reject the null hypothesis of homoscedasticity, again at the 95% confidence level. Therefore, there is sufficient evidence to compare the individual clusters to determine which groups significantly differ in association with N3.4, N1.2, N4, and SDI.

Multiple Comparisons and SST Anomaly Composites

Even on qualitative inspection of group median values for N3.4, N1.2, N4, and SIOD (Table 4-2), C4 appears to be associated with El Niño and negative SIOD, while C6 and C3 appear to be highly associated with La Niña and positive SIOD. This relates well with previous work in the basin in that a strong La Niña group (C6) originates in the east and has very westward oriented trajectories, while a strong El Niño group (C4) originates in the west and is characterized by south and eastward motion (Evans and Allan, 1992; Vitart *et al*., 2003; Ho *et al*., 2006; Kuleshov *et al*., 2008 and 2009). Noticeably however, C3 forms in the western region but is apparently more associated with La Niña, in contrast to C4. In order to provide statistical support for this perceived relationship, and to explore further associations, KW multiple comparison z-value tests

are performed based on median values of N3.4, N1.2, N4, and SIOD across all seven clusters.

Test results show that there is statistical evidence at $\alpha=0.05$ to support the claim that C4 is significantly more associated with El Niño as compared to the six other groups and based on all three Niño index regions (Tables 4-3, 4-4, and 4-5). The sea surface temperature anomaly (SSTA) composite for C4 (Figure 4-7) corroborates this finding well, with positive SSTA evident from the South American littoral west to 170°E. Also present is a SSTA pattern in the SIO suggestive of the negative SIOD, which exhibits warm anomalies from Madagascar eastward along 20°S into the eastern ocean (Behera and Yamagata, 2001; Suzuki *et al*., 2004). Indeed, the SIOD multiple comparisons (Table 4-6) show that C4 is significantly more associated with the negative SIOD phase than all other clusters.

El Niño is well known to associate with westerly wind anomalies over the SIO during austral warm season (van Loon and Rogers, 1981; Meehl, 1987; Karoly, 1989; Reason *et al*., 2000; Yoo *et al*., 2006). Likewise, TTTs are associated with anomalous westerlies over the same geographic area, which extend from the boundary layer up to 500 hPa and have a longitudinal signature that can extend across the entire SIO (Todd and Washington, 1999). Reason (2002) found these TTTs to vary in association with SIOD, and several authors found that the deepest convection coincident with TTTs shifts over the SIO in association with El Niño (Cook, 2000; Pohl *et al*., 2009; Fauchereau *et al*., 2009; Manhique *et al*., 2009). Given the high significance of both El Niño and negative SIOD for C4, and the propensity of TTTs to prevail over Madagascar and the western SIO during both of these phenomena, the conclusion is

that C4 type TCs occur when ENSO is in warm phase and SIOD is in negative phase. The longitudinally shifted and latitudinally amplified TTTs then explain the mechanism by which TCs in C4 are swept southeastward away from Madagascar.

Having established the ocean-atmospheric connections for C4, it is logical now to compare with the cluster that forms in the same region yet threatens land with far greater frequency, C3. This group is significantly different in N3.4, N1.2, and N4, and SDI from C4, which strongly suggests that C3 occurs with La Niña and/or a positive SIOD (Tables 4-3, 4-4, 4-5, and 4-6). The SSTA map (Figure 4-8) suggests a similar conclusion, with cool anomalies in the equatorial Pacific and warm anomalies south and southeast of Madagascar. According to the multiple comparison tests for N3.4, N1.2, N4, and SDI, C3 is not significantly different from any other group other than C4, and this suggests that the phasing of La Niña and the positive SIOD is not as prevalent in this group as was described for C4 with ENSO in warm phase, SIOD in negative mode, and TTTs consequently shifted north and east into the tropical SIO.

The known regional patterns during La Niña should support more westward moving TCs that would threaten Madagascar, with enhanced easterly and southeasterly trades across the tropical SIO (Wolter, 1987; Reason *et al*., 2000; Larkin and Harrison, 2001; Vitart *et al*., 2003). In accordance with positive SIOD, warm SSTA off of southern Africa increase convection over the far southern reaches of the continent coincident with the southwestward shifted TTTs (Reason, 2002; Todd and Washington, 1999). For storms in C3 that reached south of 25°S, interaction with upstream continental TTTs would explain late recurvature. A difference map of C4 SSTA minus C3 SSTA (Figure 4-9), coupled with the Z-values in the multiple comparisons, support the assertion that

both ENSO and SIOD phases should be accounted for to gain a fuller understanding of the mechanisms under which TC motion is more likely to mirror the C4 type with TTT interaction and southeastward movement or the C3 type with stronger trades and westward movement.

The trajectory type that develops in the eastern region and tracks far westward, group C6, also is strongly associated with the positive SIOD phase and La Niña. Readily identifiable La Niña and positive SIOD signals are apparent both in the high significance of C6 in the multiple comparisons (Tables 4-3, 4-4, 4-5, and 4-6) and in the SSTA map (Figure 4-10). The composite map shows equatorial cool anomalies in the Pacific as well as coherent warm anomalies off the southeast coast of Africa into the southwest IO. Cool anomalies also extend eastward from Madagascar along 15°S-25°S across the SIO. This is crucial because these cool SSTA are largely induced by increased sea to air latent and sensible heat exchange and Ekman transport associated with the strong easterly and southeasterly winds (Behera and Yamagata, 2001). Therefore, the presence of these SSTA allows inference of anomalously strong easterly trade winds across the SIO north of 25°S which could serve to steer TCs on long duration westward zonal tracks, as in Vitart *et al*. (2003). Therefore, when La Niña and positive SDI occur simultaneously, the TCs of this group remain at lower latitudes because the strong subtropical SIO high and associated easterlies preclude repeated intrusions of mid-latitude transient waves which in turn fail to foster eastward propagation of convective elements associated with the Angola/Zambia thermal trough. Thus, the conclusions of Vitart *et al*. (2003) can be improved upon.

While TCs in group C6 develop in the eastern SIO and track far westward, TCs in the counterpart group C1 also develop in the east but recurve into the mid-latitudes in the central or eastern SIO. The SSTA composite map (Figure 4-11) for C1 does not depict a strong ENSO warm or cool SSTA pattern. However, the data exhibit a northwest-southeast warm SSTA in the central and southeast subtropical IO which strongly resembles the negative SIOD mode. A map of the differences in the C1 and C6 composites (Figure 4-12) show significant differences in SSTA patterns in the ENSO and SIOD regions. In particular, the presence of warm SSTA in the central and eastern tropical/subtropical SIO and cool SSTA in the southwest sbutropical SIO indicates weakened trade winds and more frequent frontal intrusions. This would mean stronger cold advection and anomalous westerlies allowing for greater sea to air sensible and latent heat flux to the south. Also, reduced Ekman transport from the usual trades to the north, in conjunction with increased air to sea heat flux from warm advection ahead of the cold fronts, would allow for warm SSTA patterns associated with negative SIOD and/or El Niño. Therefore, with troughs moving farther north into the central/eastern SIO, this would influence C1 TCs to recurve more abruptly into the subtropics than C6 TCs.

The multiple comparisons (Tables 4-3, 4-4, 4-5, and 4-6) lend credence to the SSTA patterns and provide support to the assertion that group C1 is more of a negative SIOD related phenomenon and perhaps less dependent on warm/cool ENSO phase. This is in contrast to the eastern counterpart group C6, which occurs when ENSO is in cool phase and SIOD is in warm (positive) phase. The fact that C1 is composed of generally recurving TCs but does not have a strong El Niño signal supports the notion

that significant alteration in the TC steering wind patterns via a shift or weakening of the subtropical high can happen without strong ENSO influence (Behera and Yamagata, 2001; Fauchereau *et al*., 2003; Washington and Preston, 2006).

The TC cluster with genesis in the central region and movement to the west and southwest is C2. C2 is not significantly different from other groups in the ENSO tests save for C4 and only significantly different from C6 in the SDI multiple comparisons (Tables 4-3, 4-4, 4-5, and 4-6). However, Figure 4-6 should not be interpreted to mean that C2 shows a strong relationship to with SIOD that is opposite in sign to the strong relationship that is apparent between C6 and SIOD. It is a strong relationship compared to a weak one, not a strong positive relationship compared to a strong negative relationship. The SSTA composite map for C2 displays an easily recognizable La Niña pattern in the equatorial Pacific east of 180° (Figure 4-13), which is expected given the more east to west motion in the group that should accompany stronger SIO trade winds (Wolter, 1987; Reason *et al*., 2000; Larkin and Harrison, 2001). Though not statistically significant according to Tables 4-3, 4-4, or 4-5, the ENSO indices also indicate a possible weak association with La Niña (Table 4-2). However, there is not an easily identifiable pattern in the C2 SSTA map that would indicate a trade wind pattern shift associated with the SIOD, congruent with earlier discussion of the weak statistical SDI signal.

Since TCs of type C2 sometimes threaten inhabited places in the SIO, it is important again to compare the C2 SSTA anomaly map with another group (C7) which shares the central genesis region but is characterized by TCs that track more eastward through the open SIO. C2 and C7 are not statistically different when compared simply

by the index values for ENSO and SDI. There are signs of an El Niño pattern in the SSTA map in the N1.2 region for C7, however there is not a strong contiguous warm SSTA from South America to the date line (Figure 4-14). The difference map of C7 minus C2 SSTA (Figure 4-15) assists in identification of the equatorial Pacific as a region of importance, with warm SSTA off of South America and somewhat incoherently spread westward to the date line. Overall, there is not a significant statistical nor a strong geospatial difference between C2 and C7 that would allow for concise interpretation (Tables 4-3, 4-4, 4-5, and 4-6). The SSTA patterns in the SIO that might typically point to a positive/negative SIOD appear to have been disrupted by the TCs in both C2 and C7, with cold anomalies present along the TC tracks likely linked to cold water upwelling in the wake of the TCs.

Finally, group C5 which formed mainly near or within the Mozambique Channel did not show any significance in the multiple comparison tests with respect to ENSO or SDI. An SSTA composite map was constructed for C5, but no coherent ENSO or SIOD patterns are evident (Figure 4-16). This is somewhat surprising in that these storms are located in close proximity to the region where TTTs often occur. The lack of a clear signal may be a function of the relatively small number of storms that form in this region. From 1979-2008, only 40 of 339 (11.8%) TCs of any intensity in the western SIO formed in this region, and only 17 of those are included in the present study. Therefore, it can only be said from this study that no strong ENSO or SIOD signal was found when only more intense TCs of this region that occurred during the period 1979-2008 were considered. An in-depth analysis of these storms on a case-by-case basis could yield a

better understanding of their relationship with TTTs, as suggested by Mavume *et al*. (2009).

Discussion

In this chapter, KW ANOVA tests were performed to compare the median values of N3.4, N1.2, N4, and SDI across the seven main TC trajectory clusters from Chapter 3. All ENSO indices and the SDI showed significant differences when all groups were tested together. Given that Vitart *et al*. (2003) suggested a basin-wide influence of El Niño/La Niña on TC steering flow, the ENSO results (particularly for N3.4) were not unexpected. Likewise, given the association between SSTA and the strength of the trade winds in the SIO, it was not surprising that the SIOD was implicated in TC trajectory variability at high significance levels comparable to ENSO (Behera and Yamagata, 2001; Suzuki *et al*., 2004; Huang and Shukla, 2007). The link between SIOD and TC trajectories shown here represents a new finding not seen in previous literature.

To explore the TC-SIOD-ENSO links further, multiple comparisons were made to find where the significance exists between clusters, and SSTA composite maps were constructed to aid interpretation of geospatial patterns. Group C4 (western genesis, south motion) was found to associate highly with both El Niño and negative SIOD in comparison to all other clusters. The proposed physical mechanism behind this association is the northeastward shift of TTTs from southern Africa into the western SIO that often accompanies both El Niño and negative SIOD (Mason and Jury, 1997; Todd and Washington, 1999; Cook, 2000; Reason, 2002; Fauchereau *et al*., 2009; Manhique *et al*., 2009). Anomalous westerly winds from the lower troposphere up to 500 hPa accompany the TTTs and are deep enough to steer TCs in the western SIO south and

eastward away from Madasgascar. The eastward shift of TTTs during El Niño and negative SIOD has been well documented in previous literature relating to African rainfall, but has not previously been linked to TC trajectories in the SIO.

TCs that form in the western SIO and tend to move west or southwestward (group C3) were found to be significantly different than group C4 and are more associated with La Niña and the positive phase of SIOD. Both La Niña and positive SIOD have been previously linked to stronger east and southeasterly trade winds in the tropical/subtropical SIO (Wolter, 1987; Behera and Yamagata, 2001; Vitart *et al*., 2003). This finding is important to discern the oceanic-atmospheric environment of TCs that form near Madagascar but track eastward over the ocean from those that form in the same region and often make landfall. Consideration of ENSO phase alone is not sufficient to capture shifts in the subtropical/tropical TC steering flow in the SIO associated with the subtropical high and TTTs. The phase of the SIOD should be considered as well, as SSTA in this region can provide additional explanation for the variability of TC trajectories. This would be particularly useful when ENSO is neutral and SIOD is either strong positive or negative. Likewise, when ENSO is in warm (cool) phase and SIOD is concurrently in negative (positive) phase, these interact to produce relatively persistent eastward (westward) TC steering environments.

For example, Klinman and Reason (2008) noted that TC Favio in February 2007 followed a track south of Madagascar and then northwest making landfall in Mozambique. The system followed a highly unusual path given its occurrence during a weak El Niño year, and the authors noted that such a TC did not fit neatly into the ENSO-TC track paradigm of Vitart *et al*. (2003) wherein Mozambique is under threat for

landfall during La Niña. Applying the results from this study, the SIOD was strongly positive in Feb. 2007, which is associated with more zonally oriented westward TC tracks. Therefore, in this case consideration of both ENSO and SIOD phases allows the track of Favio to fit within a more robust framework.

A similar dichotomy was found for groups C6 and C1 in the eastern SIO. TCs that form in the eastern SIO and follow westward trajectories (C6) were significantly more associated with La Niña and positive SIOD than any other group. The physical mechanism is anomalously strong southeast and easterly trade winds which are known to accompany both of these patterns (Wolter, 1987; Behera and Yamagata, 2001; Vitart *et al*., 2003). Group C1 is characterized by TCs that also form in the eastern region, except these tend to recurve into the subtropics and remain well east of the inhabited western rim of the SIO. This group was found to be strongly associated with negative SIOD, yet not strongly associated with any ENSO phase. The TTTs, though most often studied in the context of southern African rainfall, may extend even into the central and eastern subtropical SIO during negative SIOD (Todd and Washington, 1999; England *et al*., 2006). Thus, once againin the eastern SIO a more complete understanding of the oceanic-atmospheric differences between low-latitude westward moving TCs and those that recurve into the mid-latitudes can be achieved by considering the SIOD phase in tandem with the ENSO phase.

A review of previous literature revealed that the degree of association between ENSO and SIOD is not fully understood. The SIOD was noticed in EOF analysis of Indo-Pacific SSTs as the second EOF behind a leading EOF that was apparently strongly linked to ENSO (Behera and Yamagata, 2001; Suzuki *et al*., 2004). It does not

necessarily follow that the underlying cause(s) associated with EOF2 is unrelated to the underlying cause(s) associated with EOF1 (Fauchereau *et al*., 2003; Washington and Preston, 2006). The spatial patterns of SSTA can only be interpreted as orthogonal centers of variability, not symptoms of two independent and non-interactive causes. In this study, N3.4 and SDI have a contemporaneous Spearman's rank correlation of -0.1665 (p-value=0.0251), and neither N1.2 nor N4 are significantly correlated (not shown). Thus, there is statistical significance in their simultaneous association, but not to a level where one can be said to drive the other. Future research should explore the relationship between ENSO forcing and internal SIO forcing more comprehensively, as interpretable lag-lead relationships may be found. It has already been suggested from coral reef analysis that the spatial patterns of SST and sea level pressure (SLP) resulting from ENSO-SIOD interactions has changed since the 1970s (Zinke *et al*., 2004). These changes likely produce alterations in TC trajectories, and it is important to try and determine if socially and economically vulnerable societies can expect increased or decreased exposure to negative TC impacts.

Given that the results described above suggest the importance of considering both ENSO and SIOD, a contingency table (Table 4-7) is constructed stratifying the seven clusters by TCs that occurred in four categories of ENSO/SIOD interaction: positive ENSO with positive SIOD (E+S+), positive ENSO with negative SIOD (E+S-), negative ENSO with positive SIOD (E-S+), and negative ENSO with negative SIOD (E-S-). Fisher's Exact Test is known to provide exact p-values for contingency table tests, thereby remaining robust in the presence of small samples (Higgins, 2004). Therefore, using Fisher's Test the groups from the same TC genesis regions as defined in the

earlier cluster analysis are tested for association with the interactive ENSO/SIOD categories.

The results of the Fisher's Test indicate that TC trajectories and type of interaction between ENSO and SIOD are significant for the western and eastern regions of the study area. For the western region, a highly significant association is found between the type of TC trajectories and the type of interaction between ENSO and SIOD (p-value=0.00002). Out of 22 (36) TCs in C4 (C3), 16 (4) occurred when ENSO was positive and SIOD was negative. In contrast, one (13) out of 22 (36) occurred when ENSO was negative (La Niña) and SIOD was positive. For the eastern region, a significant association again exists between the type of TC trajectories and the type of interaction between ENSO and SIOD (p-value=0.025). Out of 39 (16) TCs in C1 (C6), 13 (0) occurred when ENSO was positive and SIOD was negative, whereas when ENSO was negative and SIOD was positive the ratios were 10/39 (7/16). No such significant association exists in the central region between C2 and C7 (p-value=0.195). These results further support the notions that type C4 storms are highly associated with an anti-phasing of ENSO (warm) and SIOD (negative) wherein conditions are very favorable for TC-trough interaction, and that type C6 storms are also associated with the opposite anti-phasing of ENSO (cool) and SIOD (positive) wherein conditions are unfavorable for trough interaction across the entire SIO.

Conclusion

The KW ANOVA and subsequent tests described in this chapter have allowed comparisons between the TC trajectory clusters from Chapter 3 in terms of their associations with three ENSO indices and a SIOD index. There is statistical evidence that ENSO phase is an important factor for TC trajectories in the SIO, a finding that is in

agreement with previous research (Vitart *et al*., 2003). There is also statistical evidence that SIOD phase is an equally important factor for TC trajectories in the SIO. TTTs are important producers of rainfall on the western rim of the SIO, and their most intense tropical convective clusters often shift over the western SIO during El Niño and/or the negative SIOD phase. A broad literature base exists on the topic because TTTs contribute substantially to warm season rainfall in southern Africa. However, TTTs as synoptic features integrally linked with tropical convection have not been linked to TC trajectories in the SIO. The significance of ENSO and SIOD on SIO TC trajectories is logically explained in this study through the existing framework from the TTT literature.

The ENSO/SIOD interaction is an important consideration which is not found in the existing literature. Previous research suggests that SIOD fluctuations may develop independent of ENSO phase (Behera and Yamagata, 2001; Fauchereau *et al*., 2003; Washington and Preston, 2006). ENSO alone does not account for the observed variability of SIO TC trajectories, but when ENSO and SIOD are considered in tandem, a better accounting can be made for changes in strength and position of the SIO subtropical high and the TTTs of the South Indian Convergence Zone (SICZ). Thus, when ENSO and SIOD are in anti-phase there can be higher confidence of the direction and magnitude of anomalous TC steering winds in the SIO.

The proposed importance of ENSO/SIOD interaction was then tested, and the results from the western and eastern regions give further weight to the assertion that anti-phasing of ENSO and SIOD is significantly associated with both anomalously westward and eastward moving TCs. The statistical inferences are linked to physical mechanisms of TC steering flow because the ENSO and SIOD indices give

approximations on the strength and extent of SIO southeast trades versus anomalous low-middle tropospheric westerlies associated respectively with the SIO subtropical high and the tropical-temperate troughs. The following chapter will conclude this study by summarizing the important results and pointing to future directions in SIO TC research.

Table 4-1. P-values for KW ANOVA and Modified-Levene Equal-Variance Tests. All tests evaluated with alpha level at 0.05 and red text indicates statistical significance at the given alpha level. KW ANOVA p-values are corrected for ties.

	Niño 3.4	Niño 1.2	Niño 4	SDI
KW ANOVA	0.0002	0.0051	0.0017	0.0002
Mod. Levene	0.7516	0.1114	0.0901	0.1048

Table 4-2. Standardized median anomalies for Niño-3.4 (N3.4) sea surface temperature, Niño-1.2 (N1.2), Niño-4 (N4), and Subtropical Dipole Index (SDI). Positive values of N1.2, N3.4, and N4 indicate a trend toward El Niño conditions, while negative values indicate a trend toward La Niña conditions. SDI is positive when the southwest IO is warmer than average while the southeast IO is cooler and SDI is negative when the inverse pattern occurs.

Cluster ID	Niño 3.4	Niño 1.2	Niño 4	SDI
C1	0.02	-0.20	0.05	-0.19
C2	-0.23	-0.31	-0.16	-0.06
C3	-0.41	-0.29	-0.16	0.34
C4	0.71	0.54	0.68	-0.70
C5	-0.08	0.09	-0.04	0.32
C6	-0.58	-0.54	-0.58	0.77
C7	0.03	0.21	0.10	0.14

Table 4-3. KW Multiple Comparison Z-Value Tests for Niño-3.4 region stratified by clusters. Text shaded in red or blue indicates significant differences of median Niño-3.4 values at alpha level of 0.05. Text shaded only in red indicates significance using a Bonferroni correction to account for experiment-wide accumulated probability of Type I errors.

Niño-3.4	C1	C2	C3	C4	C5	C6	C7
C1	0.0000	0.9546	1.8630	2.9438	0.2625	2.0139	0.2301
C2		0.0000	0.9027	3.7362	0.4777	1.2830	0.9189
C3			0.0000	4.5029	1.1811	0.5944	1.5750
C4				0.0000	2.6551	4.1913	2.0765
C5					0.0000	1.4921	0.4086
C6						0.0000	1.8231
C7							0.0000

Table 4-4. KW Multiple Comparison Z-Value Tests for Niño-1.2 region stratified by clusters. Text shaded in red or blue indicates significant differences of median Niño-1.2 values at alpha level of 0.05. Text shaded only in red indicates significance using a Bonferroni correction to account for experiment-wide accumulated probability of Type I errors.

Niño-1.2	C1	C2	C3	C4	C5	C6	C7
C1	0.0000	0.4709	0.6646	3.1539	1.7057	0.9658	1.9593
C2		0.0000	0.1925	2.7421	1.3345	1.3192	1.6126
C3			0.0000	2.5787	1.1846	1.4660	1.4727
C4				0.0000	1.0631	3.4173	0.6690
C5					0.0000	2.2379	0.3175
C6						0.0000	2.4431
C7							0.0000

Table 4-5. KW Multiple Comparison Z-Value Tests for Niño-4 region stratified by clusters. Text shaded in red or blue indicates significant differences of median Niño-4 values at alpha level of 0.05. Text shaded only in red indicates significance using a Bonferroni correction to account for experiment-wide accumulated probability of Type I errors.

Niño-4	C1	C2	C3	C4	C5	C6	C7
C1	0.0000	0.5731	0.8373	2.8491	0.0272	2.1490	0.3357
C2		0.0000	0.2625	3.3199	0.4709	1.7067	0.7486
C3			0.0000	3.5429	0.6755	1.5065	0.9394
C4				0.0000	2.3175	4.2364	1.9070
C5					0.0000	1.8476	0.2670
C6						0.0000	2.0219
C7							0.0000

Table 4-6. KW Multiple Comparison Z-Value Tests for Subtropical Dipole Index (SDI) region stratified by clusters. Text shaded in red or blue indicates significant differences of median SDI values at alpha level of 0.05. Text shaded only in red indicates significance using a Bonferroni correction to account for experiment-wide accumulated probability of Type I errors.

SDI	C1	C2	C3	C4	C5	C6	C7
C1	0.0000	0.6145	1.8983	2.1023	1.4886	3.0697	1.0640
C2		0.0000	1.2843	2.6152	1.0129	2.5881	0.6123
C3			0.0000	3.6928	0.0106	1.5729	0.3405
C4				0.0000	3.0512	4.4799	2.6093
C5					0.0000	1.3277	0.3018
C6						0.0000	1.5845
C7							0.0000

Table 4-7. Tropical cyclones by cluster and ENSO/SDI phases. Red (blue) text signifies positive (negative) phase of ENSO or SDI. Western region in orange (Fisher's test p-value 0.00002). Eastern region in green (p-value 0.025). Central region in black (p-value 0.195). The SDI is not available after 2007, hence the sample size is only 181.

	C1	C2	C3	C4	C5	C6	C7	Total
ENSO/SDI	6	9	9	3	4	5	4	40
ENSO/SDI	13	8	4	16	5	0	5	51
ENSO/SDI	10	10	13	1	5	7	2	48
ENSO/SDI	10	11	10	2	2	4	3	42
Total	39	38	36	22	16	16	14	181

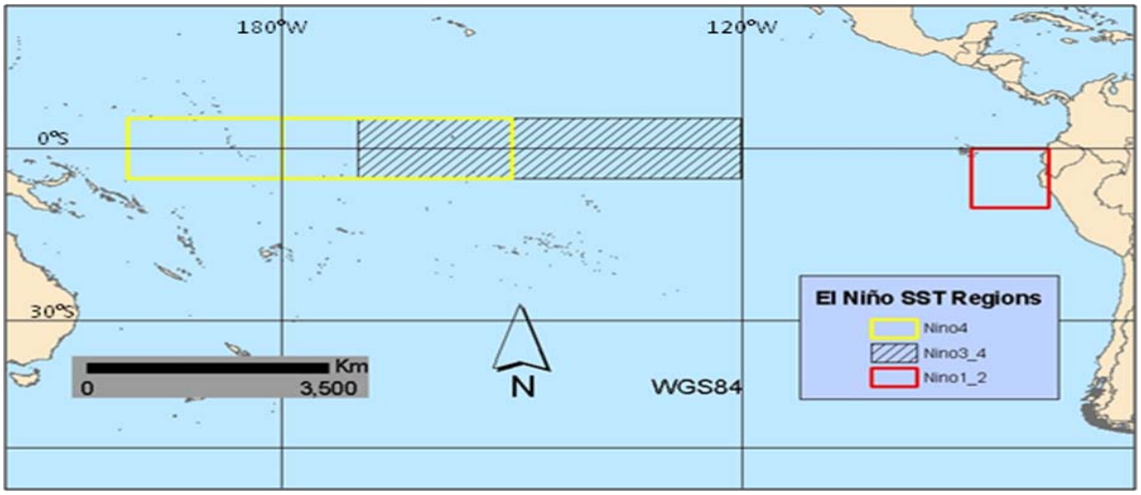

Figure 4-1. El Niño sea surface temperature index regions. Nino-1+2 is outlined in red, Niño-3.4 in hatching, and Niño-4 in yellow.

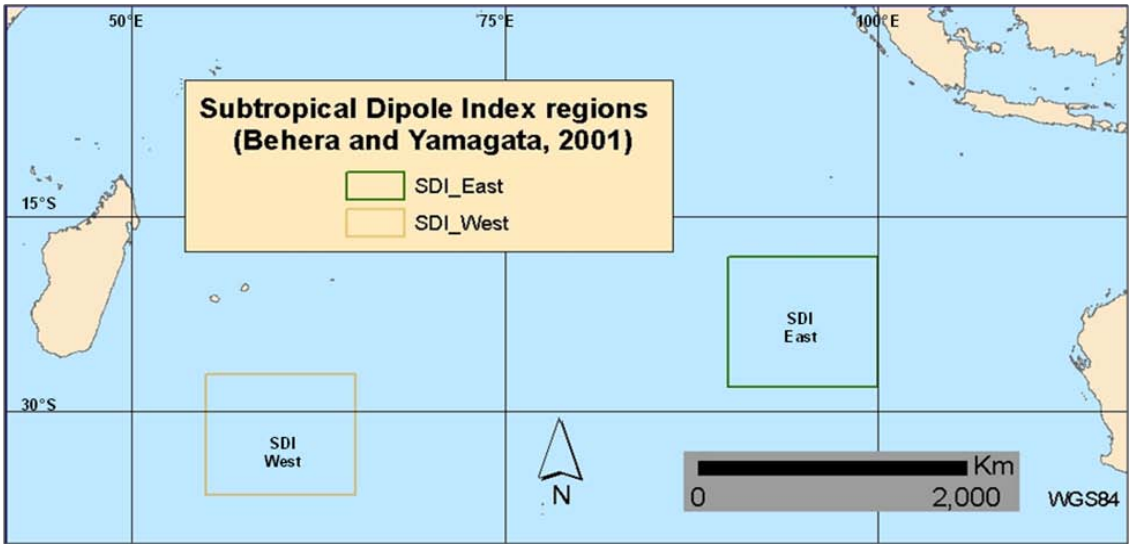

Figure 4-2. Subtropical Dipole Index SST regions. Dipole West (SDI West) in orange, and Subtropical Dipole East (SDI_East) in green.

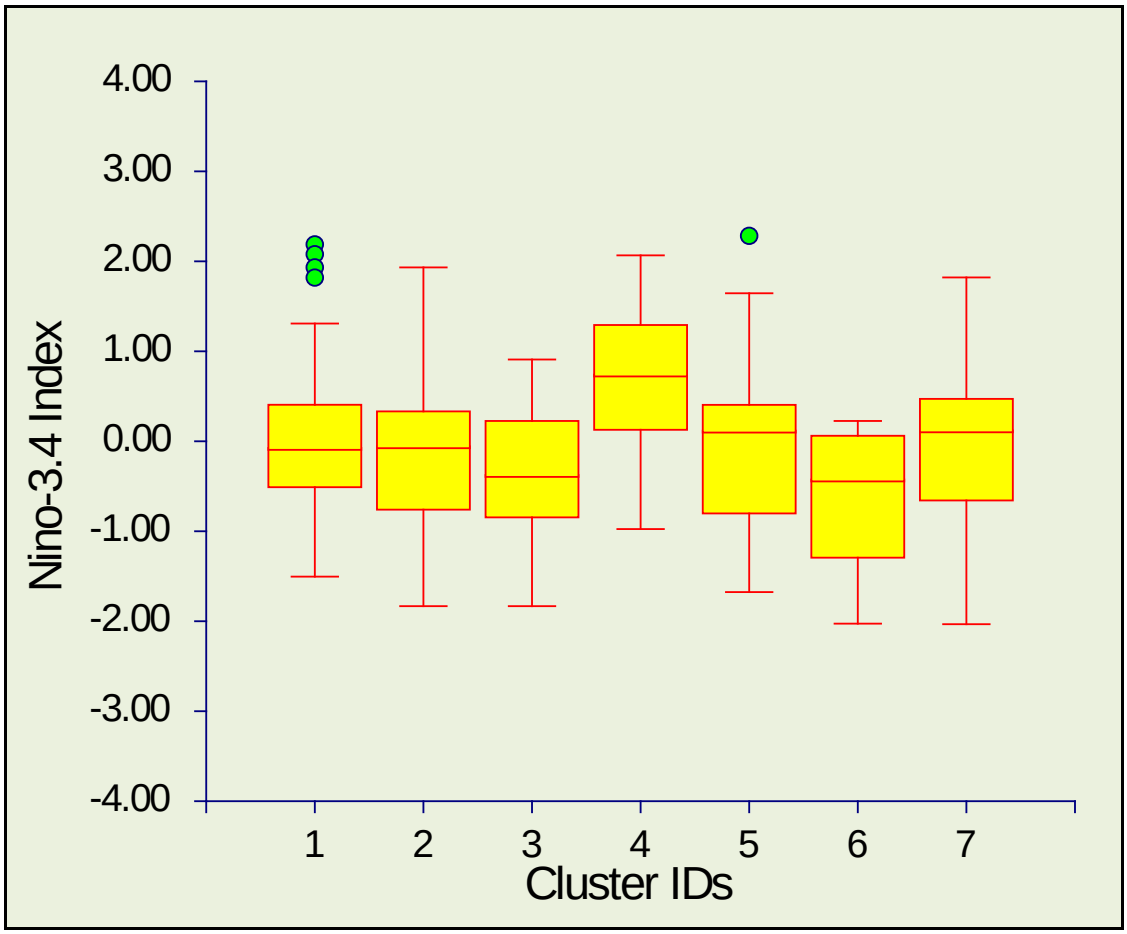

Figure 4-3. Box plots of standardized sea surface temperature anomalies for the Niño-3.4 region stratified by cluster ID.

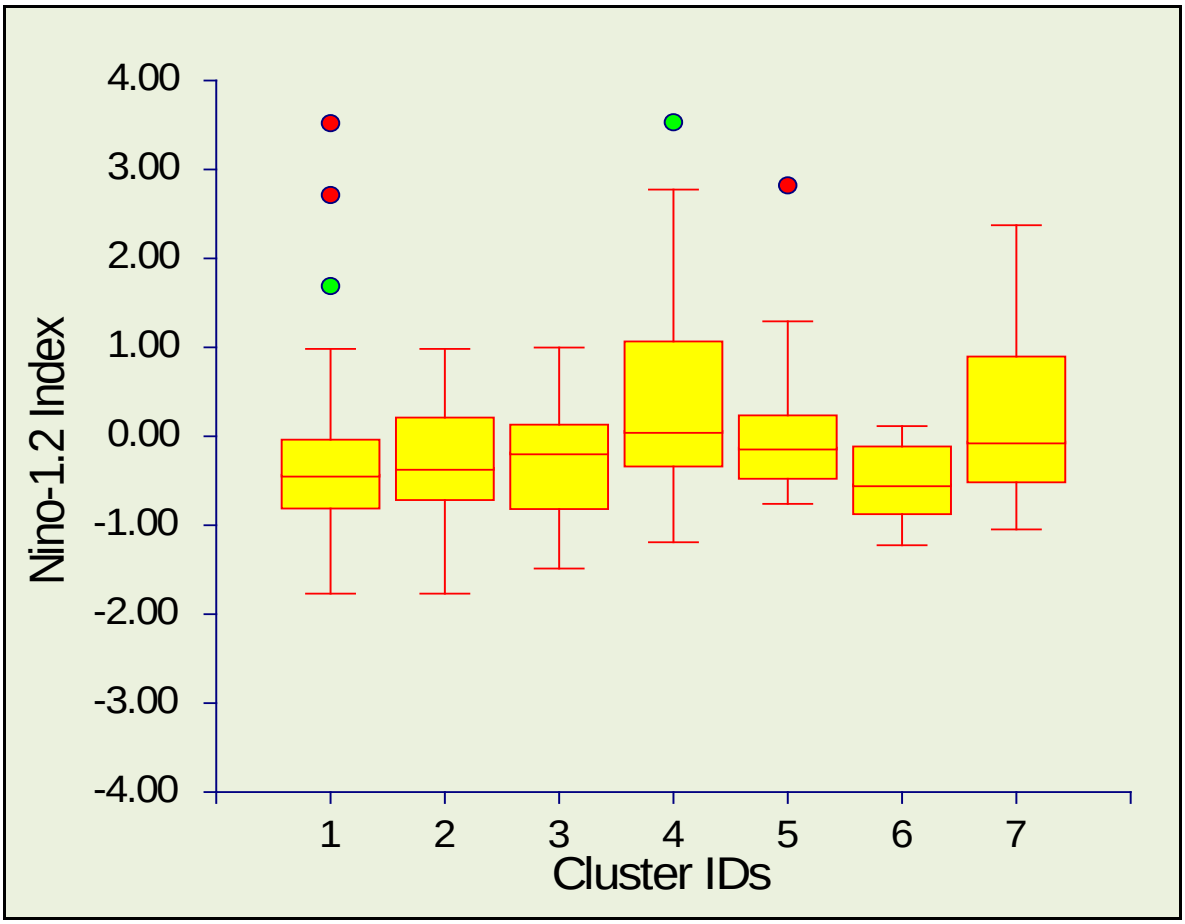

Figure 4-4. Box plots of standardized sea surface temperature anomalies for the Niño-1.2 region stratified by cluster ID.

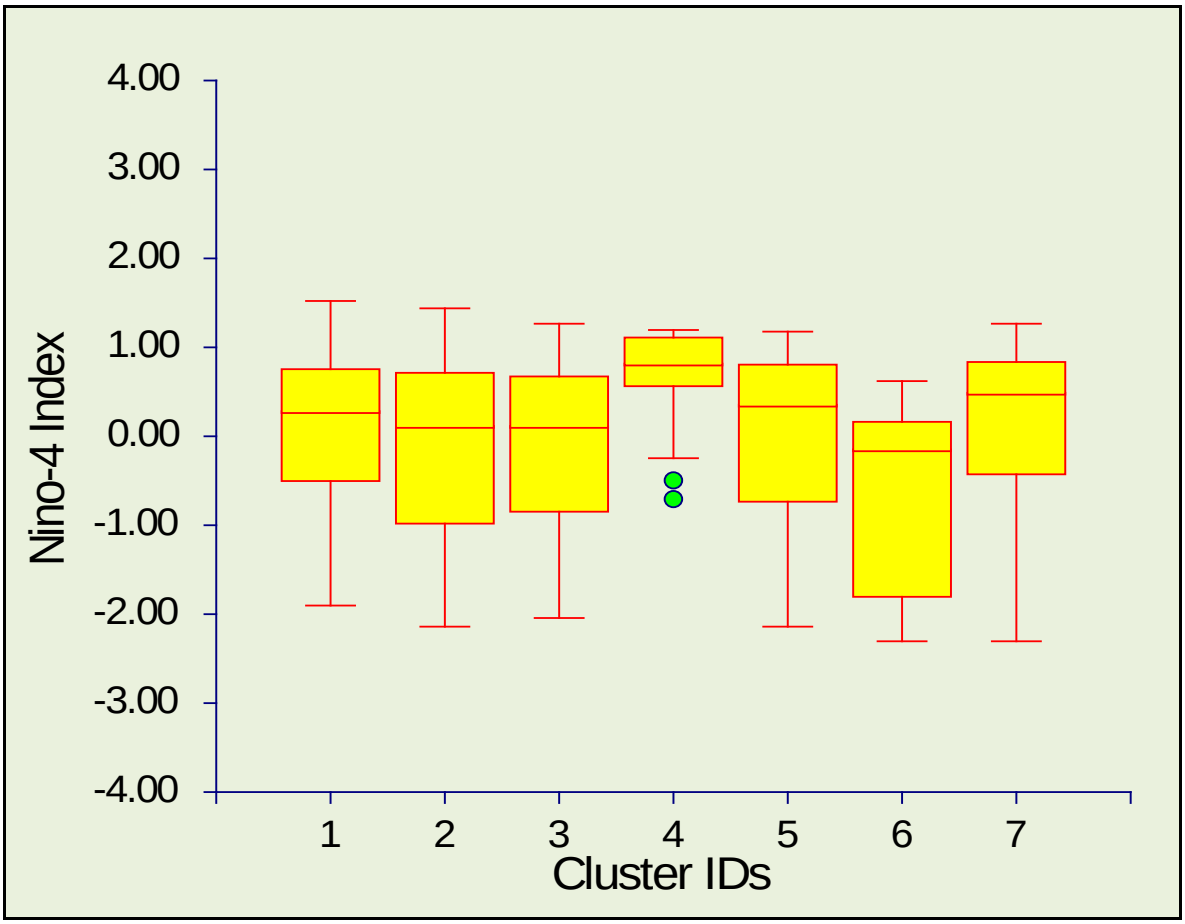

Figure 4-5. Box plots of standardized anomalies for the Niño-4 region stratified by cluster ID.

Figure 4-6. Box plots of standardized anomalies for the Indian Ocean Subtropical Dipole Index (SDI) stratified by cluster ID.

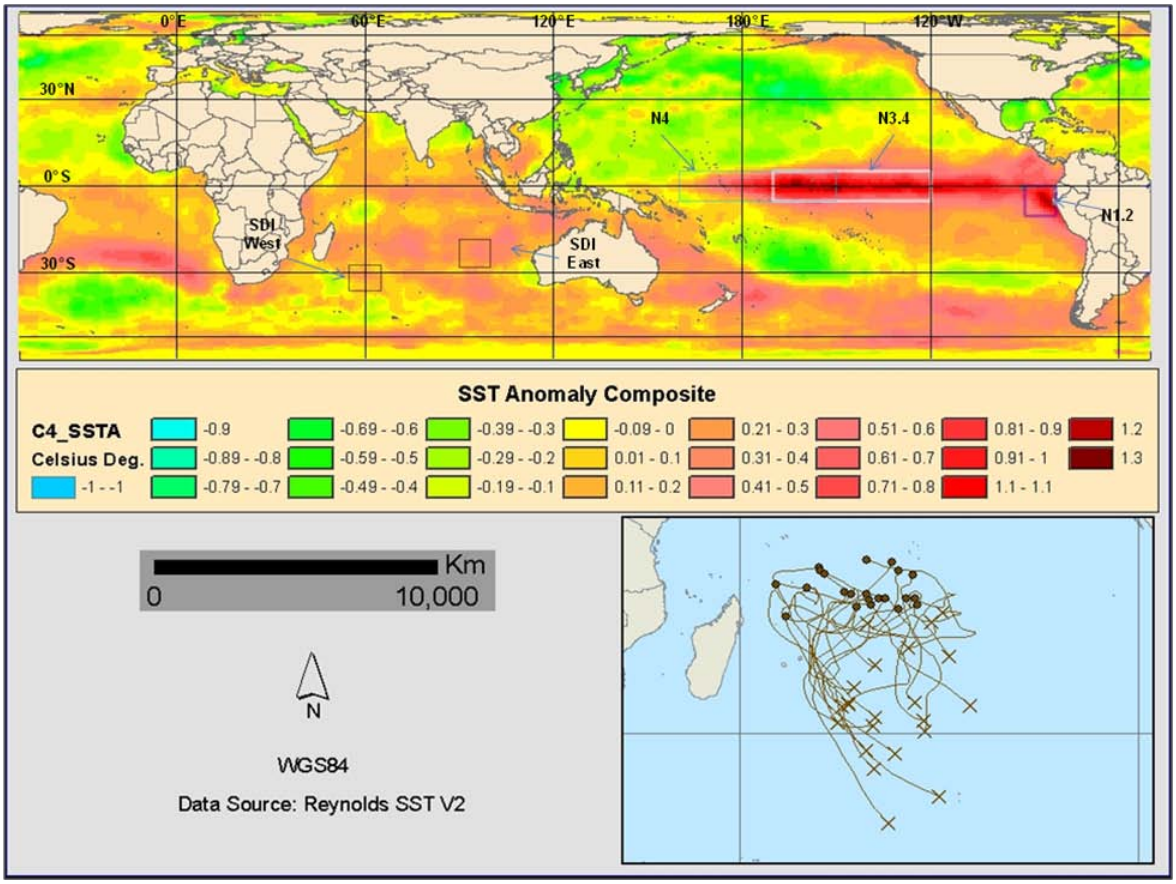

Figure 4-7. Composite map of sea surface temperature anomalies for Cluster 4 (C4), western region, south motion.

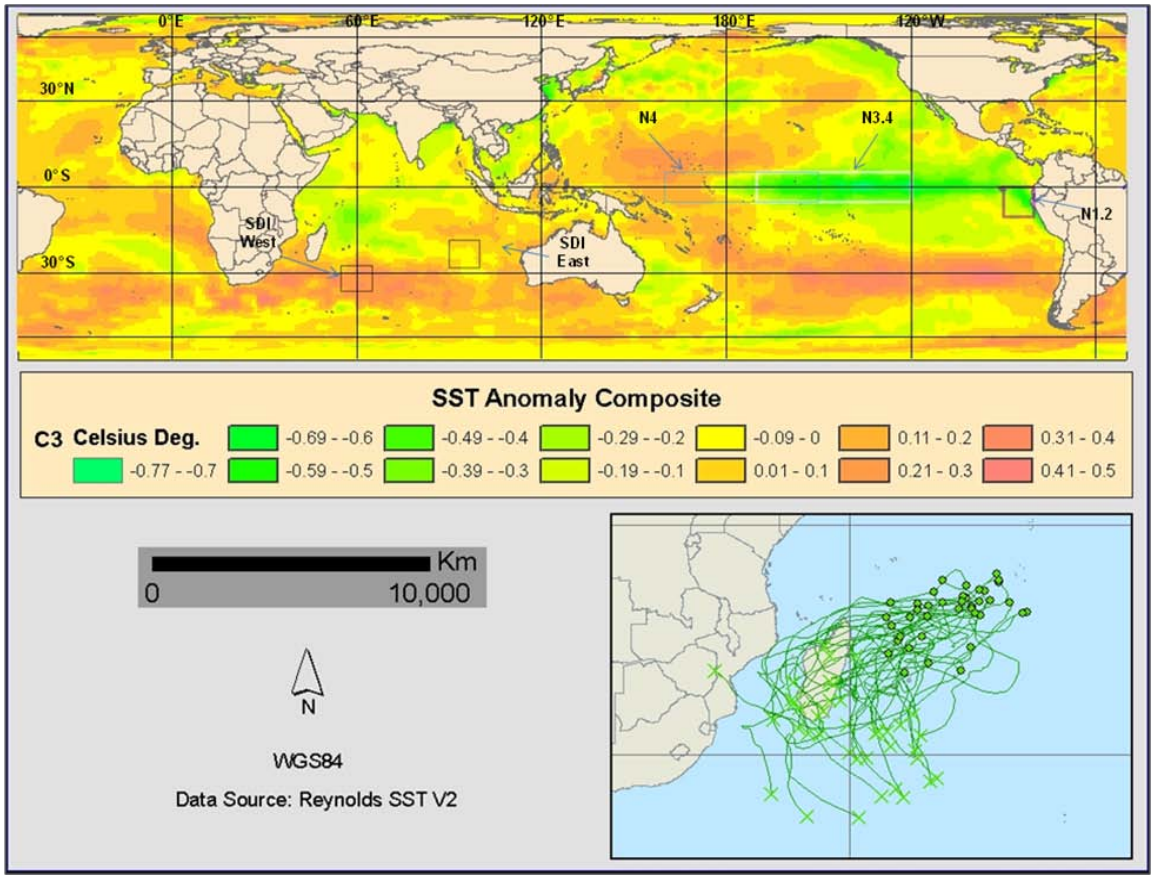

Figure 4-8. Composite map of sea surface temperature anomalies for Cluster 3 (C3), western region, southwest motion.

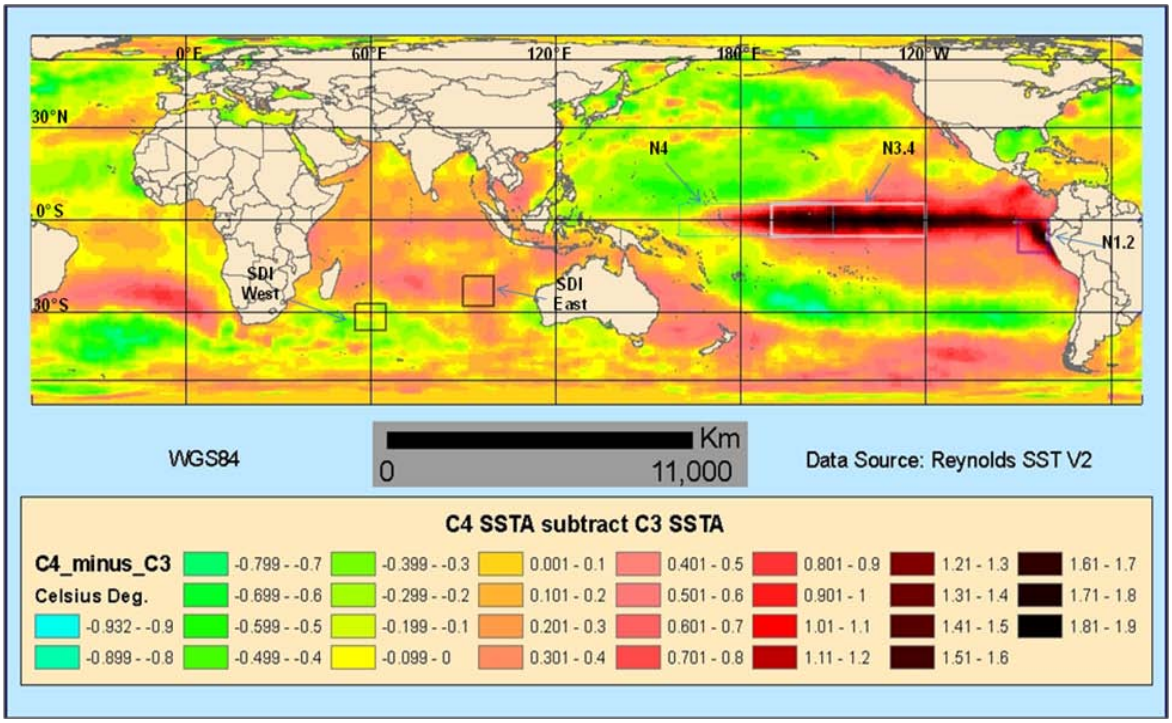

Figure 4-9. Difference of sea surface temperature anomalies between C4 and C3.

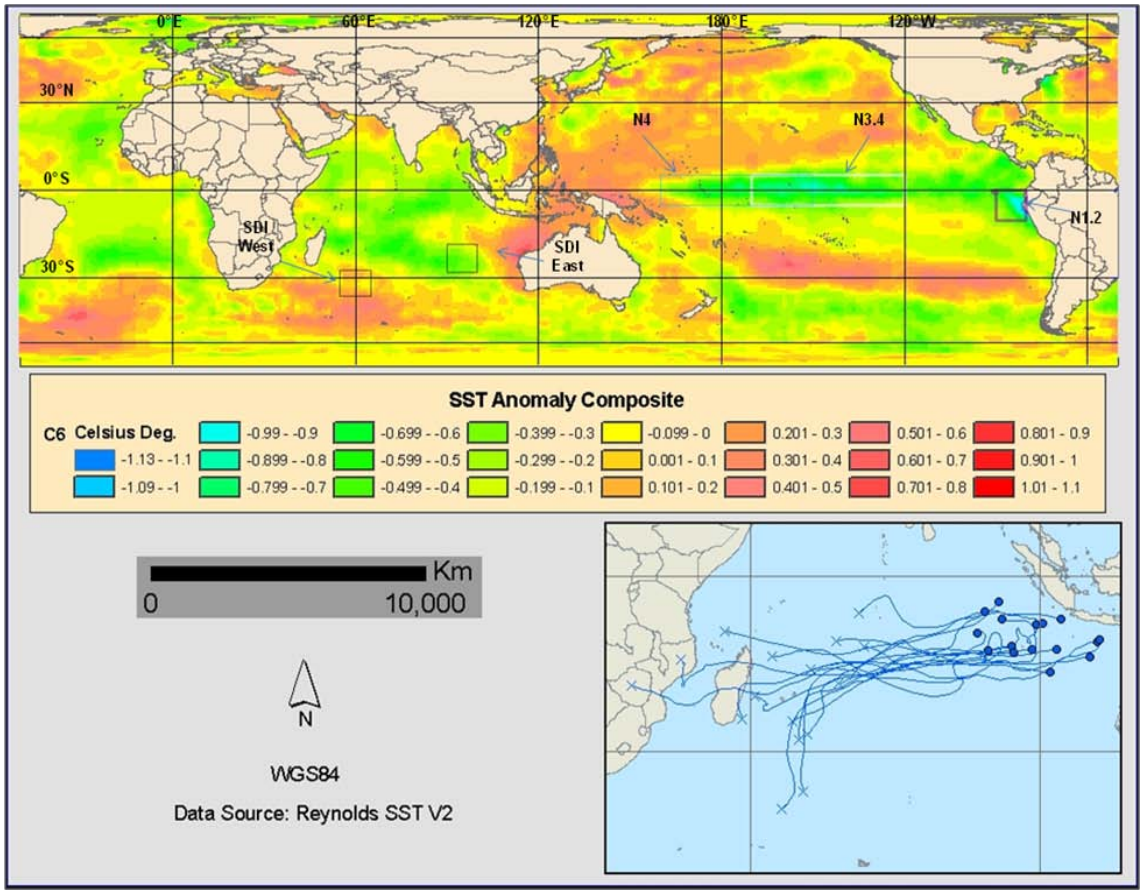

Figure 4-10. Composite map of sea surface temperature anomalies for Cluster 6 (C6), eastern region, west motion.

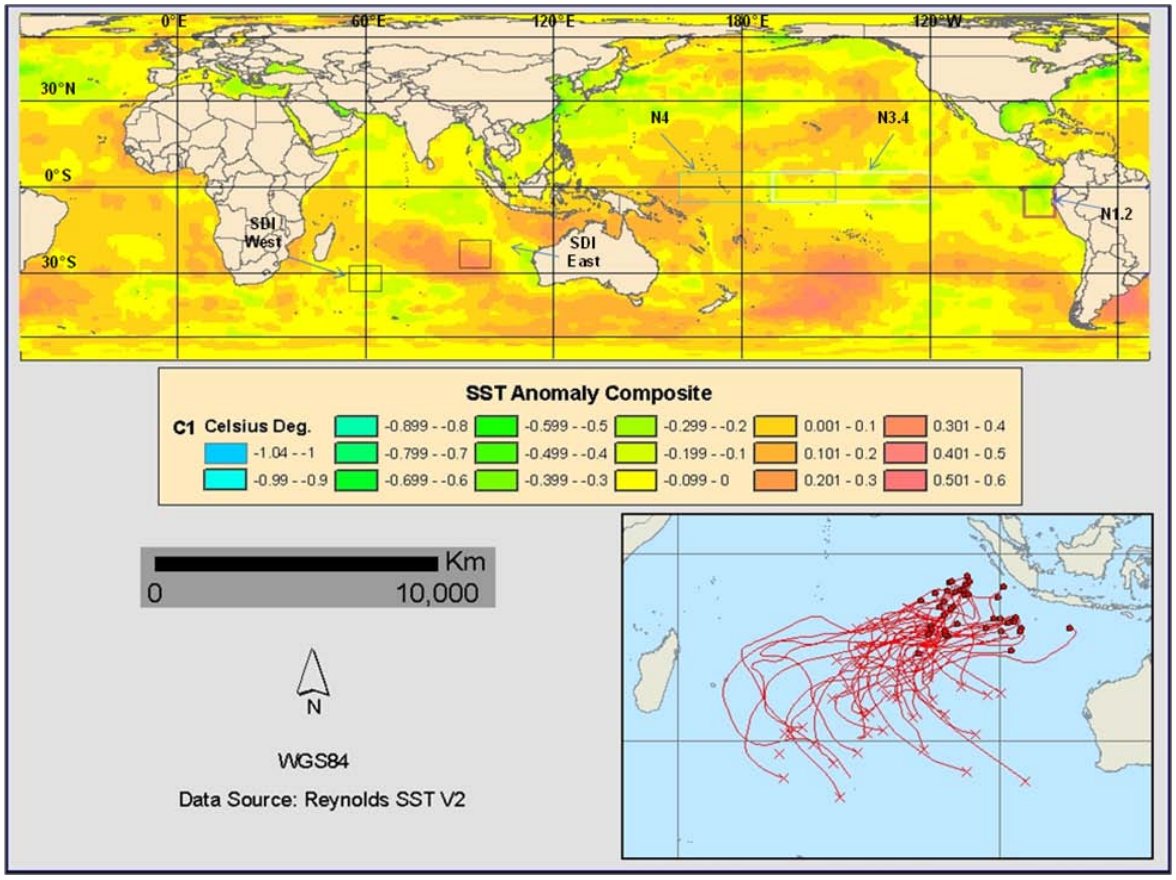

Figure 4-11. Composite map of sea surface temperature anomalies for Cluster 1 (C1), eastern region, south motion.

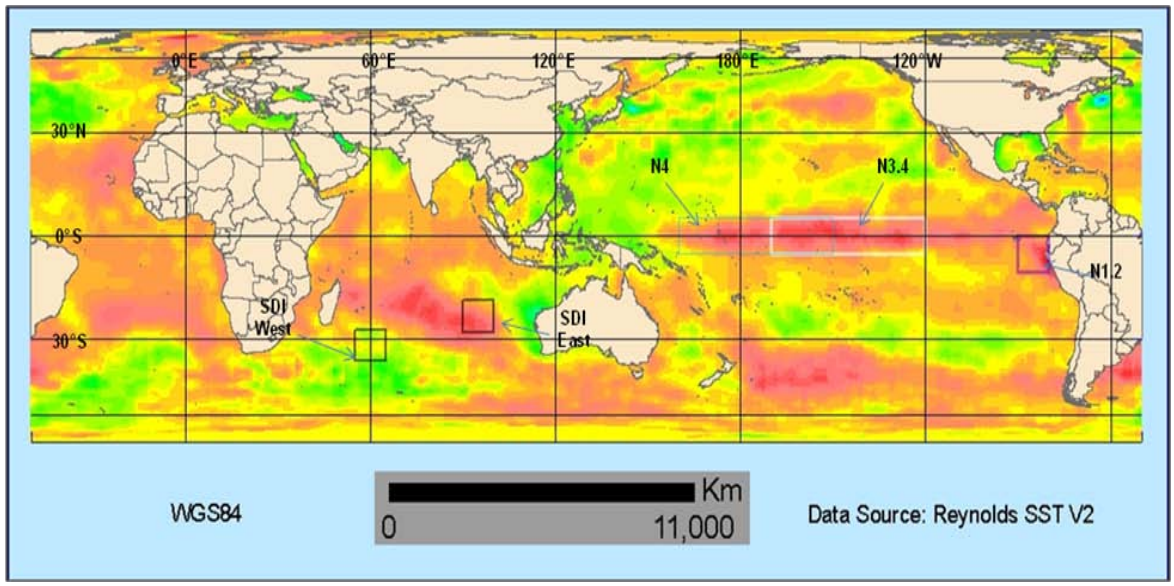

Figure 4-12. Difference of sea surface temperature anomalies between C1 and C6.

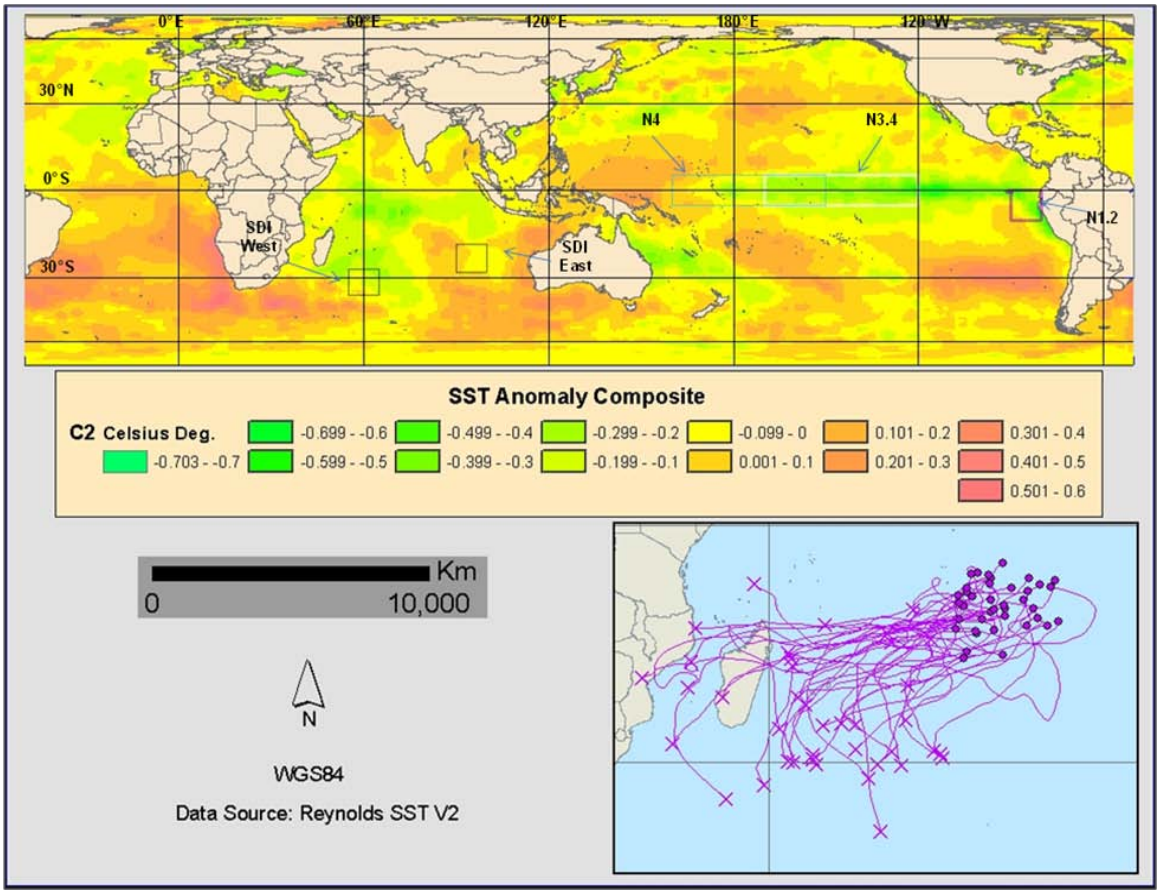

Figure 4-13. Composite map of sea surface temperature anomalies for Cluster 2 (C2), central region, southwest motion.

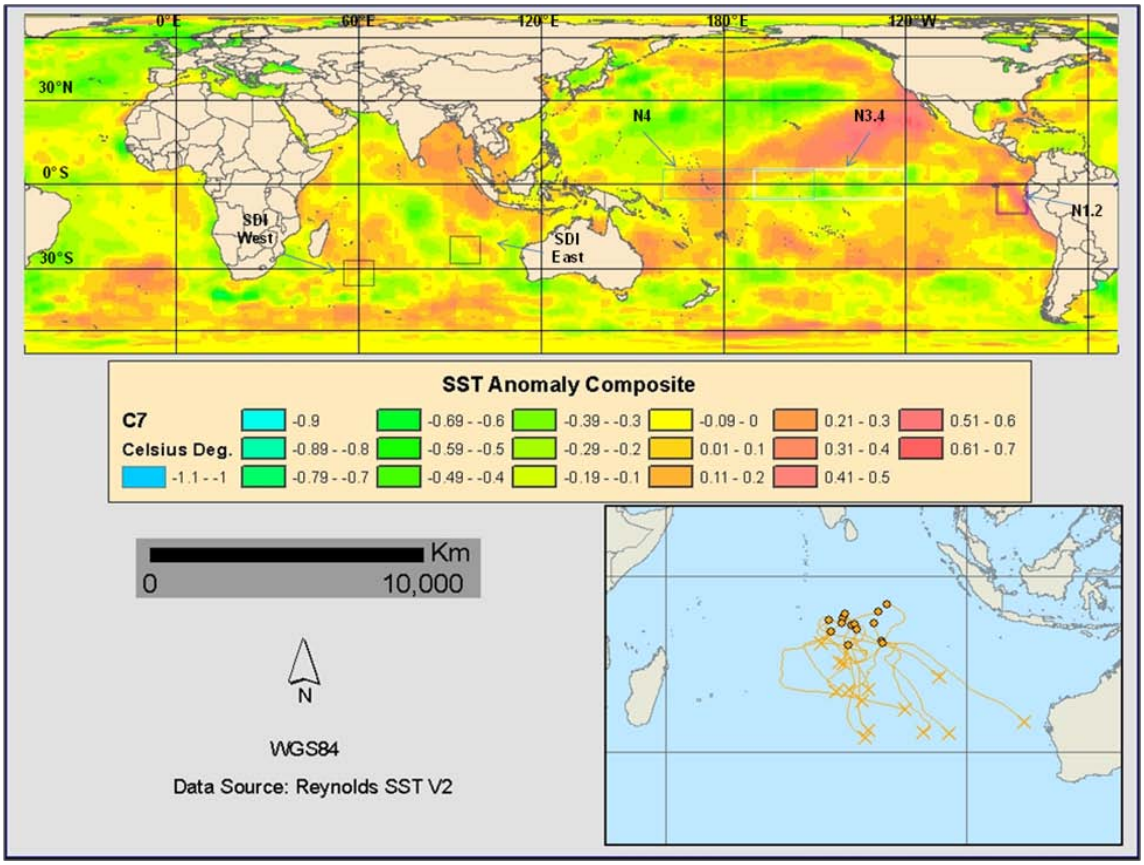

Figure 4-14. Composite map of sea surface temperature anomalies for Cluster 7 (C7), central region, south motion.

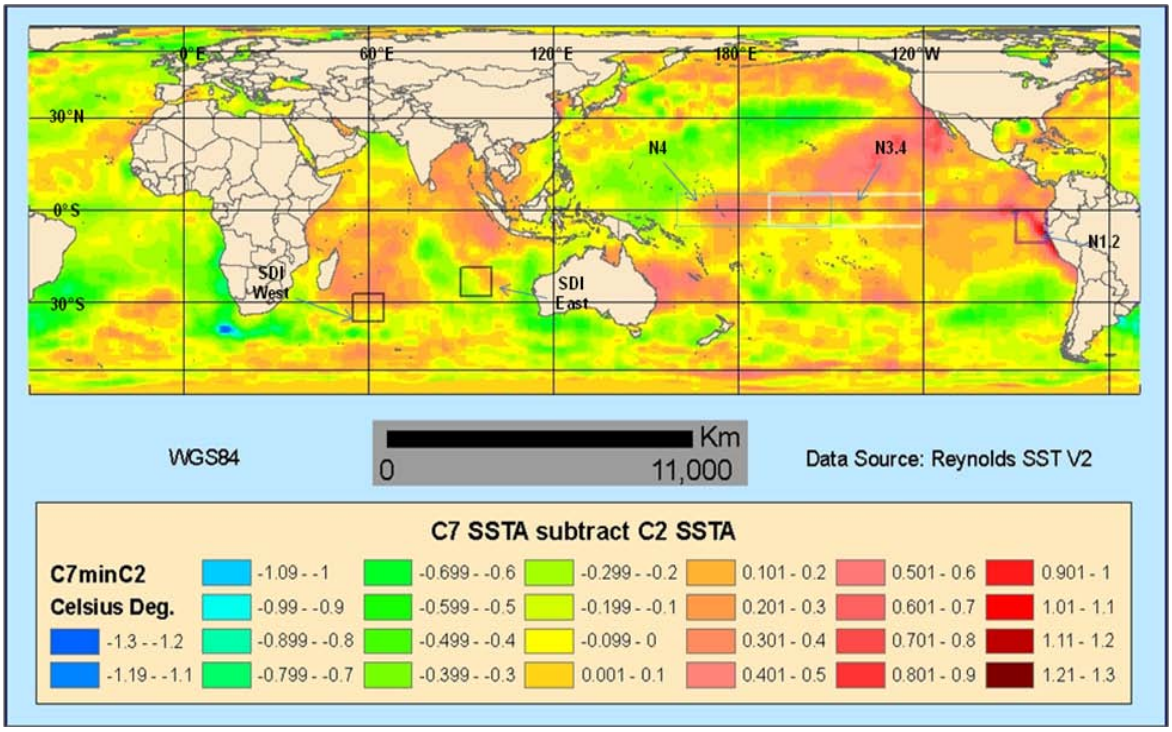

Figure 4-15. Difference of sea surface temperature anomalies between C7 and C2.

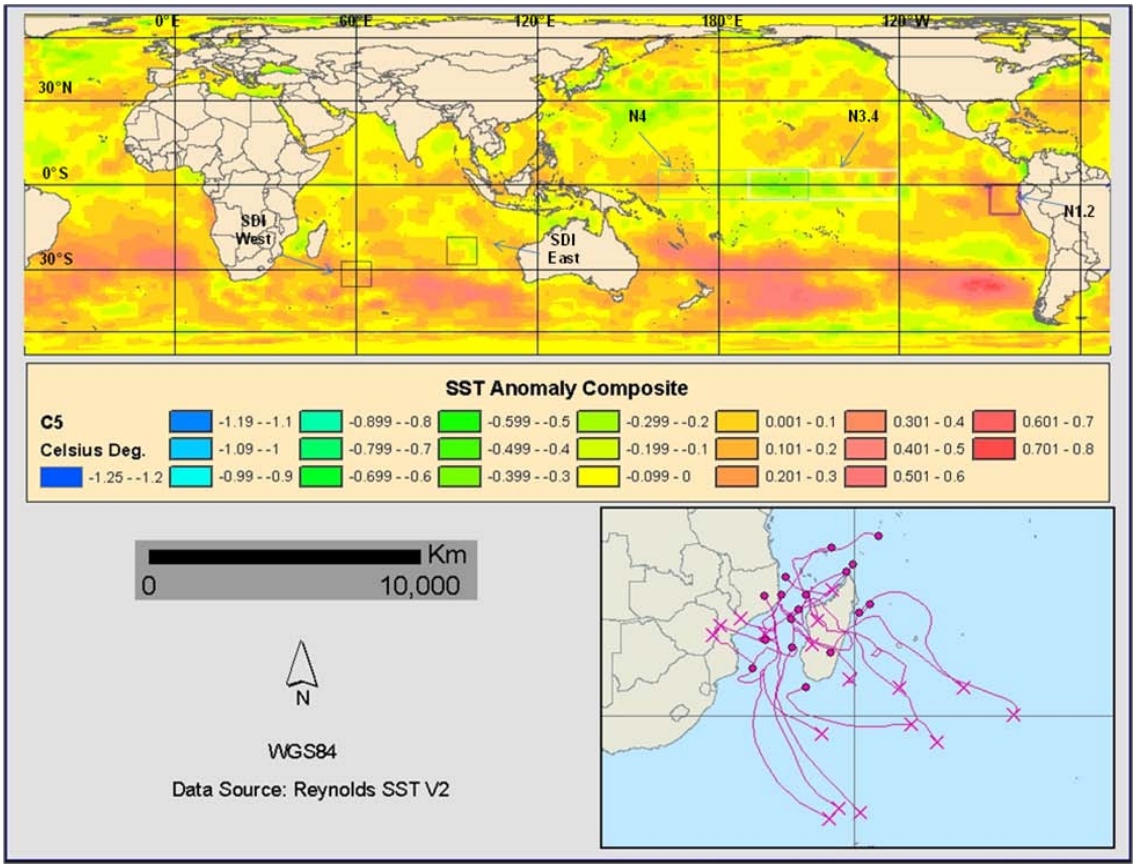

Figure 4-16. Composite map of sea surface temperature anomalies for Cluster 5 (C5), Mozambique Channel region.

CHAPTER 5
CONCLUSIONS

This study tested the hypotheses that tropical cyclone (TC) trajectories in the South Indian Ocean (SIO) are influenced by oceanic-atmospheric variability associated with El-Niño-Southern Oscillation (ENSO) and/or the internal sea surface temperature (SST) dipoles of the subtropical SIO. The significance of this work is largely in testing SIOD for association with SIO TC trajectories to build upon the previously known, but insufficient association with ENSO. The results of Fisher's Test in Chapter 4 hone in on the most specific conclusion from this study: SIOD and ENSO together have the greatest explanatory power for highly exceptional types of TC trajectories such as C4 and C6. These TCs represent easily identifiable departures from normal which occurs when ENSO and SIOD are in anti-phase. In the case of C4, the TCs track southeastward away from land, whereas in the case of C6, TCs track much farther westward than usual and can threaten populated regions of the SIO. It is paramount to understand their potential influence on the tracks of SIO TCs, which regularly threaten and disrupt the lives of the region's inhabitants during the austral warm season.

The broad steering mechanisms of TCs are now well understood, as related to short-term interactions between a TC and its surrounding environment. The goal here was to extend and apply this understanding across a large sample of events to relate the sample of TCs to larger scale synoptic regimes known to vary according to ENSO and SIOD. Hierarchical cluster analysis (CA) was employed to group TCs into four main genesis regions: western (55°E-73°E), central (74°E-86°E), eastern (88°E-104°E), and Mozambique Channel (west of 55°E). Subsequently, these were grouped by the geographic location at which the storms' life cycles ended, which resulted in seven main

groups of SIO TC trajectories, one in the Mozambique Channel and two in each of the other three genesis regions. This structuring allowed for groups from the same TC genesis region but with disparate trajectory directions to be tested in relation to ENSO and SIOD, which are known to associate with changes in the SIO atmospheric circulation.

Using non-parametric Kruskal-Wallis analysis of variance (KW ANOVA), inferential testing was performed for ENSO using the Niño-3.4, Niño-1.2, and Niño-4 indices and for the Subtropical Indian Ocean Dipole (SIOD) using the Subtropical Dipole Index (SDI). The ANOVA results and follow-on multiple comparisons indicated statistically significant differences between groups. Group C4 (western genesis, south and east motion) was more associated with El Niño and the negative mode of SIOD, while group C3 (western genesis, west and southwest motion) was more associated with La Niña and the positive mode of SIOD. Within the eastern genesis region, group C6 (west motion) was more associated with La Niña and negative SIOD, while group C1 (south motion) occurred more often during El Niño and positive SIOD. The findings were cross-validated qualitatively through SST anomaly (SSTA) composite maps which depicted easily discernible spatial SSTA patterns in/near the indexed regions for Niño-3.4 and SDI.

It was not surprising that ENSO phase was implicated by the data as significantly affecting TC trajectories, as this was found before in the SIO and other ocean basins. However, ENSO, while a necessary factor for consideration, is not sufficient to account for variability in SIO TC trajectories. The identification in this study of the SIOD as significantly relating to TC trajectories in the SIO is a new finding. SIOD is known to

associate with strong (weak) subtropical east and southeasterly trade winds and a strong (weak) parent SIO subtropical high during a positive (negative) event. Therefore, during a positive event TCs follow more westward trajectories than normal, swept along within the strong trade winds, as seen in groups C6 and C3.

In contrast, weakened trades during a negative SIOD event allow for extratropical influences on the TC trajectories, as in groups C4 and C1 which display more poleward and eastward movement than their counterparts. Based on previous literature relating to variability in African rainfall, the physical mechanisms proposed to influence this increased poleward motion for groups C4 and C1 are tropical-temperate troughs (TTTs). During a negative SIOD event, the trade winds weaken and shift these TTTs northeast over northern Mozambique and Madagascar and into the western SIO, with the deepest convection sometimes focusing over the warm waters of the western SIO. Concurrent with the weakened subtropical high, mid-latitude troughs penetrate farther equatorward and may interact with the eastward shifted continental African cyclonic circulation to extend anomalous westerlies into the SIO. These atypical winds from the TTTs can extend throughout the troposphere, deep enough to influence the track of a TC to turn poleward or eastward. Therefore, this study is unique in suggesting a link between increased (decreased) tendencies of TC recurvature in the SIO during negative (positive) SIOD events through the mechanism of TTTs.

The TTTs are also known to display very similar patterns during El Niño and La Niña with the negative (positive) SIOD patterns mirroring El Niño (La Niña). However, it has been established that the SIOD can occur largely independent of ENSO. Using the CA structure and stratifying by coincidences of El Niño (La Niña) with both positive and

negative SIOD events, it was found that the frequency of recurving (zonal) moving TCs is enhanced (reduced) when SIOD is negative (positive) and ENSO is simultaneously in warm (cool) phase. This finding builds on the work of Vitart *et al*. (2003), who admitted that while important ENSO does not account for times when SIO TC steering flow varies independent of the ENSO signal. The results from this study suggest SIOD as a useful additional measure to account for the strength of the subtropical high through the SSTA forced by anomalous trade winds. Furthermore, if SIOD is useful in accounting for anomalous TC tracks, then it should also be useful in consideration of vertical wind shear across the SIO. The extent and magnitude of vertical wind shear should in theory relate to the phase and magnitude of SIOD.

There are many more unanswered questions to be addressed. Future work should consider SIOD alongside ENSO when assessing probabilities of TC strikes. However, other relationships should be explored as well. The North Atlantic Oscillation (NAO) is known to affect the circulation and moisture fluxes associated with the convergent zones over southern Africa (McHugh and Rogers, 2001). Chang-Seng and Jury (2010b) also suggested a link between the boreal winter circulation and SIO TC activity via outflow from the Asian monsoon system. These inter-hemispheric exchanges may affect the position and structure of the TTTs and thus whether they may translate eastward over the western SIO. Much more investigation should focus on the causes of variability in the SIO subtropical high, as it is a key mechanism through which TCs either remain at low latitudes or recurve into the temperate westerlies. SIOD may be characterized as a proxy measurement for the trade winds associated with the high, and though use of the Subtropical Dipole Index (SDI) showed statistically significant

results in this study it would be fruitful to represent the broader environmental atmospheric flow with an index not limited to such small centers of action. Reason (2001) noted that rainfall variability in southern Africa is sensitive to the geographic location of the warmest SSTA in the SIOD, meaning that either a larger area could be used to index the SIOD (as in Suzuki *et al*., 2004) or that another index could represent warm SSTA closer to the African coast. Any improved accounting of the position and/or strength of the SIO subtropical high could potentially improve the ability to predict broad trends in SIO TC steering flow.

It is important, especially for the developing nations along the western rim of the SIO, to be able to withstand the impacts of natural disturbances, including TCs. If understanding of teleconnections and the internal variability of the Indian Ocean can be improved, it would be beneficial to forecast whether a TC that might form one or three months in the future will be more or less likely to approach inhabited places. This information would not specify the exact point of landfall, for example, but could be given in probabilistic terms. Given the formation of a hypothetical TC, if some threshold probability were to be exceeded (meaning high confidence in a more westerly or easterly movement), then early disaster plans could be enacted. Crops could be harvested two weeks in advance, while food supplies and other necessary resources could be strategically relocated. The findings and explanations presented in this study can serve to spur further investigation of SIO TC trajectories, as the direction of their movement is of great importance in determining their ultimate societal impacts.

APPENDIX
TROPICAL CYCLONES ANALYZED IN THE PRESENT STUDY

Name	Season	Gen Month	Lys Month	Vmax
Ivan	1979	3	3	60
Albine	1980	11	12	100
Viola/Claudette	1980	12	12	110
Hyacinthe	1980	1	1	70
Jacinthe	1980	2	2	100
Fred	1980	2	2	95
Kolia	1980	2	3	60
Laure	1980	3	3	100
Florine	1981	1	1	105
Johanne	1981	3	3	80
Olga	1981	4	4	120
None	1982	10	10	85
Armelle	1982	11	11	80
Chris/Damia	1982	1	1	120
Justine	1982	3	3	75
Karla	1982	4	5	100
Bemany	1983	11	12	65
Dadafy	1983	12	12	65
Elinah	1983	1	1	65
Naomi	1983	4	4	60
Oscar	1984	10	10	70
Andry	1984	12	12	130
Bakoly	1984	12	12	90
Fanja	1984	1	1	75
Jaminy	1984	2	2	100
Daryl	1984	3	3	75
Kamisy	1984	4	4	100
Celestina	1985	1	1	65
Ditra	1985	1	2	70
Gerimena	1985	2	2	65
Kirsty	1985	3	3	105
Helisaonin	1985	4	4	110
Delifina	1986	1	1	110
Costa	1986	1	1	70
Erinesta	1986	1	2	115
Gista	1986	2	2	85
Honorinina	1986	3	3	110

Name	Season	Gen Month	Lys Month	Vmax
Jefotra	1986	3	4	105
Alison/Krisostoma	1986	4	4	75
Billy_Lila	1986	5	5	95
Alinina	1987	1	1	75
Daodo	1987	3	3	75
Elizabeta	1987	4	4	75
Calidera	1988	1	1	65
Doaza	1988	1	2	115
Gwenda/Ezenina	1988	2	2	90
Filao	1988	2	3	80
Gasitao	1988	3	3	130
Adelinina	1989	10	11	75
Barisaona	1989	11	11	100
Calasanjy	1989	1	1	75
Edme	1989	1	1	115
Firinga	1989	1	2	90
Leon/Hanitra	1989	2	3	125
Gizela	1989	2	2	65
Jinabo	1989	3	3	65
Krisy	1989	3	4	105
Pedro	1990	11	11	65
Alibera	1990	12	1	135
Baomavo	1990	12	1	85
Cezera	1990	2	2	80
Dety	1990	1	2	95
Edisoana	1990	2	3	100
Gregoara	1990	3	3	110
Alison	1991	1	1	65
Bella	1991	1	2	130
Debra	1991	2	3	90
Elma	1991	2	3	60
Fatima	1991	3	4	90
Alexandra	1992	12	12	105
Harriet/Heather	1992	2	3	120
Farida	1992	2	3	120
Jane_Irna	1992	4	4	120
Aviona	1993	9	10	65

Name	Season	Gen Month	Lys Month	Vmax
Colina	1993	1	1	95
Edwina	1993	1	1	110
Finella	1993	2	2	75
Jourdanne	1993	4	4	125
Konita	1993	4	5	90
Alexina	1994	11	11	60
Cecilia	1994	12	12	85
Daisy	1994	1	1	95
Pearl/Farah	1994	1	1	95
Geralda	1994	1	2	145
Hollanda	1994	2	2	105
Ivy	1994	2	2	100
Litanne	1994	3	3	130
Mariola	1994	3	3	90
Nadia	1994	3	4	120
Odille	1994	3	4	105
Albertine	1995	11	12	115
Dorina	1995	1	1	100
Gail	1995	1	2	75
Ingrid	1995	2	3	100
Josta	1995	3	3	65
Kylie	1995	3	3	85
Marlene	1995	3	4	125
Agnielle	1996	11	11	150
Bonita	1996	12	1	135
Hubert/Coryna	1996	1	1	75
Doloresse	1996	2	2	75
Edwige	1996	2	2	95
Flossy	1996	2	3	115
Hansella	1996	4	4	95
Itelle	1996	4	4	140
Jenna	1996	4	5	60
Antoinette	1997	10	10	65
Melanie/Bellamine	1997	10	11	125
Chantelle	1997	11	12	65
Daniella	1997	12	12	120
Phil	1997	12	1	85

Name	Season	Gen Month	Lys Month	Vmax
Fabriola	1997	12	1	60
Pancho/Helinda	1997	1	2	125
Gretelle	1997	1	1	115
Iletta	1997	1	1	75
Josie	1997	2	2	90
Karlette	1997	2	2	65
Lisette	1997	2	3	75
Rhonda	1997	5	5	100
Selwyn	1998	12	1	65
Anacelle	1998	2	2	115
Victor/Cindy	1998	2	2	90
Elsie	1998	3	3	90
Gemma	1998	4	4	70
Alda	1999	1	1	65
Damien/Birenda	1999	1	2	80
Davina	1999	3	3	110
Frederic/Evrina	1999	3	4	140
Astride	2000	12	1	65
Babiola	2000	1	1	90
Connie	2000	1	2	120
Leon/Eline	2000	2	2	115
Felicia	2000	2	2	65
Hudah	2000	3	4	125
Ando	2001	12	1	120
Bindu	2001	1	1	100
Charly	2001	1	1	105
Dera	2001	3	3	90
Evariste	2001	4	4	75
Bessi/Bako	2002	11	12	75
Dina	2002	1	1	130
Eddy	2002	1	1	75
Francesca	2002	1	2	115
Guillaume	2002	2	2	120
Hary	2002	3	3	140
Ikala	2002	3	3	110
Dianne/Jery	2002	4	4	105
Kesiny	2002	5	5	65

Name	Season	Gen Month	Lys Month	Vmax
Boura	2003	11	11	75
Crystal	2003	12	12	90
Ebula	2003	1	1	65
Gerry	2003	2	2	105
Hape	2003	2	2	90
Japhet	2003	2	3	115
Kalunde	2003	3	3	140
Manou	2003	5	5	75
Beni	2004	11	11	100
Cela	2004	12	12	65
Jana	2004	12	12	80
Elita	2004	1	2	65
Frank	2004	1	2	125
Gafilo	2004	3	3	140
Helma	2004	3	3	65
Oscar/Itseng	2004	3	3	115
Juba	2004	5	5	65
Arola	2005	11	11	65
Bento	2005	11	12	140
Chambo	2005	12	1	105
Ernest	2005	1	1	100
Gerard	2005	2	2	60
Hennie	2005	3	3	65
Adeline/Juliet	2005	4	4	125
Bertie/Alvin	2006	11	11	115
Boloetse	2006	1	2	100
Carina	2006	2	3	130
Bondo	2007	12	12	135
Clovis	2007	12	1	65
Dora	2007	1	2	115
Favio	2007	2	2	120
Gamede	2007	2	3	105
Humba	2007	2	3	80
Indlala	2007	3	3	120
Jaya	2007	3	4	110
Ariel	2008	11	11	60
Bongwe	2008	11	11	65

Name	Season	Gen Month	Lys Month	Vmax
Fame	2008	1	2	85
Gula	2008	1	2	90
Hondo	2008	2	2	130
Ivan	2008	2	2	125
Jokwe	2008	3	3	110
Kamba	2008	3	3	115

LIST OF REFERENCES

Anderson DE. 1918. *The Epidemics of Mauritius, with a Descriptive and Historical Account of the Island*. HK Lewis: London.

Behera SK, Salvekar PS, Yamagata T. 2000. Simulation of Interannual SST Variability in the Tropical Indian Ocean. *Journal of Climate* **13**: 3487-3499.

Behera SK, Yamagata T. 2001. Subtropical SST dipole events in the southern Indian Ocean. *Geophysical Research Letters* **28**: 327-330.

Bessafi M, Lasserre-Bigorry A, Neumann CJ, Pignolet-Tardan F, Lee-Ching-Ken, M. 2002. Statistical Prediction of Tropical Cyclone Motion: An Analog-CLIPER Approach. *Weather and Forecasting* **17**: 821-831.

Bessafi M, Wheeler MC. 2006. Modulation of South Indian Ocean Tropical Cyclones by the Madden-Julian Oscillation and Convectively Coupled Equatorial Waves. *Monthly Weather Review* **134**: 638-656.

Bjerknes J. 1969. Atmospheric Teleconnections from the Equatorial Pacific. *Monthly Weather Review* **97**: 163-172.

Blender R, Fraedrich K, Lunkeit F. 1997. Identification of cyclone-track regimes in the North Atlantic. *Quarterly Journal of the Royal Meteorological Society* **123**: 727-741.

Brown ML. 2009. Madagascar's Cyclone Vulnerability and the Global Vanilla Economy. *The Political Economy of Hazards and Disasters*. Eds. Jones EC, Murphy AD. Altamira Press: New York.

Brown MB, Forsythe AB. 1974. Robust Tests for the Equality of Variances *Journal of the American Statistical Association* **69**:364-367.

Buchan A. 1901. Charles Meldrum. *Nature* **65**: 9-11.

Cabin RJ, Mitchell RJ. 2000. To Bonferroni or Not to Bonferroni: When and How Are the Questions. *Bulletin of the Ecological Society of America* **81**: 246-248.

Camargo SJ, Robertson AW, Gaffney SJ, Smyth P, Ghil M. 2007a. Cluster Analysis of Typhoon Tracks. Part I: General Properties. *Journal of Climate* **20**: 3635-3653.

Camargo SJ, Robertson AW, Gaffney SJ, Smyth P, Ghil M. 2007b. Cluster Analysis of Typhoon Tracks. Part II: Large-Scale Circulation and ENSO. *Journal of Climate* **20**: 3654-3676.

Camargo SJ, Emanuel KA, Sobel AH. 2007c. Use of a Genesis Potential Index to Diagnose ENSO Effects on Tropical Cyclone Genesis. *Journal of Climate* **20**: 4819-4834.

Camargo SJ, Robertson AW, Barnston AG, Ghil M. 2008. Clustering of eastern North Pacific tropical cyclone tracks: ENSO and MJO effects. *Geochemistry Geophysics Geosystems* **9**: Q06V05.

Camargo SJ, Sobel AH, Barnston AG, Klotzbach PJ. 2009. The influence of natural climate variability on tropical cyclones and seasonal forecasts of tropical cyclone activity. *Global Perspectives on Tropical Cyclones, 2nd edition*. World Scientific: New York; in press.

Caroff P. Operational practices for best-track elaboration at RSMC La Reunion. Presented 5 May 2009 at the International Best-Track Archive for Climate Stewardship (IBTrACS) Workshop, NOAA National Climatic Data Center, Asheville, NC.

Chambers DP, Tapley BD, Stewart RH. 1999. Anomalous warming in the Indian Ocean coincident with El Niño. *Journal of Geophysical Research* **104**: 3035-3047.

Chan JCL. 2005. The Physics of Tropical Cyclone Motion. *Annual Review of Fluid Mechanics* **37**: 99-128.

Chan JCL, Gray WM. 1982. Tropical Cyclone Movement and Surrounding Flow Relationships. *Monthly Weather Review* **110**: 1354-1374.

Chang-Seng DS, Jury MR. 2010a. Tropical cyclones in the SW Indian Ocean. Part 1: inter-annual variability and statistical prediction. *Meteorology and Atmospheric Physics*, in press.

Chang-Seng DS, Jury MR. 2010b. Tropical cyclones in the SW Indian Ocean. Part 2: structure and impacts at the event scale. *Meteorology and Atmospheric Physics*, in press.

Choi K-S, Kim B-J, Choi C-Y, Nam J-C. 2009. Cluster analysis of Tropical Cyclones making landfall on the Korean Peninsula. *Advances in Atmospheric Sciences* **26**: 202-210.

Chu JH, Sampson CR, Levine AS, Fukada E. 2002. The Joint Typhoon Warning Center tropical cyclone best-tracks, 1945-2000. *Naval Research Laboratory Reference Number NRL/MR/7540-02-16*.

Chu P-S. 2004. ENSO and tropical cyclone activity. *Hurricanes and Typhoons: Past, Present, and Future*. Eds. Murnane RJ, Liu K-B. Columbia University Press: New York.

Cook KH. 2000. The South Indian Convergence Zone and Interannual Rainfall Variability over Southern Africa. *Journal of Climate* **13**: 3789-3804.

Dunn OJ. 1964. Multiple Comparisons Using Rank Sums. *Technometrics* **6**: 241-252.

Dvorak VF. 1975. Tropical Cyclone Intensity Analysis and Forecasting from Satellite Imagery. *Monthly Weather Review* **103**: 420-430.

Elsner JB. 2003. Tracking Hurricanes. *Bulletin of the American Meteorological Society* **84**: 353-356.

Elsner JB, Kara AB. 1999. *Hurricanes of the North Atlantic*. Oxford University Press: New York; 488.

Elsner JB, Liu K-B. 2003. Examining the ENSO-typhoon hypothesis. *Climate Research* **25**: 43-54.

Emanuel K. 2003. Tropical Cyclones. *Annual Review of Earth and Planetary Sciences* **31**: 75-104.

Emanuel K. 2005a. *Divine Wind: The History and Science of Hurricanes*. Oxford University Press: New York; 285.

Emanuel K. 2005b. Increasing destructiveness of tropical cyclones over the past 30 years. *Nature* **436**: 686-688.

England MH, Ummenhofer CC, Santoso A. 2006. Interannual Rainfall Extremes over Southwest Western Australia Linked to Indian Ocean Climate Variability. *Journal of Climate* **19**: 1948-1949.

Evans JL, Allan RJ. El Niño/Southern Oscillation Modification to the Structure of the Monsoon and Tropical Cyclone Activity in the Australasian Region. *International Journal of Climatology* **12**: 611-623.

Fauchereau N, Trzaska S, Richard Y, Roucou P, Camberlin P. 2003. Sea-surface temperature co-variability in the Southern Atlantic and Indian Oceans and its connections with the atmospheric circulation in the Southern Hemisphere. *International Journal of Climatology* **23**: 663-677.

Fauchereau N, Pohl B, Reason CJC, Rouault M, Richard Y. 2009. Recurrent daily OLR patterns in the Southern Africa/Southwest Indian Ocean region, implications for South African rainfall and teleconnections. *Climate Dynamics* **32**: 575-591.

Frank WM, Young GS. 2007. The Interannual Variability of Tropical Cyclones. *Monthly Weather Review* **135**: 3587-3598.

Fritz S, Wexler H. 1960. Cloud Pictures from Satellite TIROS I. *Monthly Weather Review* **88**: 79-87.

Gaffney SJ, Robertson AW, Smyth P, Camargo SJ, Ghil M. 2007. Probabilistic clustering of extratropical cyclones using regression mixture models. *Climate Dynamics* **29**: 423-440.

Gong X, Richman MB. 1995. On the Application of Cluster Analysis to Growing Season Precipitation Data in North America East of the Rockies. *Journal of Climate* **8**: 897-931.

Gray WM, Sheaffer JD. 1991. El Niño and QBO influences on tropical cyclone activity. *Teleconnections linking worldwide climate anomalies*. Eds. Glantz MH, Katz RW, Nicholls N. Cambridge University Press: Cambridge, UK; 535.

Gutzler DS, Harrison DE. 1987. The Structure and Evolution of Seasonal Wind Anomalies over the Near-Equatorial Eastern Indian and Western Pacific Oceans. *Monthly Weather Review* **115**: 169-192.

Hanley DE, Bourassa MA, O'Brien JJ, Smith SR, Spade ER. 2003. A Quantitative Evaluation of ENSO Indices. *Journal of Climate* **16**: 1249-1258.

Harangozo SA, Harrison MSJ. 1983. On the Use of Synoptic Data in Indicating the Presence of Cloud Bands over Southern Africa. *South African Journal of Science* **79**: 413-414.

Harr PA, Elsberry RL. 1991. Tropical Cyclone Track Characteristics as a Function of Large-Scale Circulation Anomalies. *Monthly Weather Review* **119**: 1448-1468.

Harrison DE, Larkin NK. 1998. El Niño-Southern Oscillation Sea Surface Temperature and Wind Anomalies, 1946-1993. *Reviews of Geophysics* **36**: 353-399.

Hastenrath S. 1995. Recent Advances in Tropical Climate Prediction. *Journal of Climate* **8**: 1519-1532.

Hastenrath S. 2000. Zonal Circulations over the Equatorial Indian Ocean. *Journal of Climate* **13**: 2746-2756.

Higgins JJ. 2004. *An Introduction to Modern Nonparametric Statistics*. Brooks/Cole: Pacific Grove, CA; 366.

Ho C-H, Kim J-H, Jeong J-H, Kim H-S, Chen D. 2006. Variation of tropical cyclone activity in the South Indian Ocean: El Niño-Southern Oscillation and Madden-Julian Oscillation effects. *Journal of Geophysical Research* **111**: D22101.

Hope JR, Neumann CJ. 1970. An Operational Technique for Relating the Movement of Existing Tropical Cyclones to Past Tracks. *Monthly Weather Review* **98**: 925-933.

Horel JD, Wallace JM. 1981. Planetary-Scale Atmospheric Phenomena Associated with the Southern Oscillation. *Monthly Weather Review* **109**: 813-829.

Huang B, Shukla J. 2007. Mechanisms for the Interannual Variability in the Tropical Indian Ocean. Part II: Regional Processes. *Journal of Climate* **20**: 2937-2960.

Huang B, Shukla J. 2008. Interannual variability of the South Indian Ocean in observations and a coupled model. *Indian Journal of Marine Sciences* **37**: 13-34.

Julian PR, Chervin RM. 1978. A Study of the Southern Oscillation and Walker Circulation Phenomenon. *Monthly Weather Review* **106**: 1433-1451.

Jury, MR. 1993. A Preliminary Study of Climatological Associations and Characteristics of Tropical Cyclones in the SW Indian Ocean. *Meteorology and Atmospheric Physics* **51**: 101-115.

Jury MR, Pathack B, Wang B, Powell M, Raholijao N. 1993. A Destructive Tropical Cyclone Season in the SW Indian Ocean: January-February 1984. *South African Geographical Journal* **75**: 53-59.

Jury MR, Parker B, Waliser D. 1994. Evolution and Variability of the ITCZ in the SW Indian Ocean: 1988-90. *Theoretical and Applied Climatology* **48**: 187-194.

Jury MR, Pathack B, Parker B. 1999. Climatic Determinants and Statistical Prediction of Tropical Cyclone Days in the Southwest Indian Ocean. *Journal of Climate* **12**: 1738-1746.

Kalnay M, Kanamitsu M, Kistler R, Collins W, Deaven D, Gandin L, Iredell M, Saha S, White G, Woollen J, Zhu Y, Chelliah M, Ebisuzaki W, Higgins W, Janowiak J, Mo KC, Ropelewski C, Wang J, Leetmaa A, Reynolds R, Jenne R, Joseph D. 1996. The NCEP/NCAR 40-Year Reanalysis Project. *Bulletin of the American Meteorological Society* **77**: 437-471.

Karoly DJ. 1989. Southern Hemisphere Circulation Features Associated with El Niño-Southern Oscillation Events. *Journal of Climate* **2**: 1239-1252.

Kidson JW. 1975. Tropical Eigenvector Analysis and the Southern Oscillation. *Monthly Weather Review* **103**: 187-196.

Kim HM, Webster PJ, Curry JA. 2009. Impact of Shifting Patterns of Pacific Ocean Warming on North Atlantic Tropical Cyclones. *Science* **325**: 77-80.

Klein SA, Soden BJ, Lau N-C. 1999. Remote Sea Surface Temperature Variations during ENSO: Evidence for a Tropical Atmospheric Bridge. *Journal of Climate* **12**: 917-932.

Klinman MG, Reason CJC. 2008. On the peculiar storm track of TC Favio during the 2006-2007 Southwest Indian Ocean tropical cyclone season and relationships to ENSO. *Meteorology and Atmospheric Physics* **100**: 233-242.

Klotzbach PJ. 2007. Recent developments in statistical prediction of seasonal Atlantic basin tropical cyclone activity. *Tellus* **59A**: 511-518.

Klotzbach PJ, Barnston AG, Bell G, Camargo SJ, Chan JCL, Lea A, Saunders M, Vitart F. 2010. Seasonal Forecasting of Tropical Cyclones. Ed. Guard C. *Global Guide to Tropical Cyclone Forecasting, 2nd edition*. World Meteorological Organization, in press.

Knaff JA. 2009. Revisiting the maximum intensity of recurving tropical cyclones. *International Journal of Climatology* **29**: 827-837.

Knaff JA, Sampson CR. 2009. Southern hemisphere tropical cyclone intensity forecast methods at the Joint Typhoon Warning Center, Part I: control forecasts based on climatology and persistence. *Australian Meteorological and Oceanographic Journal* **58**: 1-7.

Kruskal WH, Wallis WA. 1952. Use of Ranks in One-Criterion Variance Analysis. *Journal of the American Statistical Association* **47**: 583-621.

Kuleshov Y, de Hoedt G. 2003. Tropical Cyclone Activity in the Southern Hemisphere. *Bulletin of the Australian Meteorological and Oceanographic Society* **16**: 135-137.

Kuleshov Y, Qi L, Fawcett R, Jones D. 2008. On tropical activity in the Southern Hemisphere: Trends and the ENSO connection. *Geophysical Research Letters* **35**: L14S08.

Kuleshov Y, Ming FC, Qi L, Chouaibou I, Hoareau C, Roux F. 2009. Tropical cyclone genesis in the Southern Hemisphere and its relationship with the ENSO. *Annales Geophysicae* **27**: 2523-2538.

Lander MA. 1994. An Exploratory Analysis of the Relationship between Tropical Storm Formation in the Western North Pacific and ENSO. *Monthly Weather Review* **122**: 636-651.

Landsea, CW. 2000. El Niño-Southern Oscillation and the seasonal predictability of tropical cyclones. *El Niño: Impacts of Multiscale Variability on Natural Ecosystems and Society*. Eds. Diaz HF, Markgraf V. Cambridge University Press: Cambridge, UK.

Landsea CW, Bell GD, Gray WM, Goldenberg SB. 1998. The Extremely Active 1995 Atlantic Hurricane Season: Environmental Conditions and Verification of Seasonal Forecasts. *Monthly Weather Review* **126**: 1174-1193.

Larkin NK, Harrison DE. 2002. ENSO Warm (El Niño) and Cold (La Niña) Event Life Cycles: Ocean Surface Anomaly Patterns, Their Symmetries, Asymmetries, and Implications. *Journal of Climate* **15**: 1118-1140.

Lattin JM, Carroll JD, Green PE. 2003. *Analyzing Multivariate Data*. Brooks/Cole: Pacific Grove, CA; 556.

Lau N-C, Nath MJ. 2003. Atmosphere-Ocean Variations in the Indo-Pacific Sector during ENSO Episodes. *Journal of Climate* **16**: 3-20.

Leroy A, Wheeler MC. 2008. Statistical Prediction of Weekly Tropical Cyclone Activity in the Southern Hemisphere. *Monthly Weather Review* **136**: 3637-3654.

Liebmann B, Smith CA. 1996. Description of a Complete (Interpolated) Outgoing Longwave Radiation Dataset. *Bulletin of the American Meteorological Society* **77**: 1275-1277.

Lindesay JA, Harrison MSJ, Haffner MP. 1986. The Southern Oscillation and South African rainfall. *South African Journal of Science* **82**: 196-198.

Love G. 1985. Cross-Equatorial Interactions during Tropical Cyclogenesis. *Monthly Weather Review* **113**: 1499-1509.

Lyons SW. 1991. Origins of Convective Variability over Equatorial Southern Africa during Austral Summer. *Journal of Climate* **4**: 23-39.

Manhique AJ, Reason CJC, Rydberg L, Fauchereau N. 2009. ENSO and Indian Ocean sea surface temperatures and their relationships with tropical temperate troughs over Mozambique and the Southwest Indian Ocean. *International Journal of Climatology*, in press.

Mason SJ, Jury MR. 1997. Climatic variability and change over southern Africa: a reflection on underlying processes. *Progress in Physical Geography* **21**: 23-50.

Mavume AF, Rydberg L, Rouault M, Lutjeharms JRE. 2009. Climatology and Landfall of Tropical Cyclones in the South-West Indian Ocean. *Western Indian Ocean Journal of Marine Science* **8**: 15-36.

McHugh MJ, Rogers JC. 2001. North Atlantic Oscillation Influence on Precipitation Variability around the Southeast African Convergence Zone. *Journal of Climate* **14**: 3631-3642.

Meehl GA. 1987. The Annual Cycle and Interannual Variability in the Tropical Pacific and Indian Ocean Regions. *Monthly Weather Review* **115**: 27-50.

Merrill, RT. 1988. Environmental Influences on Hurricane Intensification. *Journal of the Atmospheric Sciences* **45**: 1678-1687.

Miyasaka T, Nakamura H. 2010. Structure and Mechanisms of the Southern Hemisphere Summertime Subtropical Anticyclones. *Journal of Climate*, submitted for publication.

Murnane RJ. 2004. Introduction. *Hurricanes and Typhoons: Past, Present, and Future*. Eds. Murnane RJ, Liu K-B. Columbia University Press: New York.

Naeraa M, Jury MR. 1998. Tropical Cyclone Composite Structure and Impacts over Eastern Madagascar During January-March 1994. *Meteorology and Atmospheric Physics* **65**: 43-53.

Namias J. 1976. Some Statistical and Synoptic Characteristics Associated with El Niño. *Journal of Physical Oceanography* **6**: 130-138.

Neumann CJ, Randrianarison EA. 1976. Statistical Prediction of Tropical Cyclone Motion over the Southwest Indian Ocean. *Monthly Weather Review* **104**: 76-85.

Nicholson SE. 1997. An Analysis of the ENSO Signal in the Tropical Atlantic and Western Indian Oceans. *International Journal of Climatology* **17**: 345-375.

Nicholson SE. 2003. Comments on “The South Indian Convergence Zone and Interannual Rainfall Variability over Southern Africa” and the Question of ENSO’s Influence on Southern Africa. *Journal of Climate* **16**: 555-562.

Oort AH, Yienger JJ. 1996. Observed Interannual Variability in the Hadley Circulation and Its Connection to ENSO. *Journal of Climate* **9**: 2751-2767.

Pan YH, Oort AH. 1983. Global Climate Variations Connected with Sea Surface Temperature Anomalies in the Eastern Equatorial Pacific Ocean for the 1958-73 Period. *Monthly Weather Review* **111**: 1244-1258.

Parker BA, Jury MR. 1999. Synoptic environment of composite tropical cyclones in the South-West Indian Ocean. *South African Journal of Marine Science* **21**: 99-115.

Parker D. 1999. Criteria for Evaluating the Condition of a Tropical Cyclone Warning System. *Disasters* **23**: 193-216.

Pearson M. 2003. *The Indian Ocean: Seas in History*. Series Ed. Scammell G. Routledge: London.

Philander SGH. 1985. El Niño and La Niña. *Journal of the Atmospheric Sciences* **42**: 2652-2662.

Pielke RA Jr, Pielke RA Sr. 1997. *Hurricanes: Their Nature and Impacts on Society*. John Wiley: New York; 279.

Pohl B, Fauchereau N, Richard Y, Rouault M, Reason CJC. 2009. Interactions between synoptic, intraseasonal and interannual convective variability over Southern Africa. *Climate Dynamics* **33**: 1033-1050.

Reason CJC. 2001. Subtropical Indian Ocean SST dipole events and southern African rainfall. *Geophysical Research Letters* **28**: 2225-2227.

Reason CJC. 2002. Sensitivity of the Southern African Circulation to Dipole Sea-Surface Temperature Patterns in the South Indian Ocean. *International Journal of Climatology* **22**: 377-393.

Reason CJC. 2007. Tropical cyclone Dera, the unusual 2000/01 tropical cyclone season in the southwest Indian Ocean and associated rainfall anomalies over Southern Africa. *Meteorology and Atmospheric Physics* **97**: 181-188.

Reason CJC, Allan RJ, Lindesay JA, Ansell TJ. 2000. ENSO and Climatic Signals Across the Indian Ocean Basin in the Global Context: Part I, Interannual Composite Patterns. *International Journal of Climatology* **20**: 1285-1327.

Reason CJC, Keibel A. 2004. Tropical Cyclone Eline and Its Unusual Penetration and Impacts over the Southern African Mainland. *Weather and Forecasting* **19**: 789-805.

Reynolds RW, Rayner NA, Smith TM, Stokes DC, Wang W. 2002. An Improved In Situ and Satellite SST Analysis for Climate. *Journal of Climate* **15**: 1609-1625.

Roberts SE, Marlow PB. 2002. Casualties in dry bulk shipping (1963-1996). *Marine Policy* **26**: 437-450.

Romesburg HC. 1984. *Cluster Analysis for Researchers*. Wadsworth: North Carolina; 334.

Roux F, Chane-Ming F, Lasserre-Bigorry A, Nuissier O. 2004. Structure and Evolution of Intense Tropical Cyclone Dina near La Réunion on 22 January 2002: GB-EVTD Analysis of Single Doppler Radar Observations. *Journal of Atmospheric and Oceanic Technology* **21**: 1501-1518.

Saji NH, Goswami BN, Vinayachandran PN, Yamagata T. 1999. A dipole mode in the tropical Indian Ocean. *Nature* **401**: 360-363.

Sampson CR, Goerss JS, Schrader AJ. 2005. A concensus track forecast for southern hemisphere tropical cyclones. *Australian Meteorological Magazine* **54**: 115-119.

Shanko D, Camberlin P. 1998. The Effects of the Southwest Indian Ocean Tropical Cyclones on Ethiopian Drought. *International Journal of Climatology* **18**: 1373-1388.

Silva JA, Eriksen S, Ombe ZA. 2010. Double exposure in Mozambique's Limpopo River Basin. *The Geographical Journal*, in press.

Streten NA. 1973. Some Characteristics of Satellite-Observed Bands of Persistent Cloudiness Over the Southern Hemisphere. *Monthly Weather Review* **101**: 486-495.

Suzuki R, Behera SK, Iizuka S, Yamagata T. 2004. Indian Ocean subtropical dipole simulated using a coupled general circulation model. *Journal of Geophysical Research* **109**: C09001.

Todd M, Washington R. 1998. Extreme Daily Rainfall in Southern African and Southwest Indian Ocean Tropical-Temperate Links. *South African Journal of Science* **94**: 64-70.

Todd M, Washington R. 1999. Circulation anomalies associated with tropical-temperate troughs in southern Africa and the south west Indian Ocean. *Climate Dynamics* **15**: 937-951.

Todd MC, Washington R, Palmer PI. 2004. Water Vapour Transport Associated with Tropical-Temperate Trough Systems over Southern Africa and the Southwest Indian Ocean. *International Journal of Climatology* **24**: 555-568.

Trenberth KE. 1976. Spatial and temporal variations of the Southern Oscillation. *Quarterly Journal of the Royal Meteorological Society* **102**: 639-653.

Trenberth KE. 1990. Recent Observed Interdecadal Climate Changes in the Northern Hemisphere. *Bulletin of the American Meteorological Society* **71**: 988-993.

Trenberth KE. 1991. General Characteristics of El Niño-Southern Oscillation. *Teleconnections linking worldwide climate anomalies*. Eds. Glantz MH, Katz RW, Nicholls N. Cambridge University Press: Cambridge, UK; 535.

Trenberth KE. 1997. The Definition of El Niño. *Bulletin of the American Meteorological Society* **78**: 2771-2777.

Trenberth KE, Caron JM. 2000. The Southern Oscillation Revisited: Sea Level Pressures, Surface Temperatures, and Precipitation. *Journal of Climate* **13**: 4358-4365.

Trenberth KE, Stepaniak DP. 2001. Indices of El Niño Evolution. *Journal of Climate* **14**: 1697-1701.

Trigo IF, Davies TD, Bigg GR. 1999. Objective Climatology of Cyclones in the Mediterranean Region. *Journal of Climate* **12**: 1685-1696.

Tyson PD, Preston-Whyte RA. 2000. *The Weather and Climate of Southern Africa*. Oxford University Press: Oxford, UK; 396.

Uppala SM, Kallberg PW, Simmons AJ, Andrae U, Da Costa Bechtold V, Fiorino M, Gibson JK, Haseler J, Hernandez A, Kelly GA, Li X, Onogi K, Saarinen S, Sokka N, Allan RP, Andersson E, Arpe K, Balmaseda MA, Beljaars ACM, Van De Berg L, Bidlot J, Bormann N, Caires S, Chevallier F, Dethof A, Dragosavac M, Fisher M, Fuentes M, Hagemann S, Holm E, Hoskins BJ, Isaksen L, Janssen PAEM, Jenne R, Mcnally AP, Mahfouf JF, Morcette JJ, Rayner NA, Saunders RW, Simon P, Sterl A, Trenberth KE, Untch A, Vasiljevic D, Viterbo P, Woollen J. 2006. The ERA-40 re-analysis. *The Quarterly Journal of the Royal Meteorological Society* **131**: 2961-3012.

van Loon H, Madden RA. 1981. The Southern Oscillation. Part I: Global Associations with Pressure and Temperature in Northern Winter. *Monthly Weather Review* **109**: 1150-1162.

van Loon H, Rogers JC. 1981. The Southern Oscillation. Part II: Associations with Changes in the Middle Troposphere in the Northern Winter. *Monthly Weather Review* **109**: 1163-1168.

Visher SS. 1922. Tropical Cyclones in Australia and the South Pacific and Indian Oceans. *Monthly Weather Review* **50**: 288-295.

Vitart F, Anderson D, Stockdale T. 2003. Seasonal Forecasting of Tropical Cyclone Landfall over Mozambique. *Journal of Climate* **16**: 3932-3945.

Wang Y, Holland GJ. 1996. Tropical Cyclone Motion and Evolution in Vertical Shear. *Journal of the Atmospheric Sciences* **53**: 3313-3332.

Ward RDC. 1902. Current Notes on Meteorology. *Science* **15**:435-437.

Washington R, Todd M. 1999. Tropical-Temperate Links in Southern African and Southwest Indian Ocean Satellite-Derived Daily Rainfall. *International Journal of Climatology* **19**: 1601-1616.

Washington R, Preston A. 2006. Extreme wet years over southern Africa: Role of Indian Ocean sea surface temperatures. *Journal of Geophysical Research* **111**: D15104.

Waylen PR, Henworth S. 1996. A Note on the Timing of Precipitation Variability in Zimbabwe as Related to the Southern Oscillation. *International Journal of Climatology* **16**: 1137-1148.

Webster PJ, Moore AM, Loschnigg JP, Leben RR. 1999. Coupled ocean-atmosphere dynamics in the Indian Ocean during 1997-98. *Nature* **401**: 356-360.

Wilks DS. 2006. *Statistical Methods in the Atmospheric Sciences*. Elsevier: Boston; 627.

Wolter K. 1987. The Southern Oscillation in Surface Circulation and Climate over the Tropical Atlantic, Eastern Pacific, and Indian Oceans as Captured by Cluster Analysis. *Journal of Applied Meteorology* **26**: 540-558.

Wyrtki K. 1975. El Niño—The Dynamic Response of the Equatorial Pacific Ocean to Atmospheric Forcing. *Journal of Physical Oceanography* **5**: 572-584.

Yip CL, Wong KY, Li PW. 2006. Data Complexity in Tropical Cyclone Positioning and Classification. *Data Complexity in Pattern Recognition*. Eds. Basu M, Ho TK. Springer-Verlag: Heidelberg.

Yoo S-H, Yang S, Ho C-H. 2006. Variability of the Indian Ocean sea surface temperature and its impacts on Asian-Australian monsoon climate. *Journal of Geophysical Research* **111**: D03108.

Xie S-P, Annamalai H, Schott FA, McCreary, JP Jr. 2002. Structure and Mechanisms of South Indian Ocean Climate Variability. *Journal of Climate* **15**: 864-878.

Zinke J, Dullo W-C, Heiss GA, Eisenhauer A. 2004. ENSO and Indian Ocean subtropical dipole variability is recorded in a coral record off southwest Madagascar for the period 1659 to 1995. *Earth and Planetary Science Letters* **228**: 177-194.

BIOGRAPHICAL SKETCH

Kevin Ash was born in Tulsa, Oklahoma in 1978 and lived there until the age of ten when his family moved to Oklahoma City. He graduated from Westmoore High School in 1997 and later finished a Bachelor of Arts in geography at the University of Oklahoma in May 2004. Kevin then worked for Weathernews, Inc. in Norman, OK for nearly four years, hired originally for his geography background. After two years at Weathernews, he moved into a position in which he provided weather forecasts and route recommendations to commercial cargo vessels. Though he quite enjoyed the work, Kevin decided to leave and pursue a Masters degree in the fall of 2008 after being accepted into the Department of Geography at the University of Florida. After graduating in May 2010, he plans to pursue a PhD in geography.